Author:
Randell, Matthew J

Title:
Developing novel luminescence methods for measuring antibodies

Developing Novel Luminescence Methods for Measuring Antibodies

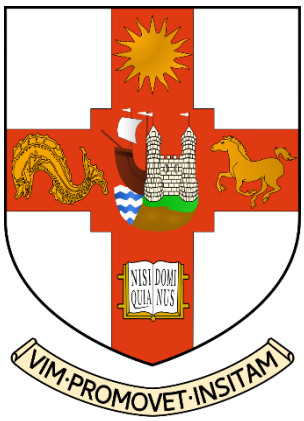

Matthew J Randell

A dissertation submitted to the University of Bristol in accordance with the requirements for award of the degree of MSc by Research in the faculty of Health Sciences.

June 2022

Word count: 27,683

Abstract

Type 1 diabetes (T1D) is a chronic autoimmune disease characterised by destruction of the insulin-producing pancreatic β-cells. Islet autoantibodies to antigens such as the protein tyrosinephosphate (PTP)-like region of Islet Antigen 2 (IA-2) predict progression to T1D. SARS-CoV-2 is a betacoronovirus which causes COVID-19. Antibodies to the spike protein of the virus provide important information regarding exposure and the magnitude and waning of the immune response, either to natural infection or vaccination. This project aimed to develop plate-based 'bridging' luciferase assays as alternative testing methods with improved performance for large-scale screening for antibodies to SARS-CoV-2 spike and IA-2.

NanoLuciferase-tagged IA-2 or SARS-CoV-2 receptor binding domain were diluted and used to label plates of sera. This mixture was then incubated in high-binding optiplates coated with unlabelled PTP-IA-2 or unlabelled spike protein. The specific antibodies in the sera formed a bridge between the plate-bound protein and the free luciferase-tagged conjugate antigens, trapping the reporter for detection.

Results were expressed as units/ml using a standard curve of serially diluted positive sera. Receiver operator characteristic (ROC) curve analysis for the IA-2A bridging assay was carried out using sera from 265 schoolchildren (aged 9-13 years) and 139 people with type 1 diabetes (aged 1-21, samples taken within 3 months of diagnosis) from the Bart's-Oxford Family Study (BOX). The assay was then compared with the PTP-IA-2 radiobinding assay in a blinded set of 150 samples from the 2020 Islet Autoantibody Standardisation Program Workshop. ROC curve analysis for the SARS-CoV-2 spike antibody bridging assay was performed using sera from 401 known negative samples and 46 individuals with PCR-confirmed SARS-CoV-2 infection. The assay was then compared with the Roche anti-spike antibody test in a blinded set of 182 samples.

The optimised bridging assays required only 2-3µl of serum. The IA-2A bridging assay had 70% sensitivity at 99% specificity, and the area under the ROC curve was 0.858 (95% CI 0.811-0.905). There was good correlation with the PTP-IA-2 results measured by radioimmunoassay (Spearman's r=0.84, p<0.001). Future work will evaluate the assay in a blinded validation sample set. The SARS-CoV-2 spike antibody bridging assay had 99% specificity and 96% sensitivity, and the area under the ROC curve was 0.997 (95% CI 0.993-1.000). The assay can detect anti-spike antibodies even at acute stages of the disease (<21 days since infection/symptom onset).

We established novel, non-radioactive, high-performance tests for autoantibodies to IA-2 and antibodies to SARS-CoV-2's spike protein. This plate-based format facilitates automation and therefore high-throughput, large-scale screening for pre-type 1 diabetes or humoral immunity in COVID-19.

COVID-19 Statement

When this half-time Masters by Research project was initiated in January 2020, it was solely focused on developing novel methods of detecting islet autoantibodies. This followed on from my undergraduate BSc project in the school of Cellular and Molecular Medicine, University of Bristol. Less than three months into the project, the COVID-19 pandemic caused the laboratory to close. While this closure was brief, my return to laboratory work was only permitted if working on SARS-CoV-2. As a research group specialising in detecting antibodies, and a clear need for such tests for this new virus, a key objective of the research group became to optimise a high throughput luciferase assay for antibodies to SARS-CoV-2 using the strategy I had been using for islet autoantibodies to IA-2. This was an exciting new research direction, but completely different to my original plan. It set back my planned Masters by Research project in several ways.

1) From April 2020 for almost a year the lab focused on developing a series of tests for SARS-CoV-2 and my focus was the Spike-RBD Bridging assay. Because of social distancing procedures we worked a 7 day per week rota until the SARS-CoV-2 assays were fully validated (Spring 2021).
2) When the laboratory was reopened to diabetes research, my 50% technical role was hugely busy because most international studies, including TEDDY, had continued to recruit, so there was a backlog of samples requiring islet autoantibody results and social distancing measures were still required. The laboratory was also negatively affected by staff having to self-isolate several times.
3) I was severely restricted in the amount of laboratory time available for me to focus on development of the IA-2 autoantibody version of the bridging assay. Ultimately, I did not have an opportunity to restart my original project of development of an IA-2A bridging assay until June 2021.
4) Throughout my Masters I had to begin a new literature search and write about a new disease, in real time during a period of rapid discovery.

Contribution Statement

All the work described in the thesis on development of the PTP-IA-2A bridging assay was carried out by myself. Multiple luciferase immunoprecipitation systems assays for SARS-CoV-2 were developed in our laboratory over the year between April 2020 March 2021. This work was carried out in tandem with a team in Professor Adam Finn's laboratory, School of Cellular and Molecular Medicine, University of Bristol developing ELISAs in order to compare both platforms. Much of this work is included in a preprint, Halliday et al. 2022, which is referenced throughout this thesis. I led the development of the SARS-CoV-2 Spike-RBD bridging assay as described in this thesis. Other members of the team (Ilana Kelland, Yassin Ben Khoud, Georgina Mortimer, Olivia Ball, Simon Scoltock, Ben Gillard, and Hannah Wilson) also helped with sample processing (including heat inactivation of sera for Health and Safety procedures), as well as blinding and testing of validation samples. The Roche N antibody assay was carried out by Dr Jorgen McKernon, Clinical Scientist, North Bristol Trust.

Dedication and Acknowledgement

This thesis is dedicated to my late supervisor, Dr. Alistair Williams. The assays described here would not exist without him and his passionate dedication to his field. His wealth of knowledge, attention to detail, and dry humour were all greatly missed in the latter 15 months of this project. Al gave a lot of his time supporting young people getting started in research, and I know we are all grateful.

I would like to thank my supervisors: Dr. Anna Long, who has been consistently brilliant, kind, and patient in the face of my repeated trivial queries, and Professor Kathleen Gillespie, who took on the impossible task of filling Al's shoes, and did the best anyone could. Her big-picture perspective became especially invaluable as this project neared its end.

I would also like to thank the wider Diabetes & Metabolism team for making me feel at home these last few years, and for generally helping and supporting me and this project. I am especially grateful to Ilana Kelland, who was somehow able to facilitate my completion of this MRes without compromising our routine technician laboratory work, or our friendship.

Lastly, I would like to thank my family, especially my parents, for the frequent motivational comments and persistent discouragement of distraction. I might have been able to do it without you, but it would have taken way longer.

Author’s Declaration

I declare that the work in this dissertation was carried out in accordance with the requirements of the University's *Regulations and Code of Practice for Research Degree Programmes* and that it has not been submitted for any other academic award. Except where indicated by specific reference in the text, the work is the candidate's own work. Work done in collaboration with, or with the assistance of, others, is indicated as such. Any views expressed in the dissertation are those of the author.

SIGNED: [redacted] DATE: 13/06/2022

Table of Contents

ABSTRACT ..... **I**

COVID-19 STATEMENT ..... **III**

CONTRIBUTION STATEMENT ..... **IV**

DEDICATION AND ACKNOWLEDGEMENT ..... **VI**

AUTHOR'S DECLARATION ..... **VIII**

TABLE OF CONTENTS ..... **IX**

LIST OF TABLES ..... **XIII**

LIST OF FIGURES ..... **XIV**

PUBLICATIONS THAT HAVE ARISEN DURING THIS STUDENTSHIP ..... **XV**

PREPRINT, SUBMITTED TO JOURNAL OF CLINICAL INVESTIGATION INSIGHT XV

POSTER ABSTRACT, ACCEPTED BY DIABETES UK PROFESSIONAL CONFERENCE XV

LIST OF ABBREVIATIONS ..... **XVI**

1 INTRODUCTION **1**

1.1 TYPE 1 DIABETES 1

1.1.1 Burden of Type 1 Diabetes *1*

1.1.2 Pathogenesis of Type 1 Diabetes *2*

1.1.3 Genetic Associations with Type 1 Diabetes *3*

1.1.4 Islet Autoantibodies *4*

1.2 SARS-COV-2 6

1.2.1 Structure of SARS-CoV-2 ..... *6*

1.2.2 Transmission and Burden of SARS-CoV-2 ..... *7*

1.2.3 Immune Response to SARS-CoV-2 ..... *8*

1.3 INCREASED BURDEN OF TYPE 1 DIABETES IN COVID-19 8

1.4 BIOMARKERS FOR SARS-COV-2 INFECTION 10

1.5 EXISTING ANTIBODY ASSAY METHODS 10

1.5.1 Islet Cytoplasmic Autoantibodies (ICA) *11*

1.5.2 Radiobinding Assay (RBA) *13*

1.5.3 Enzyme-Linked Immunosorbent Assay (ELISA) *14*

1.5.4 Chemiluminescence Immunoassay (CLIA) *15*

1.5.5 Chemiluminescent Microparticle Immunoassay (CMIA) *17*

1.5.6 Antibody Detection by Agglutination-PCR (ADAP) *18*

1.5.7 Luciferase Immunoprecipitation System (LIPS) *19*

1.5.8 Surrogate Virus Neutralization Test (sVNT) *19*

1.5.9 Cell-free PCR assay (cfPCR) *20*

1.6 NOVEL BRIDGING ASSAY METHOD 21

1.7 HYPOTHESIS 22

1.8 AIMS 22

2 MATERIALS AND METHODS **23**

2.1 SAMPLES 25

2.1.1 Standard Curves and Quality Control Samples *28*

2.1.2 Serum vs Plasma *29*

2.2 BUFFERS 29

2.3 IA-2 Expression 30
2.3.1 GST-PTP-IA-2 Expression 30
2.3.2 IA-2ic Transformation 31
2.3.3 IA-2ic Expression 31
2.3.4 Sonication 31
2.3.5 SDS-PAGE Gel Electrophoresis 32
2.3.6 Fast Protein Liquid Chromatography (FPLC) 32
2.3.7 Quantifying Concentrations 32
2.3.8 Midiprep 33
2.3.9 Sequencing 33
2.3.10 Biotinylating IA-2 33
2.4 IA-2A Bridging Assay Methods 33
2.5 SARS-CoV-2 Spike Antibody Bridging Assay Methods 35
2.5.1 Initial Spike LIPS Assay Method 35
2.5.2 Optimising Initial LIPS Method 35
2.5.3 Novel Bridging Assay Method 36
2.6 Statistical Analysis 37

3 RESULTS 38

3.1 IA-2 Expression and Purification 38
3.2 IA-2A Bridging Assay Variations 39
3.3 Glutathione Variation of the IA-2A Bridging Assay 40
3.3.1 The optimal concentration of PTP-IA-2-GST to coat the glutathione-coated optiplate is 5ng/well 40
3.3.2 Cell-made single label preparation offers superior spread compared to other labels 42
3.3.3 A 2 hour label incubation and 1.5 hour incubation in a coated plate is sufficient to discriminate well between positive and negative samples 44
3.3.4 Blocking via incubation with 1% casein does not reduce background 46
3.4 Biotinylated Variation of the IA-2A Bridging Assay Results 47
3.4.1 Biotinylated IA-2 can be stored at -4°C or -80°C, at least short term, but glycerol reduces binding 47
3.4.2 Incubating biotinylated IA-2 in the label buffer boosted signal compared to incubating it separately 49
3.4.3 Biotinylated IA-2 diluted to 10ng/well provided optimal signal without increasing background .. 50
3.4.4 Neutravidin-coated plates do not require additional blocking 51
3.4.5 Biotinylated IA-2 variation of the bridging assay suffered a 10-fold decrease in light units 52
3.5 Standard IA-2A Bridging Assay Optimisation Results 53
3.5.1 Unlabelled PTP-IA-2 can be stored at -80°C or 4°C for up to 7 months 55
3.5.2 Increasing label total counts to $1x10^7$ improves signal without affecting background 56
3.5.3 NanoGlo® Assay Reagent can be further diluted to reduce cost 57
3.5.4 Additional reagents in label buffer do not improve assay performance 59
3.6 IA-2A Bridging Assay Threshold Setting 61
3.7 PTP-IA-2A Bridging Assay correlates well with PTP-IA-2 RBA 61
3.8 Bridging assays frequently have great intra-assay variation 62
3.9 SARS-CoV-2 Bridging Assay Variations 63
3.10 SARS-CoV-2 Spike-RBD Bridging Assay Optimisation Results 65
3.10.1 A variety of buffers could be used to dilute unlabelled protein to coat plates 65
3.10.2 Coating plates with 100ng/well is the optimal concentration of unlabelled spike protein 66
3.10.3 Reducing the number of washes increases the background of the assay 67
3.10.4 Coated plates can be stored up to 3 months at 4°C 69
3.10.5 Room temperature label incubation is sufficient to achieve good and distinct range of positive signal 70
3.10.6 Casein in Label Buffer does not lower the background 70
3.11 Spike-RBD Bridging Threshold Setting 73

3.12 Comparison with the Roche assay 73
3.13 Spike-RBD Bridging Assay Validation 74

4 DISCUSSION 75

4.1 SARS-CoV-2 Spike-RBD Antibody bridging Assay 75
4.2 PTP-IA-2A Bridging Assay 75
4.3 Strengths of the bridging assay format 76
4.3.1 Bridging assays detect all isotypes of antibody response 76
4.3.2 Bridging assays only capture specific antibodies 77
4.3.3 Bridging assays can be sensitive and specific 77
4.3.4 The Spike-RBD Bridging assay detects even acute infection 78
4.3.5 Bridging assays require very low sample volume 79
4.3.6 Bridging assays are low cost to perform 80
4.3.7 Bridging assays can be high throughput 81
4.4 Limitations of the bridging assay format 84
4.4.1 Bridging assays have great intra-assay variation 84
4.4.2 Plate-based assays can suffer from epitope obscuration 84
4.4.3 Bridging assays rely on existing luciferase constructs and Promega kits 85
4.4.4 The Spike-RBD bridging assay is unable to differentiate between responses to vaccination and natural SARS-CoV-2 infection 86
4.4.5 The biotinylated IA-2 is not suitable for long-term storage at 4°C 87
4.4.6 The IA-2A bridging assay uses a truncated antigen 87
4.5 Application: General Population Screening for Islet Autoantibodies 87
4.6 Application: Large-scale screening for anti-SARS-Cov-2 spike antibodies 91
4.7 Conclusion and Future Work 92

5 APPENDIX 94

5.1 Buffers 94
5.2 IA-2ic Sequencing Results 96
5.3 Alternate IA-2A Bridging Assay Format Methods 98
5.3.1 Glutathione-Coated Plate Variation of the IA-2A Bridging Assay Method 98
5.3.2 Biotinylated IA-2 Variation of the IA-2A Bridging Assay Method 99
5.3.3 NanoGlo® Assay Reagent can be further diluted to reduce cost in the biotinylated IA-2 format of the bridging assay 99

6 BIBLIOGRAPHY 101

List of Tables

Table 1-1 Amino acid residues of several epitopes of IA-2 by publication. 4
Table 1-2 Summary of existing antibody tests against criteria for large-scale screening. 11
Table 2-1 Materials/Equipment 24
Table 2-2 Reagents 25
Table 2-3 Details of the samples used in the IA-2A Bridging Assay 26
Table 2-4 Details of the samples used in the Spike-RBD Bridging Assay 27
Table 2-5 IA-2A bridging assay conditions optimised previously. 34
Table 2-6 SARS-CoV-2 Spike-RBD Bridging assay conditions optimised previously 36
Table 3-1 Investigated incubation conditions for the Glutathione IA-2A Bridging Assay. 44
Table 4-1 Table summarising bridging assay steps and automation potential. 83
Table 4-2 Table showing the estimated rates of type 1 and type 2 errors for Spike-RBD bridging 92
Table 5-1 Table showing all buffers used in this project and their recipes. 95
Table 5-2 Table showing assay conditions used in the glutathione and biotinylated versions of the IA-2A bridging assay previously optimised 98

List of Figures

Figure 1-1 Activation of CD8+ cytotoxic T-cells in Type 1 Diabetes 3
Figure 1-2 Structure of a SARS-CoV-2 virion 7
Figure 1-3 Unadjusted in-hospital COVID-19 mortality rates 9
Figure 1-4 Flowchart of a radiobinding assay method 13
Figure 1-5 Flowchart of an indirect ELISA method 14
Figure 1-6 Flowchart of an ECL method 16
Figure 1-7 Flowchart of an ECLIA method. 16
Figure 1-8 Flowchart of method for AdviseDX SARS-CoV-2 IgG II semi-quantitative CMIA 17
Figure 1-9 Flowchart of method for the Roche Elecysys Anti-SARS-CoV-2 CLIA/CMIA assays. 17
Figure 1-10 Flowchart of an ADAP method 18
Figure 1-11 Flowchart of a LIPS method 19
Figure 1-12 Flowchart of an sVNT method. 20
Figure 1-13 Flowchart of a cell-free PCR assay method 20
Figure 1-14 Flowchart of bridging assay method 21
Figure 1-15 Bridging assay schematic. 22
Figure 2-1 Standard Curve for the IA-2A bridging assay. 28
Figure 2-2 Standard Curve for the Spike-RBD bridging assay 28
Figure 1-2-3 pET-49b(+) plasmid map 30
Figure 3-1 SDS-PAGE Gel showing expression of PTP-IA-2 38
Figure 3-2 SDS-PAGE Gel showing FPLC-purified fractions of PTP-IA-2 and IA-2ic 39
Figure 3-3 Glutathione IA-2A Bridging Optimisation: Coated Protein Concentration 41
Figure 3-4 Glutathione IA-2A Bridging Optimisation: Label Preparation 43
Figure 3-5 Glutathione IA-2A Bridging Optimisation: Incubation Lengths 45
Figure 3-6 Glutathione IA-2A Bridging Optimisation: Blocking Method 46
Figure 3-7 Biotinylated IA-2A Bridging Optimisation: Protein Storage Temperature 48
Figure 3-8 Biotinylated IA-2A Bridging Optimisation: Protein Incubation Method 49
Figure 3-9 Biotinylated IA-2A Bridging Optimisation: Biotinylated IA-2 concentration 50
Figure 3-10 Biotinylated IA-2A Bridging Optimisation: Blocking Method 52
Figure 3-11 Biotinylated IA-2A Bridging Optimisation: Biotinylated IA-2 Degradation 53
Figure 3-12-2 IA-2A Bridging Assay Format Comparison. 54
Figure 3-13 IA-2A Bridging Optimisation: Protein Storage Temperature 55
Figure 3-14 IA-2A Bridging Optimisation: Label Total Counts 56
Figure 3-15 IA-2A Bridging Optimisation: Assay Reagent Dilution 58
Figure 3-16 IA-2A Bridging Optimisation: Additional Reagents in Label Buffer 59
Figure 3-17 Receiver Operator Characteristic (ROC) Curve for the IA-2A Bridging Assay. 61
Figure 3-18 Plot comparing IA-2A bridging and RBA in samples from the IASP2020 Workshop 62
Figure 3-19 Graph comparing the percentage error in IA-2A bridging and RBA 63
Figure 3-20 Spike-RBD Bridging Optimisation: Coated Protein 64
Figure 3-21 Spike-RBD Bridging Optimisation: Coated Protein Diluent 65
Figure 3-22 Spike-RBD Bridging Optimisation: Coated Protein Concentration 67
Figure 3-23 Spike-RBD Bridging Optimisation: Number of Washes 68
Figure 3-24 Spike-RBD Bridging Optimisation: Coated Plate Viability 69
Figure 3-25 Spike-RBD Bridging Optimisation: Label Incubation temperature 70
Figure 3-26 Spike-RBD Bridging Optimisation: Casein in Label Buffer 71
Figure 3-27 Receiver Operator Characteristic (ROC) Curve for the Spike-RBD bridging assay 73
Figure 3-28 Graph comparing the Roche N and Spike-RBD bridging antibody tests 74

Figure 5-1 Five prime IA-2ic sequencing results. 96
Figure 5-2 Three prime IA-2ic sequencing results. 97
Figure 5-3 Biotinylated IA-2A Bridging Optimisation: Assay Reagent Dilution 100

Publications that have arisen during this studentship

Preprint, submitted to Journal of Clinical Investigation Insight

Alice Halliday, Anna E Long, Holly E Baum, Amy C Thomas, Kathryn L Shelley, Elizabeth Oliver, Kapil Gupta, Ore Francis, Maia Kavanagh Williamson, Natalie di Bartolo, **Matthew J Randell**, Yassin Ben-Khoud, Ilana Kelland, Georgina Mortimer, Olivia Ball, Charlie Plumptre, Kyla Chandler, Ulrike Obst, Massimiliano Secchi, Lorenzo Piemonti, Vito Lampasona, Joyce Smith, Michaela Gregorova, Lea Knezevic, Jane Metz, Rachael Barr, Begonia Morales-Aza, Jennifer Oliver, Lucy Collingwood, Benjamin Hitchings, Susan Ring, Linda Wooldridge, Laura Rivino, Nicholas Timpson, Jorgen McKernon, Peter Muir, Fergus Hamilton, David Arnold, Derek N Woolfson, Anu Goenka, Andrew D. Davidson, Ashley M Toye, Imre Berger, Mick Bailey, Kathleen M Gillespie, Alistair JK Williams, Adam Finn. Development and evaluation of low-volume tests to detect and characterise antibodies to SARS-CoV-2. *medRxiv.* 2022:2022.2005.2003.22274395.

Poster abstract, accepted by Diabetes UK Professional Conference

M. J. Randell; K. T. Elvers; V. Lampasona; A. J. K. Williams; K. M. Gillespie; A. E. Long. Development of a novel, low volume, non-radioactive luminescence method of detecting islet autoantibodies in serum for large-scale screening. Diabetic Medicine, 2022. Basic and clinical science posters: Screening and prediabetes, P72.

SIGNED: [redacted] DATE: 13/06/2022

SIGNED: [redacted] DATE: 15/06/2022

List of Abbreviations

- ACE2 = angiotensin converting enzyme-2
- ADAP = Antibody Detection by Agglutination-PCR
- ALSPAC = Avon Longitudinal Study of Parents and Children
- APS = Ammonium Persulfate
- AUC = Area under the receiver operator characteristic curve
- CDC = Centers for Disease Control and Prevention
- cfPCR = Cell-Free PCR assay
- CI = confidence interval
- CLIA = Chemiluminescence Immunoassay
- CMIA = Chemiluminescent Microparticle Immunoassay
- COVID-19 = Coronavirus Disease 2019
- CP = Cell Pellet
- cVNT = Conventional Virus Neutralization Test
- DAISY = Diabetes Autoimmunity Study in the Young
- DASP = Diabetes Antibody Standardization Program
- Denver LIPS/TBST Higher Tween = Tris-Buffered saline + 0.5% Tween
- Denver/TBST Low Tween = Tris-buffered saline + 0.15% Tween
- DiPis = Diabetes Prediction in Skåne
- DIPP = Type 1 Diabetes Prediction and Prevention Project
- DKA = Diabetic Ketoacidosis
- DNA = Deoxyribonucleic acid
- E protein = envelope
- *E. coli* = *Escherichia coli*
- ECLIA = Electrochemiluminescence Immunoassay Analyzer
- EDTA = Ethylenediaminetetraacetic acid
- ELISA = Enzyme-Linked Immunosorbent Assay
- Fab region = fragment antigen-binding region
- Fc region = fragment crystallizable region
- FLuc = Firefly Luficerase
- FPLC = Fast Protein Liquid Chromatography
- GAD(A) = (autoantibodies to) glutamic acid decarboxylase
- GDP = Gross Domestic Product)
- GRS = Genetic Risk Score
- GST = Glutathione S-Transferase
- HLA = Human Leukocyte Antigen
- HRP = Horseradish Peroxidase
- IA-2(A) = (autoantibodies to) tyrosine phosphatase-related islet antigen 2
- IA-2ic = the intracellular/cytoplasmic domain of IA-2
- IAA = autoantibodies to insulin
- IASP = Islet Autoantibody Standardization Program
- ICA = Islet Cytoplasmic Autoantibodies

- IFN-γ = interferon gamma
- Ig = immunoglobulin
- IL-1β = interleukin 1 beta
- IL-6 = interleukin 6
- IPTG = Isopropyl β-D-1-thiogalactopyranoside
- JM = the juxtamembrane domain of IA-2
- K_D = Dissociation constant
- LB = lysogeny broth
- LIPS = Luciferase Immunoprecipitation System
- M protein = membrane
- MERS-CoV = Middle East Respiratory Syndrome Coronavirus
- MHC = Major Histocompatibility Complex
- MHRA = Medicines and Healthcare products Regulatory Agency
- MSD = Meso Scale Discovery Company
- N protein = nucleocapsid proptein
- NEQAS = National External Quality Assessment Service
- NHS = National Health Service
- NIBSC = National Institute for Biological Standards and Control (NIBSC)
- NIDDK = National Institute of Diabetes and Digestive and Kidney Disease
- NIH = National Institutes of Health
- NLuc = Nanoluciferase enzyme
- OD = Optical Density
- PBS = Phosphate-Buffered Saline
- PCR = Polymerase Chain Reaction
- POInT = Primary Oral Insulin Trial
- PTP = the tyrosine phosphatase domain of IA-2
- QC = quality control sample
- qPCR = Quantitative Polymerase Chain Reaction
- RBA = radiobinding assay
- RBD = receptor binding domain
- RIA = radioimmunoassay
- RLuc = Renilla Luficerase
- RNA = ribonucleic acid
- ROC = Receiver Operator Characteristic
- RT = Room temperature
- S = Supernatant
- S protein / S1+S2 = spike protein
- SARS = Severe Acute Respiratory Sydrome
- SARS-CoV-2 = Severe Acute Respiratory Syndrome Coronavirus 2
- SDS-PAGE = Sodium dodecyl sulfate-polyacrylamide gel electrophoresis
- SNP = Single Nucleotide Polymorphism
- SNR = Signal-to-Noise Radio

- sVNT = Surrogate Virus Neutralization Test
- T1D = Type 1 Diabetes
- T2D = Type 1 Diabetes
- TBS = Tris-buffered saline
- TEDDY = The Environmental Determinants of Diabetes in the Young
- TEMED = Tetramethylethylenediamine
- TMB = Tetramethylbenzidine
- TNF-α = tissue necrosis factor alpha
- Tris = *tris*(hydroxymethyl)aminomethane
- WHO = World Health Organization
- ZnT8(A) = (autoantibodies to) zinc transporter 8
- ΔC_T = difference in cycle threshold between sample and blank controls

1 Introduction

Antibodies are important in a range of conditions, from causing autoimmune disease to providing protection against infection. Their capacity to bind to specific antigens allows them to be isolated and detected in serum, while their ubiquity allows one assay format to have biomarking utility in a range of disease contexts. In this thesis I describe existing antibody tests and a possible novel solution for the niche created by their shortcomings, using type 1 diabetes and SARS-CoV-2 infection as case studies.

1.1 Type 1 Diabetes

1.1.1 Burden of Type 1 Diabetes

A chronic autoimmune disease, type 1 diabetes (T1D) is caused by damage to the insulin producing β-cells of the pancreas. Insulin is critical to regulating glucose levels in blood[1]. The lifetime risk of T1D is about 1 in 300, but this is higher in individuals with an affected first-degree relative – their lifetime risk is around 1 in 20[2].The incidence of T1D is increasing[3], particularly in young children.

Since 1921, T1D has been treated by injecting insulin to replace lost endogenous hormone secretion caused by the destruction of β-cells. Blood glucose levels need to be carefully monitored but this can be difficult, especially in young children. There are severe complications from poorly regulated insulin levels. These include diabetic ketoacidosis (DKA), cerebral oedema[4], and peripheral artery disease, potentially leading to foot amputation[5]. Microvascular complications include diabetic retinopathy, neuropathy, and nephropathy.[6] T1D patients have an estimated life expectancy 12 years shorter than that of the general population[7].

Severe DKA is life-threatening, and in England and Wales, 24% of children and adolescents with T1D are in DKA when diagnosed[8]. Even without a licenced preventative treatment, early diagnosis of T1D is critical to prevent DKA. Several paediatric studies, including BABYDIAB, The Environmental Determinants of Diabetes in the Young (TEDDY), Diabetes Autoimmunity Study in the Young (DAISY), and Type 1 Diabetes Prediction and Prevention Project (DIPP) have found T1D detected by screening results in fewer cases diagnosed in DKA, with BABYDIAB and DAISY also reporting shorter patient stays in hospitals[9-12]. There

have also been numerous intervention trials, combining prediction with potential preventative therapies, for example oral insulin in trials such as DPT-1 and Pre-POINT[13]. These trials aim to preserve function of at least a portion of an individual's β-cells, allowing some level of glycaemic control to persist. Slight delays in C-peptide decline in new onset T1D patients have been observed following some treatments, for example CTLA-4 Ig (abatacept). Few interventions have been trialled in at-risk populations, and until recently these strategies have unfortunately yielded little success in delaying progression to diabetes[13], but treatment with the anti-CD3 monoclonal antibody Teplizumab offers the potential to delay onset in "at risk" individuals[14].

Even with good glycaemic control, individuals with T1D have been found to have impaired immune systems in a variety of ways. For example, peripheral blood monocytes secrete less interleukin-1 and interleukin-6 (both well characterised pro-inflammatory cytokines) in individuals with T1D than in individuals with type 2 diabetes (T2D) or no diabetes[15]. Another example is components of the immune system becoming glycated, having a detrimental effect on the function of these aspects of immunity. This is the case for immunoglobulins, which become glycated proportionally to the increased HbA1c typical of T1D[16], although it is still unclear whether this alters the humoral response to infectious diseases such as Coronavirus Disease 2019 (COVID-19).

1.1.2 Pathogenesis of Type 1 Diabetes

There are between 3.2 and 14.8 million islet cells in a human pancreas. Insulin is secreted by β-cells, which make up an estimated 70-80% of each islet. Another 15-20% of each islet are α-cells, which secrete glucagon[17,18]. In individuals without diabetes, healthy levels of blood sugar are maintained by these cells secreting appropriate levels of their respective hormones. In individuals with T1D, lymphocytes have infiltrated the β-cells – a condition called insulitis[19]. Depending on the stage of this insulitis, different types of immune cell are involved. $CD8^+$ cytotoxic T cells are most abundant, and macrophages and $CD20^+$ cells (B cells) are also present, with the latter increasing as the disease progresses, and peaking at late insulitis. This has been reported to be age-dependent, with individuals diagnosed over 13 years of age having a consistently low proportion of infiltrating $CD20^+$, and individuals diagnosed under 7 years of age, a much higher proportion[20]. While less abundant than macrophages, $CD4^+$ helper T cells also exist in this infiltrate.[21]

B cells can differentiate into plasma cells, which produce antibodies, but B cells are also antigen-presenting cells, using Major Histocompatibility Complex (MHC) Class II to present peptides to $CD4^+$ helper T cells. In turn, $CD8^+$ cytotoxic T cells (recognised via MHC Class I and involved in β-cell destruction) are activated by these $CD4^+$ helper T cells secreting cytokines. There is also evidence of B cells cross-presenting islet peptides via MHC Class I, which may activate these cytotoxic T cells more directly[22] (figure 1-1). Additionally, some studies suggest β-cells can express MHC Class II in certain circumstances, allowing interactions with $CD4^+$ helper T cells which may expedite β-cell destruction[23].

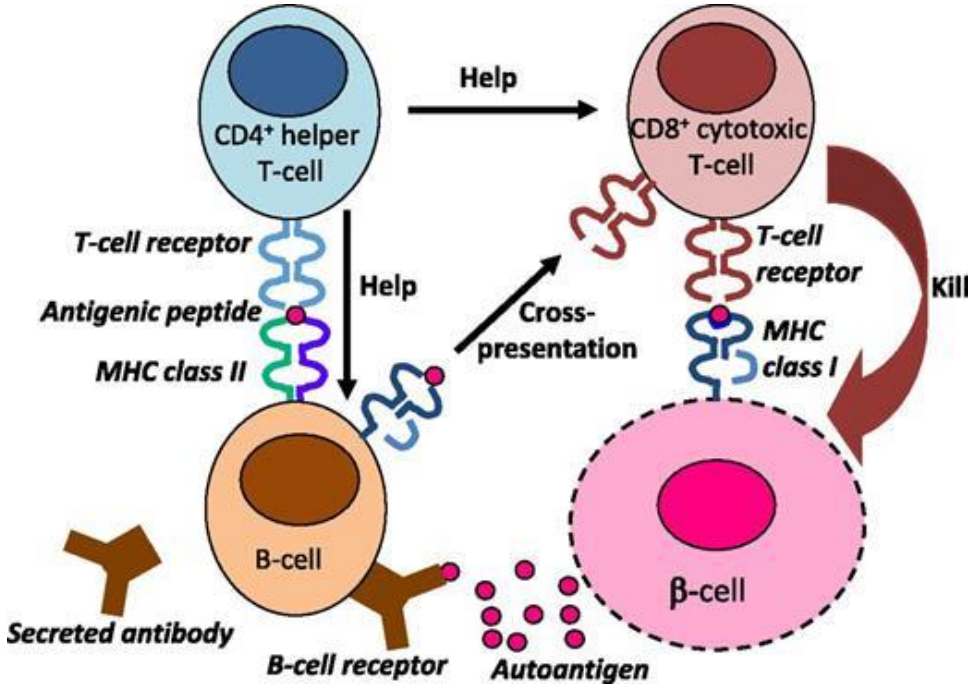

Figure 1-1 Activation of CD8+ cytotoxic T-cells in Type 1 Diabetes. Figure from Christie et al. (2016).

1.1.3 Genetic Associations with Type 1 Diabetes

Individuals with a first-degree relative who has T1D have an increased lifetime risk – 1 in 20 compared with 1 in 300[2]. Haplotypes in the Human Leukocyte Antigen (HLA) region have around 50% of genetic risk attributed to them[4] while at least 78 non-HLA single nucleotide polymorphisms (SNPs) are also associated with T1D[24]. Over the last decade, genetic risk scores (GRS) for T1D incorporating both HLA and non-HLA variants have become more widely utilised in research studies and to help classify diabetes at diagnosis[25,26]. Of Caucasian individuals with T1D, 95% have at least one of either DR3 or DR4, which are the highest risk haplotypes[27]. Despite this clear genetic association, a family history of the disease is only present in about 15% of T1D cases[28].

1.1.4 Islet Autoantibodies

The link between T1D and autoantibodies to autoantigens on the pancreatic islets is so strong that their presence has now been characterised as a stage of presymptomatic disease[28].

There are five main autoantibodies which target islet proteins: autoantibodies to insulin (IAA), glutamic acid decarboxylase (GADA), tyrosine phosphatase-related islet antigen 2 (IA-2A), zinc transporter 8 (ZnT8A), and tetraspanin-7[29-34].

IA-2 is expressed largely on neuroendocrine cells and has several notable epitopes: the cytoplasmic domain (IA-2ic), which includes parts of the juxtamembrane domain (JM) and the tyrosine phosphatase (PTP) domain. The amino acid residues of each of these epitopes vary slightly by publication, and some are summarised in table 1-1 below[35]. The antibody response to IA-2 in pre-diabetes often targets the JM domain, then spreads to the PTP domain and to IA-2β – a closely related protein[35] which is more persistent in its expression. Glucose and insulin induce IA-2 expression in β-cells, which is down-regulated by proinflammatory cytokines such as interleukin 1-beta (IL-1β), tissue necrosis factor alpha (TNF-α), and interferon gamma (IFN-γ)[36].

Epitope	**Amino Acid Residues**			
	McLaughlin et al. (2015) Clinical Immunology	**Long et al. (2013) Diabetes**	**Elvers et al. (2013) Diabetes**	**Peakman et al. (1999) Journal of Clinical Investigation**
IA-2ic	605-979	606-979	606-979	603-979
PTP	643-937	687-979	687-979	No data

Table 1-1 Amino acid residues of several epitopes of IA-2 by publication.

IA-2 has homologues in multiple species, indicating it has an important function, possibly in regulating the contents of insulin granules, but the minutiae and extent of this role has yet to be fully elucidated[36].

Children at risk of type 1 diabetes often first develop autoantibodies to insulin or GAD[37]. Autoantibodies to IA-2 and ZnT8 are rarely present in individuals with a single autoantibody,

instead appearing closer to diagnosis. These autoantibodies could therefore be considered markers of more rapid progression to type 1 diabetes[38].

The titre of autoantibodies is also important. One study found that amongst relatives of those with type 1 diabetes, individuals with a higher titre of IA-2A were much more likely to progress to T1D themselves – a 79% chance within 10 years, compared with 20% in those who were positive for IA-2A but with lower titres[39]. The importance of autoantibody titres has been clear for some time[40], and it has been analysed in some longitudinal studies[41,42]; despite this it is still the binary antibody status/positivity alone which is often considered[43,44].

The risk of progression to clinical T1D is greater in individuals with multiple autoantibodies[45]. Genetically at-risk children (n=13,377) enrolled in the studies DAISY (Colorado, USA), BABYDIAB (Germany), and DIPP (Finland), were tested for IA-2A, GADA, and IAA, and they found that 4.4% had multiple islet autoantibodies[4,46]. Individuals positive for a single autoantibody were shown to have a 14.5% risk of developing T1D within 10 years[4], while individuals with multiple autoantibodies had a 69.7% risk of progressing to clinical disease within the same period[46]. Additionally, of DAISY study participants who progressed to clinical T1D, 89% were positive for at least two autoantibodies[47]. It is of benefit for disease prediction therefore, to assay for combinations of the four islet autoantibodies, rather than just one.

Due to the predictive power of islet autoantibody and genetic tests, there has been a focus on investigating the feasibility of large-scale screening to identify “at-risk” individuals in the general population.

Type 1 Diabetes TrialNet screens around 15,000 people per year who have first- or second-degree relatives with T1D. This helps improve understanding of the natural history of the disease, as well as providing recruitment for intervention trials such as the Abatacept Prevention Study. The Fr1da study screened over 90,000 children aged 2-5 years from the general population of Bavaria, Germany, but the healthcare costs saved by reducing DKA and avoiding hospitalisation were estimated to only be one third the cost of the screening study[4] (although this does not account for quality of life improvements). Fr1da also shows that the cost of antibody test is a significant proportion of the total screening cost, and

therefore a crucial barrier in large-scale screening[48]. This highlights the need for cheaper / more high throughput screening assays.

In order to roll out islet autoantibody testing nationwide, the chosen method also ought to avoid radioactivity. Despite being considered by many to be the current gold-standard, the regulations surrounding storage and waste disposal, as well as training, greatly limits the number of laboratories/sites available to perform radiobinding/radioimmuno assays (RBA/RIA). Hence, the need for non-radioactive tests which rival the RBA in sensitivity and specificity. Another factor to be taken into consideration is the volume of serum required by the test. Capillary blood samples are less invasive than venous samples, but it can be difficult to collect high volumes. For this reason, a suitable test must require very low serum volumes. The Fr1da study reported only 0.54% of capillary samples having insufficient blood volume - these were collected by phlebotamists[49], but even self-collected samples have been found in TrialNet to be sufficient volume 84% of the time[50].

Antibodies for SARS-CoV-2 can be measured using similar laboratory methods, and may also demand remote sampling. In addition, the impact of COVID-19 on people with, or "at risk of", T1D has been a research focus.

1.2 SARS-CoV-2

Coronaviruses cause a range of diseases in animals, with seven types able to infect humans. On 31st December 2019, in China, the first patient with a new type of coronavirus was identified – severe acute respiratory syndrome coronavirus 2 (SARS-CoV-2)[51].

1.2.1 Structure of SARS-CoV-2

SARS-CoV-2 is a betacoronavirus[52], part of the *Coronaviridae* family, characterised by an envelope and a positive sense single-stranded ribonucleic acid (RNA) genome of about 30 kilobases[53]. The pleomorphic virions are ~60-140nm in diameter[54] and have four major structural proteins: nucleocapsid (N), spike (S1+S2), envelope (E), and membrane (M)[55], shown on figure 1-2 below[56]. A fragment of the spike protein (aa318-510), a discrete receptor binding domain (RBD), binds to the angiotensin converting enzyme-2 (ACE2) receptor for coronaviruses more efficiently than S1 as a whole[57].

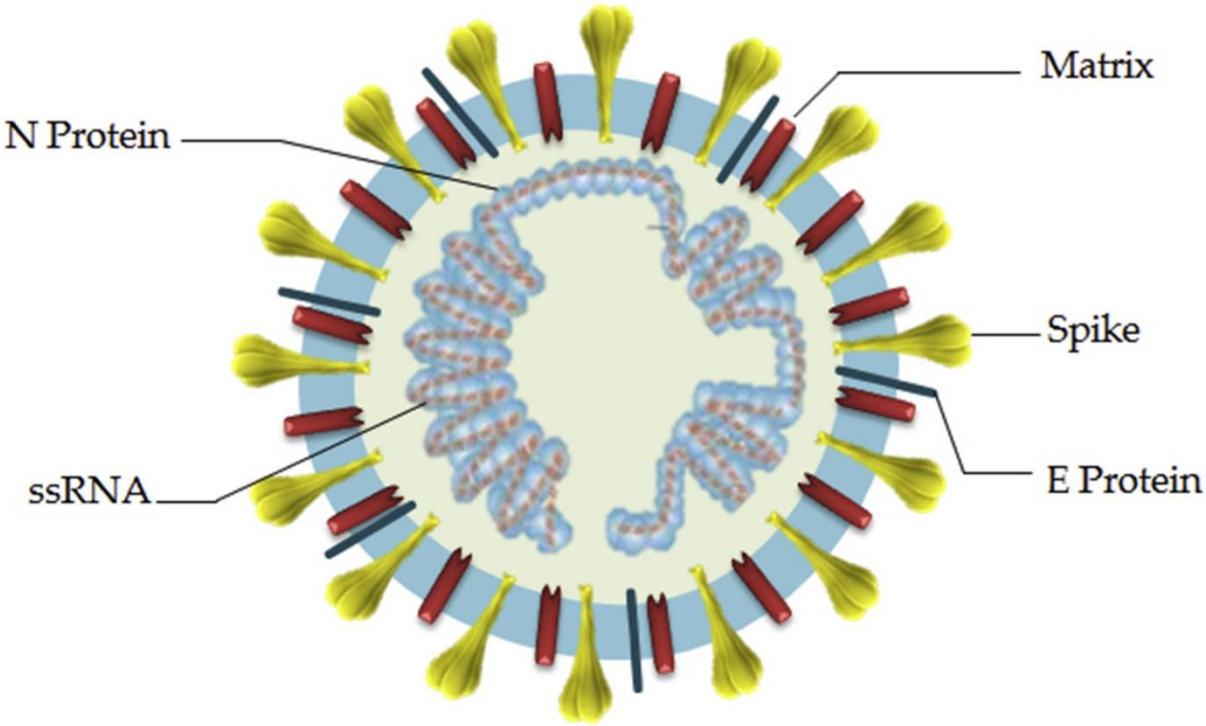

Figure 1-2 Structure of a SARS-CoV-2 virion. Taken from Astuti et al. (2020).

1.2.2 Transmission and Burden of SARS-CoV-2

SARS-CoV-2 is transmitted primarily through droplets and close contact[58]. Common symptoms of COVID-19 include fever, a cough, and fatigue; the disease can be more serious however, and the same meta-analysis which found those to be the most common symptoms also reported that 17% of hospitalised patients required intensive care, and a 7% mortality rate[59]. The vast variety in severity of symptoms (asymptomatic to fatal) can often be attributed to underlying health conditions / comorbidities. One study found that during a one-month period, 49.7% of hospitalised COVID-19 patients had hypertension, 48.3% obesity, and 34.6% chronic lung disease. In addition, 28.3% had diabetes mellitus[60]. The burden of COVID-19 cannot be overstated, with 66,479 associated deaths in England between 29/06/2020 and 31/01/2021[61]. Additionally, a great economic burden resulted from the national and local "lockdowns" restricting certain businesses from functioning. The UK Parliament's House of Commons Library has described the magnitude of the pandemic recession as "unprecedented in modern times", and quotes 2020 as having the steepest decrease in Gross Domestic Product (GDP) (9.7%) since records began[62].

1.2.3 Immune Response to SARS-CoV-2

When SARS-CoV-2 virions are detected by pathogen recognition receptors, greater interferon production is induced. COVID-19 patients also have increased expression of chemokines and cytokines – IL-6 and TNF-α, amongst others. T cells can recognise the SARS-CoV-2 antigens presented by MHC class I and MHC class II, promoting $CD8^+$ cytotoxic and $CD4^+$ helper T cells respectively[63]. These $CD4^+$ T cell responses to spike correlated well with titres of immunoglobulin G (IgG) and IgA antibodies, although are potentially cross-reactive, as one study found them in up to 60% of individuals who have not been exposed to SARS-CoV-2[64].

The N protein is highly immunogenic and is subject to an early B cell response, whereas antibodies against the spike protein tend to appear later in acute infection. IgG, IgA, and IgM antibody isotypes are all present in patients infected with SARS-CoV-2, although production varies as the disease progresses[63].

HLA association remains to be fully identified in SARS-CoV-2 infection, although potentially transferrable knowledge has been elucidated in Middle East Respiratory Syndrome Coronavirus (MERS-CoV)[63].

1.3 Increased Burden of Type 1 Diabetes in COVID-19

In addition to T1D, described above and characterised by a lack of insulin secretion, there exists another common form of the disease – type 2 diabetes (T2D). In contrast with type 1, T2D is more prevalent (making up about 90% of total UK diabetes cases)[65], and characterised by resistance to insulin[66], making exogenous insulin an inappropriate initial treatment for hyperglycaemia.

Type 1 and type 2 diabetes have both been shown to exacerbate the effects of similar viruses, for example they triple the risk of hospitalisation for H1N1 influenza[67], and were also independently associated with poor outcome in SARS-CoV-1 infection[68].

Individuals with diabetes are not becoming infected with SARS-CoV-2 at a greater rate[69], however COVID-19 patients with diabetes do have an increased risk of rapid progression to more severe disease - often characterised by uncontrolled cytokine storms and a hypercoagulable state[70]. In Wuhan, China, one study showed that 42.3% of 26 people whose deaths were caused by SARS-CoV-2 had diabetes[71].

For type 2 diabetes (T2D), the link to worse COVID-19 outcomes could be due to correlations with age and other comorbidities such as obesity[72]. Issues common across types of diabetes, such as glycaemic control, are also risk factors. One study found that 56.6% of a small cohort of people with T2D and COVID-19 (n=29) had abnormal blood glucose levels[73], and another found abnormal glucose tolerance (pre-diabetes) in individuals not diagnosed with diabetes is an independent risk factor for 28-day mortality in COVID-19 (fasting blood glucose ≥7.0 mmol/l hazard ratio: 2.30 [95% CI (confidence interval) 1.49, 3.55])[74]. Figure 1-3 below shows deaths per 100,000 due to COVID-19 in people with and without each type of diabetes. COVID-19 mortality in people with T1D is worse than in T2D[75], suggesting T1D as a co-morbidity is due to more than just glycaemic control.

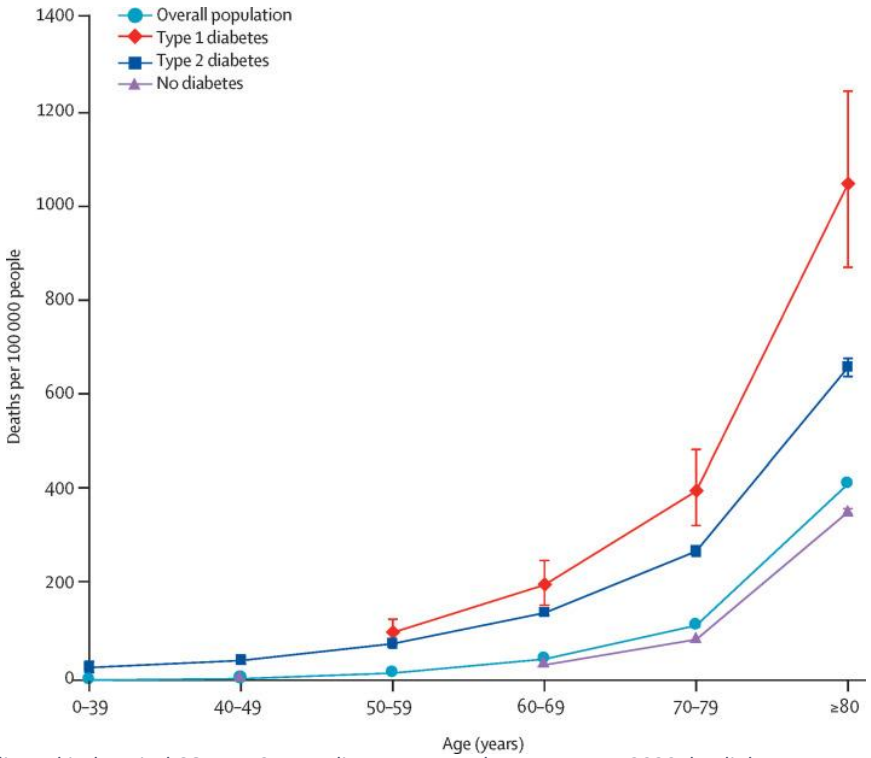

Figure 1-3 Unadjusted in-hospital COVID-19 mortality rates, March 1 to May 11, 2020, by diabetes status. Error bars show 95% CIs. Data for age groups 0–39 years and 40–49 years for type 1 diabetes and 0–39 years and 50–59 years for no diabetes have been excluded because of small numbers of events (one to four), to comply with data protection regulations. Taken from Barron et al. (2020).

The relationship between SARS-CoV-2 infections and hyperglycaemia is complex. Coronaviruses can bind to cells of the human pancreas via ACE2 receptors[76], an enzyme also occurring on a variety of other human cells, namely lung alveolar epithelial cells[77]; possibly due to this mechanism, slight islet cell degeneration has been found in pancreatic biopsies of COVID-19 patients, having caused acute temporary diabetes[78]. This has been an area of much debate, as research on pancreata from COVID-19 patients has found most islet cell

subsets have low ACE2 expression, and suggests COVID-19-related diabetes is unlikely to be caused by SARS-CoV-2 using ACE2 to infect the endocrine cells of the pancreas[79]. Most recently however, the Centers for Disease Control and Prevention (CDC) published data showing that, compared to people without COVID-19, people aged under 18 years with COVID-19 were more likely to be diagnosed with type 1 diabetes >30 days after infection[80].

1.4 Biomarkers for SARS-CoV-2 Infection

An ideal biomarker should be specific, sensitive, indicative[81] – all descriptors of good antibody tests. Antibody testing is essential to examine the relationship between the immune response to SARS-CoV-2 and protection against COVID-19. Serological tests also allow previous exposure of a population to the virus to be defined, and to confirm the adaptive immune response in infected/vaccinated individuals[82]. Although antibody testing was one of the UK government's five pillars of coronavirus response[83], good quality testing proved difficult, with the Medicines and Healthcare products Regulatory Agency (MHRA) eventually approving tests that did not meet their own requirements of sensitivity and specificity[84,85].

Furthermore, while testing for antibodies to the spike protein cannot differentiate between humoral responses to natural infection and the vaccine response, there are large populations in the world where vaccination programmes are yet to be effectively rolled out[86]. A simple assay using small volumes and little equipment could be useful in these areas, especially where the logistics of sample collection is more difficult. There was therefore a requirement for a high throughput, very high performance SARS-CoV-2 antibody test - particularly one requiring low blood volumes which could be collected remotely during lockdowns to monitor infection rate in the general population.

1.5 Existing Antibody Assay Methods

Since the discovery of antibodies, there have been many different assay formats developed for their detection in serum. Islet autoantibody detection began in the 1970s[87] with subsequent development of modern techniques. Conversely, SARS-CoV-2 has a more recent history so while some techniques are applicable in both diseases, some historic islet autoantibody detection methods (e.g. RBA) have not been applied to these anti-viral antibodies.

The National Institutes of Health/World Health Organisation (NIH/WHO) have funded efforts to harmonise islet autoantibody assays, and this has been achieved in RBAs for GADA and IA-2A[88]. The Diabetes Antibody Standardization Program (DASP), established in the early 2000s, and later the Islet Autoantibody Standardization Program (IASP), aim to standardise measurement of islet autoantibodies by sending coded serum aliquots from newly diagnosed patients and blood donor controls to laboratories across the world, for them to test in various assays for comparison[89]. An analogous blinded serum exchange programme has been suggested for SARS-CoV-2[82], and in the meantime the National Institute for Biological Standards and Control (NIBSC) and the WHO have provided reference standards to aid assay harmonisation[90]. Some detection methods for antibodies in both diseases are described below.

Criteria	**ICA**	**RBA**	**ELISA**	**CLIA**	**ADAP**	**LIPS**	**CMIA**	**sVNT**	**cfPCR**
Sensitive	Yes, on human pancreata	Yes	Yes	Yes	Yes	Yes	Yes	Yes	Unclear
Specific	No	Yes	Yes	Yes	Yes	Yes	Yes	Yes	Unclear
Low serum volume	Yes, highly diluted	Yes 4-20µl	Variable, but up to 50µl	Yes, up to 12µl	Yes, 2-10µl	Yes 2-4µ	Yes, 12-25µl	No, up to 60µl	Yes, 1µl
Commercial (C)?	In house (IH)	IH>C	C>IN	IH> C	C	IH	C	IH	IH/C
No radioactivity	Yes	No	Yes	Yes	Yes	Yes	Yes	Yes	Yes
Possibility for automation	No	No	Yes	Yes	Yes	No	Yes	Yes	Yes

Table 1-2 Summary of existing antibody detection methods against criteria for large-scale screening.

1.5.1 Islet Cytoplasmic Autoantibodies (ICA)

This method entails adding serum (for example, 25µl of a 1:32 dilution in PBS) to 4µm sections of pancreas to determine whether antibodies in the serum bind to antigens in the islets. The output is islet cytoplasmic fluorescence intensity measured by epifluorescence

microscopy on an arbitrary scale, but this can be converted to international units for inter-laboratory comparison[91].

On human pancreas, ICA provides sensitive detection of a variety of islet autoantibodies, GADA, IA-2A, and ZnT8A, but lacks the specificity of biochemical tests[91]; however, it is still used in clinical practice and in trials such as TrialNet[92]. This sensitivity allows serum to be highly diluted, removing issues of background while preserving low level ICA detection. It also helps overcome some of the difficulties caused by the presence of antinuclear antibodies which can cause false positive results[91].

Factors such as morphologic and antigenic quality of the pancreas, microscope efficiency, and being operator-dependent mean this ICA test suffers from poor inter-laboratory correlation of islet cell antibody levels[91].

This method is also limited by the availability of suitable human pancreas, since non-human pancreas can lead to antigen-binding specificity/reactivity issues when assaying human serum. Pancreas from several sources have been assessed as substitutes, with rat pancreas appearing comparable in one study from 1995[93],while tissue from pigs or cows are ineffective proxies[94]. However there have not been enough comparisons to show the differences non-human pancreata have on sensitivity and specificity. Due to the field moving onto using biochemical markers, this area is unlikely to be properly explored in future. However ICA is still used in National Health Service (NHS) laboratories, which have not pursued these questions, and broader use of biochemical tests at diagnosis are required for disease classification, particularly in adults.

ICA is ill-suited to large-scale screening, as it is very labour-intensive and has no possibility of automation[95]. When used alone, ICA has limited predictive power. The technique has been found to overestimate the number of positives in a population[96], implying a lack of specificity[97]. Now that the specific islet antigens have been identified and characterised, ICA has largely been superseded (at least in research, especially for initial screens) by techniques such as radiobinding assays or enzyme-linked immunosorbent assays[98].

1.5.2 Radiobinding Assay (RBA)

This method of measuring islet autoantibodies was the first to have good sensitivity and specificity without using large volumes of serum[89] – only 4µL to 20µL of serum is required per test. Furthermore, the RBA format can be used to identify different isotypes, depending on the protein Sepharose/agaroses used[99]. ^{35}S radiolabelled GAD, IA-2, or ZnT8, or ^{125}I radiolabelled insulin is usually used to bind the antibodies, before they are immunoprecipitated in this fluid-phase assay.

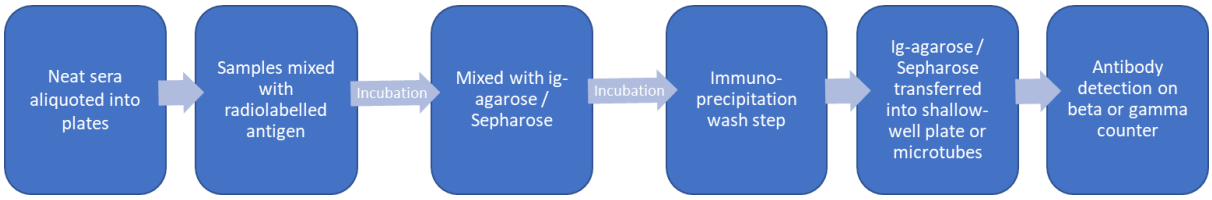

Figure 1-4 Flowchart of a radiobinding assay method. Adapted from Wyatt et al. (2016).

IAA historically required comparatively high serum volumes to allow detection, which limited their use in young children and therefore in population screening. Being a low-volume assay, the development of the RBA microassay for IAA is of particular importance when attempting to screen large populations of children[99,100], and is available via commercial assay kit suppliers such as RSR Limited[101], although there has been concern previously regarding the ability of commercial assays in comparison to in-house tests[102].

An advantage of RBAs using iodinated radiolabelled antigens is their ability to measure affinity[103], as the concentration of labelled antigen is known, and the antigen is minimally modified. Knowing the mass of the total antigen being added (both labelled and unlabelled in the case of competition assays) allows the affinity to be expressed as a reciprocal K_d value. This is of use as high-affinity autoantibodies are associated with greater risk[104].

RBAs are currently used in a variety of studies following children and adults for development of islet autoantibodies and diabetes, including TEDDY, TrialNet, and in Primary Oral Insulin Trial (POInT). The RBA for GADA and IA-2A are the only antibody assays that have been harmonised – there is a standard protocol and common National Institute of Diabetes and Digestive and Kidney Diseases (NIDDK) calibrators. This gives it a unique advantage over other assay formats in multi-centre studies[88].

The necessity for radioisotopes is the main drawback of the RBA. Regulations and licensing surrounding the use of radioactive material limits the number of laboratories able to carry the assay out. In addition, as an immunoprecipitation assay it involves a time-consuming centrifugation or filtration wash step which severely limits how high-throughput the assay can be, and reduces the possibility for automation. The use of radioactive materials also makes the test potentially dangerous to carry out, although this risk is mitigated through strict risk assessments, operating procedures, and personal protective equipment.

1.5.3 Enzyme-Linked Immunosorbent Assay (ELISA)

The indirect ELISA is a common assay for measuring proteins such as antibodies by forming a bridge between an antigen bound to the bottom of a well and an enzyme-linked reagent antibody. The level of antibody is measured through the colour change, which is caused by the addition of the chromogen in the penultimate step. ELISAs are well-established to test for islet autoantibodies[105] and these have been shown to have sensitivity and specificity rivalling the RBA – a single study reported 88% and 98% respectively for GAD_{65}, compared to RBA's 88% and 93%, in sera from the 2002 DASP workshop[106]. In the 2005 DASP workshop, the IA-2A ELISA provided an area under the Receiver Operator Characteristic (ROC) curve equivalent to that of the RBA[107].

Like the RBA, commercially available RSR ELISA kits mean the assay is widely available[101]. The ELISA has been shown to find some RSR RBA positive samples as negative, as the sandwich ELISA only detects high-affinity GAD autoantibodies. There is a lower risk of requiring insulin treatment in low-affinity GADA positive patients than in those with high-affinity GADA[108], so for population screening this specificity is valuable.

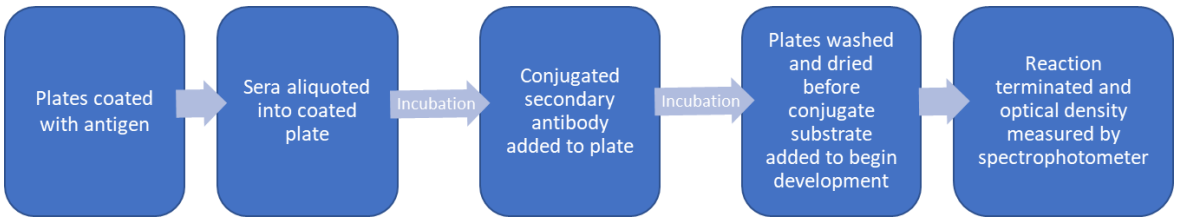

Figure 1-5 Flowchart of an indirect ELISA method. Adapted from Delic-Sarac et al. (2016).

The main limitation of many ELISA methods is their reliance on comparatively high volumes of serum, up to 25µl in replicate[106], significantly reducing usefulness for population screening due to requiring venous blood samples. Some ELISAs, while good at distinguishing

between positive and negative samples, suffer from limited dynamic range. This limits their use in answering questions that rely on the higher end of an assay's detectable range, for example waning vaccine response for SARS-CoV-2, as well as predicting progression of IA-2A positive individuals to T1D, which is greatly affected by titre[39]. Other issues include its difficulty detecting certain antibodies (such as those to insulin[109]), the cost of several of the reagents, and the time-consuming protocol, with many wash and incubation steps. Some of these disadvantages may be circumvented by automation[110], or by measuring multiple autoantibodies in a single assay (multiplexing), which has shown to be comparable to the individual (singleplex) ELISAs, at least for IA-2 and GAD_{65}[111]. A three-screen ELISA was used to screen roughly 100,000 children in the Fr1da study[49]. This multiplex assay excludes IAA, which ELISAs have historically struggled to detect, with only GADA and IA-2A methods submitted to the first IASP[112], although singleplex IAA ELISA do now exist[113] (but are not available from RSR[101]).

1.5.4 Chemiluminescence Immunoassay (CLIA)

CLIA is an umbrella term under which many assay methods fall. Electrochemiluminescence (ECL) assays have been developed to detect islet autoantibodies. The ECL assay is a fluid-phase method which uses biotinylated antigens to capture autoantibodies in serum which form a bridge to Sulfo-TAG conjugated antigens[114].

The Sulfo-TAG emits light when stimulated by an electric current pulsed through the plate. The method varies quite significantly depending on the antibody being detected, for example serum requires acid treatment in order to detect insulin autoantibodies, which could limit its potential in population screening, although a multiplex assay combining seven different autoantibody tests has been validated[115].

The ECL method provides a sensitive assay which may discriminate between low-affinity, low-risk autoantibodies and high-affinity, high-risk autoantibodies. Using samples from TrialNet, the ECL assay for GADA and IAA showed greater specificity than the RBA by

removing the low-affinity signals[116]. Furthermore, the ECL is theoretically able to detect all immunoglobulin classes, instead of just IgG, which the RBA and ELISA tend to rely on[117].

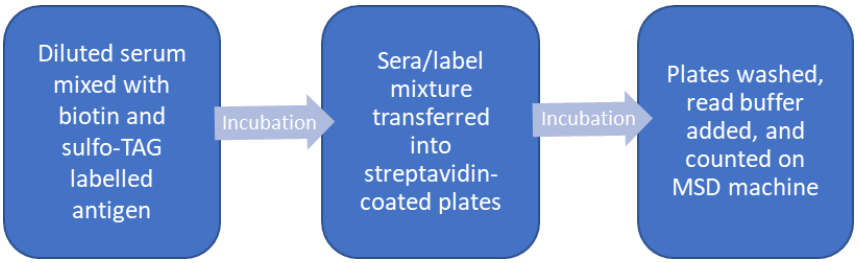

Figure 1-6 Flowchart of an ECL method. Adapted from Yu (2016). In-house preparation of biotin and sulfo-TAG labelled antigen not shown.

Limitations of the ECL are the comparatively high serum requirement, often up to 15µL per sample, and the expensive proprietary reagents and equipment[114]. For the Meso Scale Discovery Company (MSD)-IAA ECL assay, normal serum was found to inhibit the binding of IAA, both the radiolabelled mouse monoclonal and the human antibodies in the sample, so an acid-treatment step was introduced, adding to the complexity of the assay and making it less receptive to automation[104]. In addition, the method for islet autoantibodies has not easily been reproduced in other experienced laboratories (personal communication with Anna Long).

The electrochemiluminescence immunoassay analyzer (ECLIA) is a similar assay format to the ELISA. Antigen is used to coat plates, then sera is added, and then a polyclonal secondary antibody labelled with a proprietary Sulfo-TAG. The signal comes in the form of chemiluminescence, created after addition of the substrate for this Sulfo-TAG, when the plate is inserted into the reader and the substrate is converted via electric pulse[118].

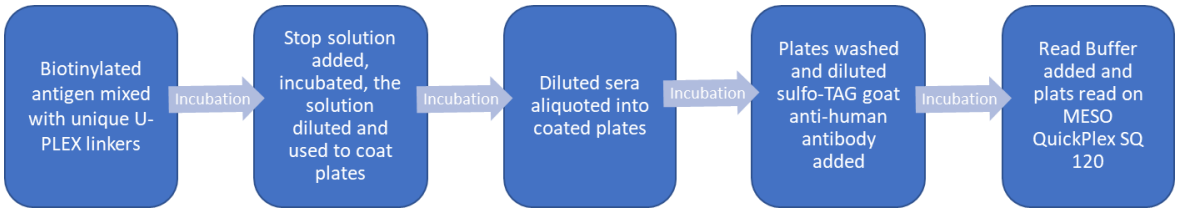

Figure 1-7 Flowchart of an ECLIA method. Adapted from Bolton et al. (2020).

1.5.5 Chemiluminescent Microparticle Immunoassay (CMIA)

Some chemiluminescence assays utilise microparticles. There are multiple different ways this can be done. For example, some CMIAs involve incubating up to 25µl serum or plasma with paramagnetic microparticles coated with antigen – RBD, in the case of the Abbott SARS-CoV-2 IgG II Quant[119]. When diluted, antibody-antigen complexes form which, after a wash cycle, are incubated with a conjugated secondary anti-human IgG antibody. Following an incubation and a second wash cycle, a chemiluminescent reaction is produced by addition of a substrate, which can be interpreted and output as relative light units by a reader such as an Alinity i[120].

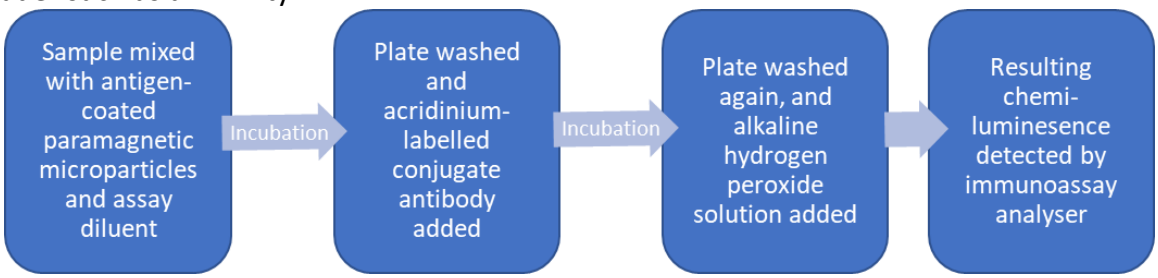

Figure 1-8 Flowchart of method for AdviseDX SARS-CoV-2 IgG II semi-quantitative CMIA. Adapted from Maine et al. (2022).

A similar assay, the Roche anti-spike antibody assay (Elecsys Anti-SARS-CoV-2 S), uses an Elecsys Cobra e801 to detect total antibodies targeting the spike protein of SARS-CoV-2. This test (described as an ECLIA) uses biotinylated RBD, as well as RBD labelled with a ruthenium complex. These reagents are incubated with 12µl of serum or plasma[119], before being incubated with streptavidin-coated microparticles, which bind the biotinylated RBD. This sandwich complex can then be captured to an electrode via magnetism[121].

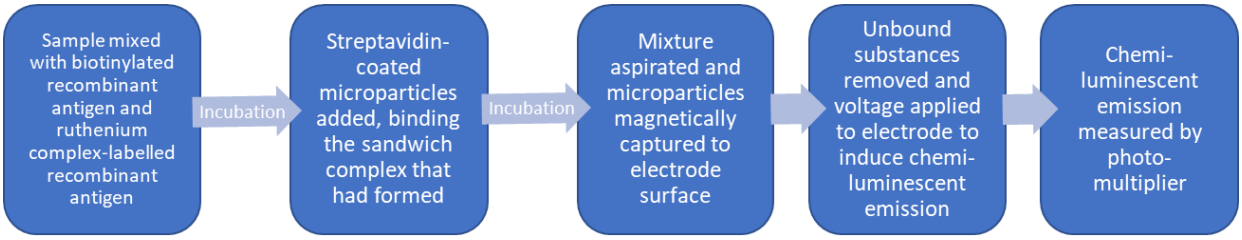

Figure 1-9 Flowchart of method for the Roche Elecysys Anti-SARS-CoV-2 CLIA/CMIA assays. Adapted from Public Health England (2021).

While CMIA methods are capable of good sensitivity and specificity[120-122], one study found limited ability to predict protection from COVID-19, potentially partly due to interference from anticoagulants in the sample tubes[123]. Many of these assays are able to be automated, providing greater throughput[122], but still tend to be more costly than alternative formats,

due to being commercially produced and involving a lot of reagents – antigen and antibody conjugates and microparticles, etc.

1.5.6 Antibody Detection by Agglutination-PCR (ADAP)

ADAP is a solution-phase method created to detect antibodies for non-linear or conformational epitopes like IAA. The assay uses synthetic antigen-DNA conjugates which are agglutinated when the antibodies bind them. Using just 2-4µL of serum[124,125] (although this is increased slightly to 6-10µl in some automated methods[125]) and standard Polymerase Chain Reaction (PCR) protocols, ADAP has a much greater sensitivity to anti-thyroglobulin autoantibodies (TGA) than the RBA or ECL[124]. ADAP detects all antibody isotypes and showed promising performance in the IASP 2018 workshop, with average clinical sensitivity of 96% and specificity of 97%[126,127]. An automated ADAP method has also been published for antibodies to SARS-CoV-2[125].

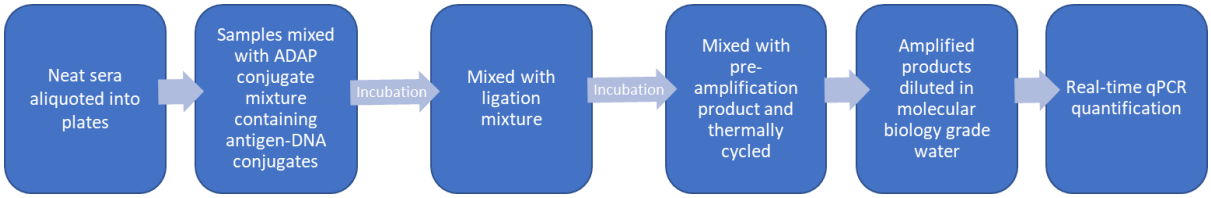

Figure 1-10 Flowchart of an ADAP method. Adapted from Karp et al. (2020).

ADAP is a new method, first published in 2016[124], with only one laboratory submitting it to the 2018 IASP workshop[126], and mixed concordance in a recent comparison with a commercial RBA[128]. Until it is more widely adopted, its true false positive rate remains to be elucidated, but planned future work includes using the test on at-risk individuals followed from birth[128]. Current publications describe the ΔC_T (difference in cycle threshold between samples and blank controls) as proportional to the initial amplicon concentrations, which itself is proportional to the level of the specific antibody in the sample.

Indeed an ADAP multiplex approach appears suitable for large scale screening; an automated triplex method is currently in use for T1Detect – a nationwide screening programme[129]. However, this method excludes ZnT8A, a critical marker of rapid progression to T1D[38], for reasons unclear. Furthermore, ADAP is a commercial assay, produced by US-based company Enable Biosciences, and while these have generally been shown to perform comparably to in-house assays[130], they are often costed higher due to being for-profit rather than provided at-cost as an in-house assay might be.

1.5.7 Luciferase Immunoprecipitation System (LIPS)

First published in 2002[131], LIPS has shown to be comparable to the RBA[131], and methods have been published for several islet autoantibodies[132-134] as well as antibodies to SARS-CoV-2[82]. LIPS is similar to the RBA method, but measures the bioluminescence emitted by the labelled antigen, e.g. IA-2ic antigen fused with the luciferase enzyme, either expressed *in vitro* via transcription translation systems, or in a plasmid transfected into mammalian cells[131], which allows post-translational modifications, such as in insulin and thyroid peroxidase. IASP has shown the smaller and more active Nanoluciferase enzyme (NLuc), derived from deep-sea shrimp *Oplophorus gracilirostris*[135], to perform better than a Renilla luciferase reporter, at least when assaying for autoantibodies to truncated GAD (amino acids 96-585). IASP 2018 also described the LIPS GADA assay as "high-performance"[126].

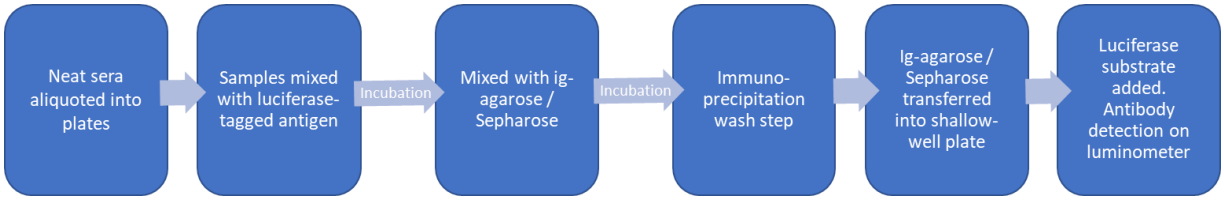

Figure 1-11 Flowchart of a LIPS method. Adapted from Liberati et al. (2018).

As well as eliminating the need for radioisotopes, LIPS' other advantage over its RBA predecessor is a slightly reduced serum volume. RBAs are relatively low volume assays, tending to peak at 20µl for a competition assay detecting antibodies to insulin[100], however the equivalent LIPS assay requires just 4µl serum[134]. While the quantified luciferase-tagged antigens allow LIPS assays to differentiate between high and low affinity antibodies, this is calculated by a proxy and cannot express the affinity in the usual way (K_D).

1.5.8 Surrogate Virus Neutralization Test (sVNT)

Virus neutralization tests (VNTs) are a gold standard in serological testing of antibodies to infectious disease. They are used on the principle that binding antibodies, such as those detected by the majority of methods described here, do not always equate to neutralising antibodies – a far more useful metric when considering humoral protection. However, these assays traditionally required live virus and high safety categorised laboratories. By purifying antigen from the virus, the need for live virus and biosafety level 3 containment is removed, allowing the tests to be performed in many more laboratories than these conventional VNTs (cVNTs) would be[136].

SD Biosensor and GenScript (cPASS™) both offer sVNTs for SARS-CoV-2, based on blocking the virus' RBD and its interactions with the host's ACE2 receptor in an antibody-mediated way. In each of these assays, horseradish peroxidase (HRP)-labelled RBD is incubated with diluted serum, before being added to plates coated with ACE2 protein. When the plate is read, a chromogenic substrate 3,3',5,5'-tetramethylbenzidine (TMB) is added, reacting with HRP to produce a detectable signal[119,136].

These assays are able to identify all isotypes of antibody to SARS-CoV-2's RBD protein, but require a high serum volume – up to 60µl in the case of SD Biosensor's STANDARD E SARS-CoV-2 nAb assay[119].

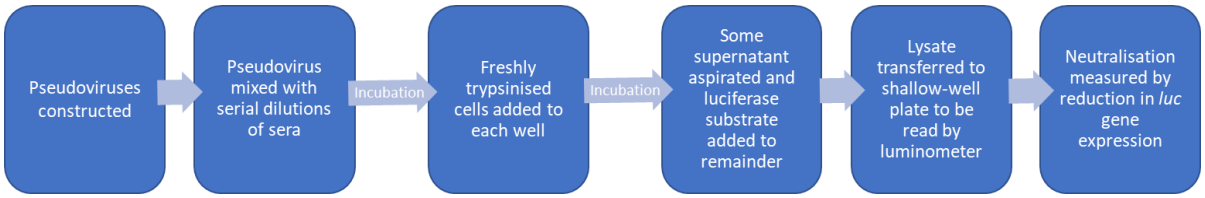

Figure 1-12 Flowchart of an sVNT method. Adapted from Nie et al. (2020).

1.5.9 Cell-free PCR assay (cfPCR)

While the sVNT does circumvent many of the concerns traditional virus plaque reduction neutralization tests engender, they are still reliant on time-consuming and costly cell-based methodologies. The cell-free PCR assay was therefore designed to detect neutralising anti-viral antibodies without the use of cells. Based on existing ADAP technology, the assay principle is incubating low volume of sera first with antigen-deoxyribonucleic acid (DNA) conjugates and then this mixture with receptor-DNA conjugates. If neutralising antibodies are present, these will bind the antigen-DNA conjugates, thus decreasing the antigen's ability to bind the receptor-DNA conjugates when that mixture is added. This competition is quantified via the addition of a ligation mixture, and the resulting solution undergoes standard PCR procedures. Readout is given as ΔC_T with a high signal (more amplifiable DNA) indicating limited binding between antigen and receptor (spike protein and ACE2 receptor, in the case of SARS-CoV-2)[137].

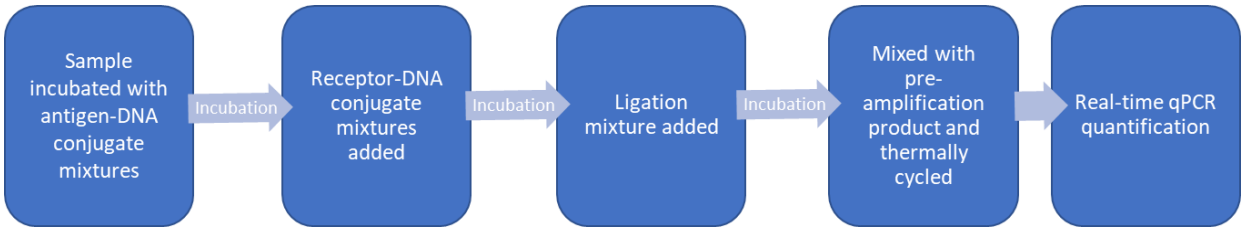

Figure 1-13 Flowchart of a cell-free PCR assay method. Adapted from Danh et al. (2020).

Despite being liquid phase, this assay does not require washing or centrifugation, allowing to be automated in a style similar to the ADAP method previously described. Even manually, the test takes very little time, just 140 minutes, meaning it could have use in urgent clinical settings. This test has so far only been tested on a small number of samples[137], and more work needs to be done to ensure its sensitivity and specificity.

Another limitation of the method is its necessity for good understanding of the cellular receptor to the antigen, as well as the antigen and antibodies themselves. While other methods are able to detect antibodies as soon as the antigen is elucidated, this method also requires research into how the pathogen attaches to host cells, potentially restricting its use in totally novel or under-researched diseases. Furthermore, it would not be a suitable test in situations where the antibody's target is intracellular, as is the case for many of the islet autoantigens[138].

1.6 Novel Bridging Assay Method

While some of these existing assay methods seem promising, there emerges no clear solution for achieving the throughput required for large-scale screening while maintain good sensitivity and specificity, in addition to acceptability through low-burden sample collection and low cost sample collection. This thesis describes a novel assay method that aims to meet these criteria.

The general principle of the bridging assay format is the antibody, if present in the sample, forms a bridge between plate-bound antigen and luciferase-tagged free antigen. Specific antigen detection is enabled by trapping the luciferase tag to the solid-phase, whereas if no complementary antibody is present, the free tagged antigen is removed in the wash step. This method is described in figure 1-14.

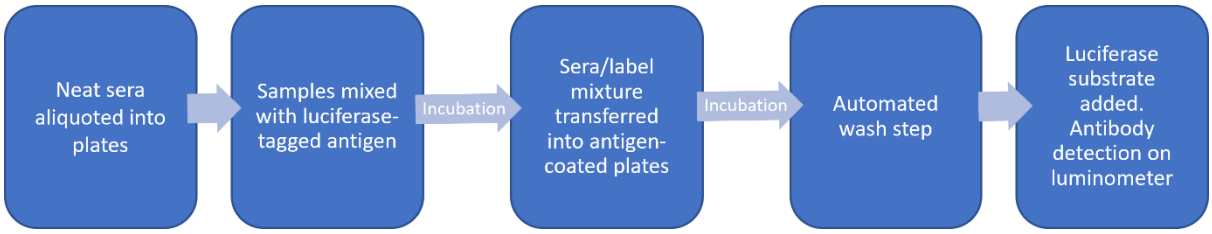

Figure 1-14 Flowchart of bridging assay method

The dual-binding bridging concept is also illustrated in a schematic, figure 1-15.

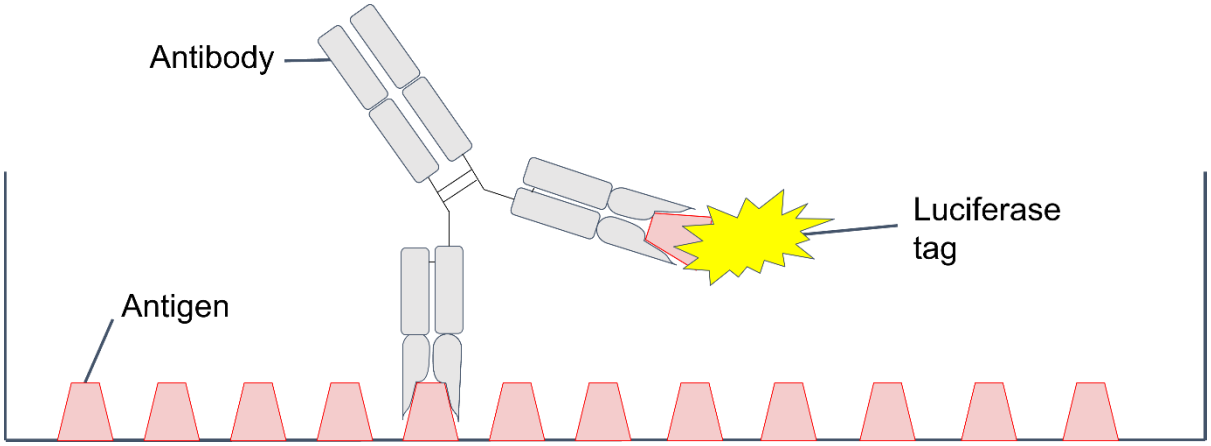

Figure 1-15 Bridging assay schematic.

1.7 Hypothesis

Plate-based, non-radioactive, low serum volume, luciferase-based antibody assays can be sensitive, specific, and high-throughput enough to be considered for large-scale testing.

1.8 Aims

1) To optimise a plate-based bridging assay for all isotypes of autoantibody to IA-2, set a threshold, and compare to the established radiobinding assay.
2) To optimise a plate-based bridging assay for all isotypes of antibody targeting the SARS-CoV-2 spike protein, set a threshold, and compare to the established Roche antibody assay.

2 Materials and Methods

Details and recipes of all buffers used in protein expression and antibody assays are in Appendix 5.1. Suppliers of materials/equipment and reagents are described in tables 2.1 and 2.2 respectively.

Material	Supplier
30ml universal tubes	GBO
Äkta Prime Plus with PrimeView software.	Cytiva
Balance	Sartorius
Category II Biological Safety Cabinets	Esco Lifesciences/Biopharma Group/ThermoFisher
Centrifuge	Thermo Scientific
Centro 963 Microplate Luminometer	Berthold
ChemiDoc Universal Hood III imager with Image Lab software.	Bio-Rad
Conical centrifuge tubes (15ml and 50ml)	Greiner Bio One Ltd
Curvettes	Fisher
Deep Well Plates	Sarstedt
ELx405 plate washer	BioTek
Gel Electrophoresis Tank/Kit	Bio-Rad
Glutathione-coated plates	Thermo Scientific
Hidex Sense Beta Luminometer	Lab Logic
High speed centrifuge	Sigma
High-Binding Optiplate	Perkin Elmer
Illustra NAP-5 Columns	SLS
Incubated Shaker	New Brunswick Scientific
Master Mix	Promega
Microfuge	Sigma
Microplate	GBO
Miscellaneous Glassware	Pyrex/Schott Duran
MTS 2/4 digital microtiter shaker	IKA
Parafilm	Fisher
PD-10 Desalting Column	Amersham Biosciences
Petri Dish	VWR
Pipette Tips (10/200/1000µl)	Alpha Labs
Pipettes (p3, p10, p20, p100, p200, p1000, p100 multichannel)	Sartorius
Powerpette Plus Pipette Controller	VWR
Serological Pipettes	FisherBrand/Falcon
SevenCompact pH Probe	Mettler Toledo
Stirrer	Bibby Scientific
Streptavidin-coated plates	Thermo Scientific
TopSeal lids	Perkin Elmer
Ultrasonic Probe Sonicator	MSE

UV-1601 Spectrophotometer	Shimadzu
Vortex	Scientific Industries
Water bath	Grant

Table 2-1 Materials/Equipment

Reagent	**Supplier**
1% Casein in PBS	Thermo Scientific
Acrylamide	PanReac AppliChem
Agar	Melford
Ammonium Persulfate	Fisher Scientific
Ampicillin	Sigma
Anhydrous Na_2CO_3	BHD
Anhydrous $NaHCO_3$	Sigma-Aldritch
Bromophenol Blue	Phi Bio
BSA	Sigma
Chloramphenicol	Sigma
cOmplete™ ULTRA Tablets, Mini, EDTA-free, EASYpack Protease Inhibitor Cocktail tablets	Roche
Desiccant	Clariant
DL-Dithiothreitol (DTT)	Sigma-Aldritch
Ethanolamine-blocked Protein G Sepharose (EB-PGS)	GE Healthcare Life Sciences
ethylenediaminetetraacetic acid (EDTA)	Melford
EZ-Link™ Sulfo-NHS-LC Biotinylation Kit	Thermo Scientific
Glacial acetic acid	Merck
Glycerol	BDH
Glycine	Melford
Glycine-blocked Protein A Sepharose fast flow (GB-PAS)	GE Healthcare Life Sciences
GSTrap FF 5ml column	GE Healthcare
GST-tagged PTP-IA-2	Expressed in-house
HCl (Hydrochloric Acid) 5M	Fisher chemical
Isopropyl β-D-1-thiogalactopyranoside (IPTG)	Melford
Kanamycin	Sigma
Methanol	Fisher Scientific
NaCl (Sodium Chloride)	Fisher Scientific
NanoGlo® Luciferase Assay System	Promega
NLuc IA-2	Dr. Vito Lampasona
NLuc RBD	Dr. Vito Lampasona
PBS Tablet	Gibco
pET49b plasmid PTP	Dr. Karen Elvers
pGEX-6P plasmid IA-2ic	Dr. Michael Christie
PhastGel Blue R stain	Sigma Aldritch
Plasmid Midi Kit	QIAGEN®
Precision Plus Protein™ All Blue Prestained Protein Standards Ladder	Bio-Rad
Qubit® Protein Assay Kit.	Thermo Fisher Scientific

RBD antigen	Dr. Kapil Gupta
Reduced Glutathione	Duchefa Biochemie
Rosetta (DE3)pLysS competent cells	Sigma
Sodium Dodecyl Sulphate (SDS)	BDH
Spike antigen	Dr. Kapil Gupta
Tetramethylethylenediamine (TEMED)	Melford
TRIS, [Tris(hydroxymethyl) aminomethane]	Melford
Tryptone	Melford
Tween 20	Sigma
Ultra-pure DNA free water	Thermo Fisher Scientific
Yeast extract	Melford
Zebra spin desalting column	Thermo Fisher

Table 2-2 Reagents

2.1 Samples

Briefly, SARS-CoV-2 positive serum samples were available as follows with grateful thanks to Bristol Biobank, the DISCOVER study and Professor Ash Toye. Pre-pandemic samples (collected no later than November 2019) were available from the Avon Longitudinal Study of Parents and Children (ALSPAC), Professor Ash Toye, the Respiratory team, and the Diabetes team at the University of Bristol. IA-2A positive and negative samples were available from the Bart's-Oxford Region (BOX) Family Study, an observational study recruiting people diagnosed with type 1 diabetes in the former Oxford health authority region, as well as their first-degree relatives, since 1985. Samples were selected for optimisation, threshold setting, and validation (see table 2.3). For the SARS-CoV-2 validation, samples from individuals who had a confirmed or suspected COVID-19 infection were further subdivided into acute (<3 weeks since symptom onset, n=47), early convalescent (3-12 weeks since symptom onset, n=105) and late convalescent (>12 weeks since symptom onset, n=70) infection.

Cohort	Collected Via	Total (n)	Positive (n)	Negative (n)	T1D (n)	Sex (n M/F)	Age at sample (median (range))	Time since T1D diagnosis (median (range))
Optimisation	BOX Family Study	35*	13	12	14	21/11	36.0 (4.5-57.6) years	-4.7 (-32.6-5.8) years
Threshold Setting / ROC curve Controls	Schoolchildren as described in Bingley et al. (1993) Diabetes Care	265	Estimated to be 6-7 (2.5%)	Estimated to be 258-259 (97.5%)	0	149/116	10.9 (9.1-13.3) years	n/a
Threshold Setting / ROC curve Patients	BOX Family Study	135	111	24	135	76/60	10.4 (1.3-21.8) years	0.0 (-0.7-2.0) months
RBA Comparison	IASP 2020 Workshop	150	50+	90+	38+	No data	No data	No data

*Table 2-3 Details of the samples used in the IA-2A Bridging Assay. Positivity status defined by IA-2ic RBA. *incomplete data on one or more samples.*

Cohort	Collected Via	Total (n)	Positive (n)	Negative (n)	Sex (n M/F)	Age at sample (median (range))	Days since symptom onset or positive PCR test (median (range))
Optimisation (total n = 396*)	CMM BioBank	60*	35 + 10 suspected *	14*	17/41*	38.6 (0.2-60.9) years*	35 (10-73) days*
	Convalescent samples provided by Professor Ash Toye	161	161	0	No data	No data	No data
	Blood Donors from 1998	120*	0	120	64/54	39.9 (19.8-62.6 years	n/a
	Local Collection	21	No data	No data	No data	No data	No data
	NEQAS	4	4 suspected	0	2/2	65 (45-75) years	27.5 (14-30) days
	Commercial Negative Sera	1	0	1	No data	No data	n/a
	NBS Plasma provided by Professor Ash Toye	27	0	27	No data	No data	n/a
Controls for ROC curve (total n = 402)	ALPSAC	148	0	148	14/32*	(7-65) years*	n/a
	CMM BioBank	1	0	1	0/1	5 years	n/a
	NBS Plasma provided by Professor Ash Toye	27	0	27	No data	No data	n/a
	Blood Donors from 1998	226	0	226	121/105	41.7 (19.0-67.5) years	n/a
Patients for ROC curve	CMM BioBank	32	32	0	10/22	33.4 (18.1-57.4 years)	39.5 (10-100) days
	DISCOVER	14*	13	0	No data	61 (39-80) years	11 (4-104) days
Roche Comparison	Various	182	176	6	79/103	52.0 (19-86)	8.6 (0.7-18.3) weeks
Validation	Various, described in Halliday et al. (2022) JCI.	807	222	585	No data	No data	No data

*Table 2-4 Details of the samples used in the Spike-RBD Bridging Assay. Positivity status was defined by positive PCR test unless otherwise stated. *incomplete data on one or more samples*

2.1.1 Standard Curves and Quality Control Samples

The IA-2A Bridging assay used the seven NIDDK calibrators (internally referred to as DK standards) to quantify antibodies into common NIDDK Units/ml. An example of the standard curve from an assay performed with the final IA-2A bridging method (described in 2.4) is below.

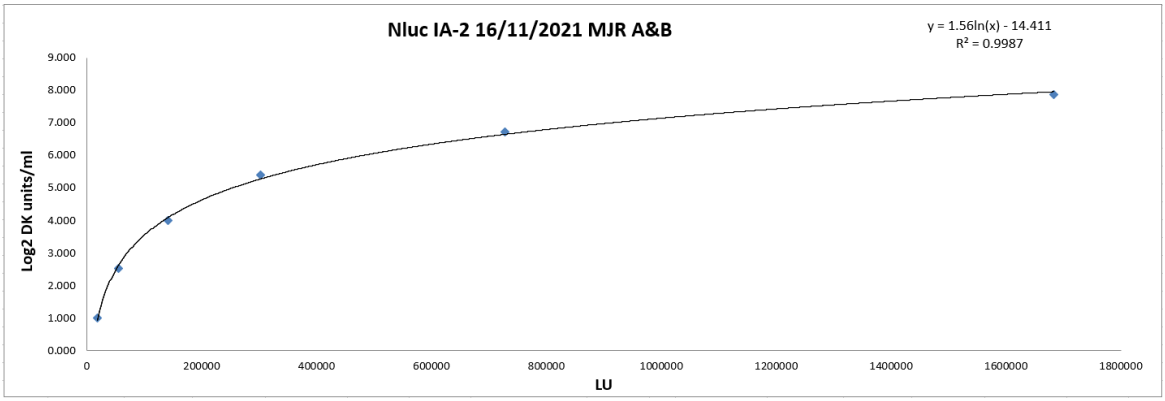

Figure 2-1 Standard Curve for the IA-2A bridging assay.

For the SARS-CoV-2 Spike-RBD Bridging assay, an eight-point in-house standard curve was generated by serially diluting a pool of high positive samples. Once this curve was established, it and its standard negative diluent were run on every plate, or split across a set of two plates, and used to calculate arbitrary local units. Figure 2-2 shows an example of the standard curve from the fully-optimised version of the Spike-RBD bridging assay.

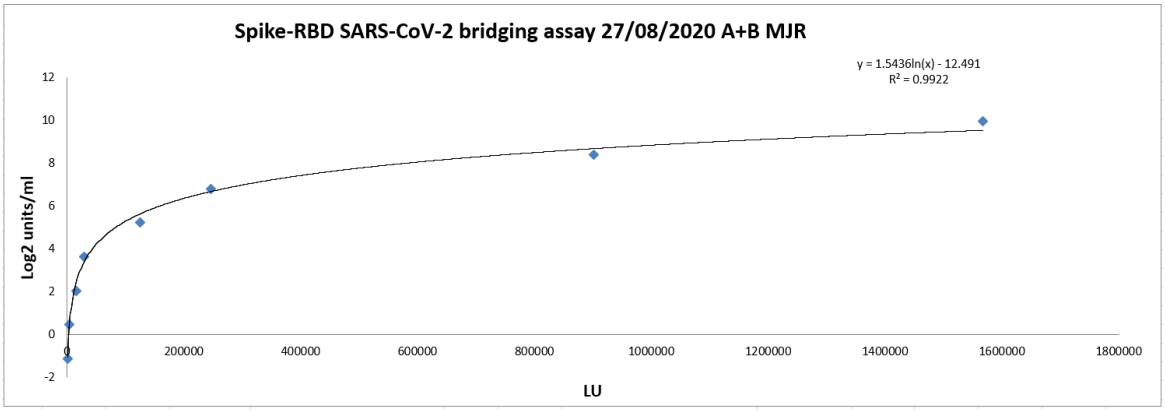

Figure 2-2 Standard Curve for the Spike-RBD bridging assay.

We also received a standard from the NIBSC which we similarly diluted and tested to try to give comparative units between our local units and the more standardised units that curve produced (data not shown).

Internal positive quality control (QC) sera were obtained (and some diluted) from a variety of the sources described above. Negative QC sera and diluent for the other QCs were

purchased commercially. At least two replicates each of a high positive, medium positive, low positive, and negative QC were on every plate of both bridging assays.

2.1.2 Serum vs Plasma

The NIBSC standard, as well as several known negative samples used throughout optimisation, were plasma samples rather than serum. These have been shown to be interchangeable in many antibody assays, for example those for detecting antibodies to mycobacterial antigens[139], and we tested matched plasma-sera samples and found very comparable results for islet autoantibodies (unpublished data).

2.2 Buffers

The primary assay buffer used in both bridging assays developed as part of this project is Tris(hydroxymethyl)aminomethane (Tris)-Buffered Saline + 0.5% Tween, referred to as Denver LIPS. Unlabelled antigen was diluted in Phosphate-Buffered Saline (PBS). A full table of buffers and their recipes can be found in Appendix 5.1.

2.3 IA-2 Expression

2.3.1 GST-PTP-IA-2 Expression

The pET49b plasmid containing genes to express the PTP region (aa687-979) of IA-2, with a Glutathione S-Transferase (GST) tag, was developed and transformed into *Escherichia coli* Rosetta (DE3)pLysS competent cells by Dr. Karen Elvers. These *E. coli* cells were stored as a 15% glycerol stock at -80°C, before being used to inoculate a 50ml lysogeny broth (LB) containing 34µ/ml chloramphenicol and 15µg/ml kanamycin. This broth was incubated at 37°C at 225rpm for 16 hours. A 1ml blank for absorbance was collected from a 1L stock of LB broth. The 50ml starter culture was used to inoculate 1L LB, containing the same concentrations of chloramphenicol and kanamycin, to an optical density (OD) at 600nm of 0.1. This was incubated at 37°C at 225rpm until the OD600nm reached ~0.8 (about 4 hours). At this point, protein expression was induced by addition of 1ml Isopropyl β-D-1-

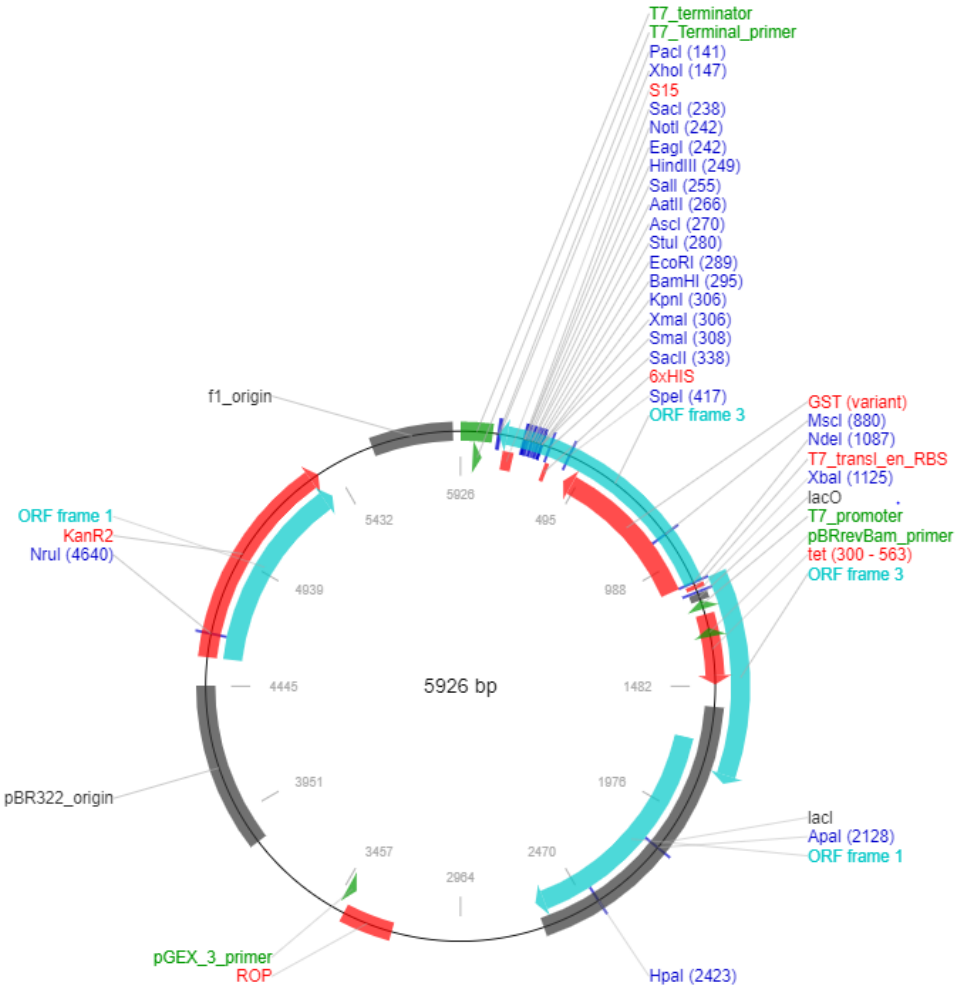

Figure 1-2-3 pET-49b(+) plasmid map. Generated by Addgene's vector database.

thiogalactopyranoside (IPTG) (1M stock). The culture was incubated for a further 4 hours with another 1ml addition of 1M IPTG after 2 hours. At baseline and every hour, 1ml samples of LB were taken for cell pellets and OD600nm measurement. Cell pellets were obtained by centrifugation at 13000 rpm for 1 minute and stored at -20°C for analysis of expression by sodium dodecyl sulfate-polyacrylamide gel electrophoresis (SDS-PAGE). After 4 hours the cultures were centrifuged at 8000rpm for 20 minutes at 4°C and the cell pellet resuspended in 15ml 15% glycerol and frozen prior to sonication.

2.3.2 IA-2ic Transformation

The pGEX-6P vector containing genes to express the 604-979aa region of IA-2 was kindly provided by Dr. Mike Christie, University of Lincoln, at a concentration of 35ng/µl. BL21 competent *E. Coli* cells were thawed on ice. The plasmid (2µl) and competent cells (30µl) were gently mixed together and incubated on ice for 20-30 minutes. This mixture was heat shocked by placing the bottom two thirds of the tube into a 42°C water bath for 45 seconds. The tube was put on ice for 2 minutes. The tube had 500µl LB broth (without antibiotics) added then was incubated for 45 minutes at 37°C at 225rpm. A small amount was taken using a flamed loop and streaked out to single colonies on an agar plate containing 100µg/ml ampicillin.

2.3.3 IA-2ic Expression

A 50ml starter culture of LB broth with 100µg/ml ampicillin was inoculated with a colony picked from the agar plate via a flamed loop and incubated for 16 hours at 37°C at 225rpm. A 1ml blank for absorbance was collected from the 1L LB broth. The starter culture was used to inoculate 1L LB with the same concentration of ampicillin, to an OD600nm of 0.1. This was incubated and expression induced using the same method described above for PTP-IA-2.

2.3.4 Sonication

Once thawed, the cell pellet from protein expression was resuspended in 1x SDS-PAGE running buffer and sonicated in an ultrasonic probe sonicator. After centrifugation for 1 minute at 13000rpm, the supernatant was taken off again, now containing the protein. An SDS-PAGE gel compared the supernatant from the sonicated cell pellet to the resuspended

whole cell to confirm the fusion protein was not present in the cell pellet. The cell pellet was disposed of and the supernatant was stored at -20°C or below until purification.

2.3.5 SDS-PAGE Gel Electrophoresis

Samples (35µl) were each mixed with 15µl loading dye. Gels were a 12% polyacrylamide gel mix (12% separating gel, 6% stacking gel), full recipes are in appendix 5.1. A Precision Plus Protein™ All Blue Prestained Protein Standards Ladder (7µl) was loaded into the first well. The sample and dye mixtures were loaded, 40µl in each remaining well. The gel was placed in a tank of 1x SDS-PAGE running buffer with a current run through it at 120V for 100 minutes. The gel was then transferred to PhastGel Blue R stain for 1 hour before this stain was replaced with destain solution. The gel was incubated on a shaker at room temperature and the destain solution refreshed every hour, before being left on the shaker overnight to fully destain. The gel was imaged the next morning on a Bio-Rad ChemiDoc Universal Hood III imager with Image Lab software.

2.3.6 Fast Protein Liquid Chromatography (FPLC)

FPLC was performed using an ÄKTA Prime Plus FPLC system with PrimeView software. The supernatant (sonicated cell pellet from protein expression) had 200µl ethylenediaminetetraacetic acid (EDTA) added while it defrosted. Binding buffer A (2.5ml) was used to dissolve two cOmplete™ ULTRA Tablets, Mini, EDTA-free, EASYpack Protease Inhibitor Cocktail tablets, and was then added to the supernatant. The system and GSTTrap FF 5ml column were primed with binding buffer A then the protein was loaded onto the column. Binding buffer A was loaded to push the remaining sample through the dead tubing. After this, High salt wash buffer B was loaded, before the column was washed again with binding buffer A to remove the high salt content. The column was removed from the system and the system was washed/primed with binding buffer A and elution buffer C. The column was reconnected and 1ml fractions were collected. Elution buffer C was loaded to flow through the column and remove the GST-IA-2 fusion protein.

2.3.7 Quantifying Concentrations

The concentration of each of the fusion proteins were quantified in fractions using a Thermo Fisher Scientific Qubit® Protein Assay Kit.

2.3.8 Midiprep

A Midiprep was performed to isolate high-quality plasmid DNA from the *E. coli* glycerol stock for sequencing. A sterilised loop was used to streak bacteria from the frozen glycerol stock onto an agar plate containing 100µg/ml ampicillin and this was incubated at 37°C overnight. The next day, a single colony from this plate was picked and used to inoculate 5ml of LB broth containing 100µg/ml ampicillin. This starter culture was incubated at 37°C and shaken at 225rpm for 4 hours, before being added to a larger volume of the same broth and incubated in the same conditions for 18 hours. This culture was then lysed and the plasmid amplified using a QIAGEN® Plasmid Midi Kit.

2.3.9 Sequencing

Sequencing and pGEX 5 prime and 3 prime primer synthesis was provided by the TubeSeq service from Eurofins Genomics. The sequencing worked well, and the full results can be found in appendix 5.2.

2.3.10 Biotinylating IA-2

PTP-IA-2 was diluted in PBS to 1mg/ml in a total volume of 10ml. The biotin reagent was equilibrated to room temperature. Biotin (2.2mg) was dissolved in 500µL ultra-pure / DNA free H_2O. This biotin solution (30.1µl) was transferred into a 15ml centrifuge tube with 1 ml of the 1 mg/ml IA-2. This mixture was vortexed and incubated at 23°C for 1 hour. The bottom of a Zebra spin desalting column was twisted off and the column placed in a collection tube. The column was centrifuged at 1000*g for 2 minutes to remove the storage solution. PBS was added to the column, and it was centrifuged again at 1000*g for 2 minutes, then this step was repeated twice more. The column was placed in a new collection tube, and the sample slowly applied to the centre of the compact resin bed. This was centrifuged at 1000*g for 2 minutes to collect the sample, and the column discarded after use.

2.4 IA-2A Bridging Assay Methods

The standard PTP-IA-2-GST bridging assay method is described below.

PTP-IA-2-GST antigen diluted to 400ng/40µl was pipetted into every well of a 96-well high-binding OptiPlate™ (Perkin-Elmer, Waltham, MA, USA) and incubated for 18hrs at 4°C. The

plate was washed 4 times in 20mM Tris 150mM NaCl pH 7.4 with 0.5% v/v Tween-20 (Denver LIPS) and blocked with 1% Casein in PBS (Thermo Scientific, Waltham, MA, USA). The plate was left to air-dry for 2-3hrs before being stored with a sachet of desiccant in a sealed plastic bag at 4°C.

The NLuc-IA-2 antigen was diluted in Denver LIPS to a concentration of $1x10^7$ LU ±5% per 25µl. Sera (1µl, 2 replicates) were pipetted into a 96-well plate and incubated with 25µl diluted NLuc antigen for 2hrs at room temperature. This mixture was transferred into the coated OptiPlate and incubated shaking (~700rpm) for 1.5hrs at room temperature. The plate was washed 8 times with Denver LIPS, excess buffer was removed by aspiration, then 40µl of a 1:2 dilution of the standard 1:50 Nano-Glo® substrate (Promega) and 20mM Tris 150mM NaCl pH 7.4 with 0.15% v/v Tween-20 (Denver) was injected into each well before counting in a Berthold Centro 963 Microplate Luminometer (Germany).

Development of this assay began in 2019 as part of my undergraduate research project. A table of previously optimised conditions in table 2-3.

Condition	**Outcome**
Coated protein concentration	400ng/well
Coated protein diluent	PBS
Incubation method	"Indirect" (incubating serum with label, then transferring the mixture to the coated optiplate)
EDTA in the label buffer	Label diluted in Denver LIPS + 5% EDTA
Plate viability	Can be stored at least up to 1 month at 4°C in a sealed bag with a sachet of desiccant
Number of washes	8 washes (2x runs of the ELISA wash programme)

Table 2-5 IA-2A bridging assay conditions optimised as part of my 2019 undergraduate research project for the school of Cellular and Molecular Medicine.

These conditions also formed the basis of a second version of the assay, using commercial glutathione-coated plates (to bind to the GST tag on the IA-2). A preliminary experiment with this assay format was conducted as part of the undergraduate project, and it was revisited in this MSc project for further

optimisation, along with a third version of the assay using biotinylated IA-2 and neutravidin-coated plates.

The methods for the glutathione-coated plate and biotinylated IA-2 variants of the IA-2A bridging assay are in the appendix, along with tables detailing conditions that had been optimised in other forms of the assay.

2.5 SARS-CoV-2 Spike Antibody Bridging Assay Methods

All LIPS/bridging SARS-CoV-2 assays used NLuc RBD label amino acids 319-541. A bridging experiment also investigated aa319-655 and found comparable results (data not shown).

2.5.1 Initial Spike LIPS Assay Method

Initially, development began of a liquid-phase luciferase immunoprecipitation system (LIPS) assay for IgG antibodies to SARS-CoV-2. The NLuc-RBD antigen (kindly provided by Dr Vito Lampasona, Milan) was diluted in 20mM Tris, 150mM NaCl, pH 7.4 with 0.5% v/v Tween-20 (Denver LIPS) and 0.05% casein to a concentration of $3.8x10^6$ – $4.2x10^6$ per 25µl. Sera (1ul, 2 replicates) were pipetted in to a 96-well plate and incubated with 25ul diluted NLuc antigen for 2 hours at RT in a dark area. Immunocomplexes were precipitated using 2.5µl glycine-blocked Protein A Sepharose 4 fast flow (GB-PAS) (GE Healthcare Life Sciences, Chicago, IL, USA) and 2.5µl ethanolamine-blocked Protein G Sepharose (EB-PGS) (GE Healthcare Life Sciences) (washed 4 times in Denver Lips) for 1hr with shaking (~700rpm). Precipitates were washed 5 times with Denver LIPS and then transferred to a 96-well Optiplate™ (Perkin-Elmer, Waltham, MA, USA) and excess buffer removed by aspiration. Diluted Nano-Glo® substrate (40µl, Promega) was injected into each well immediately before counting in a Hidex Sense Beta (Hidex, Turku, Finland).

2.5.2 Optimising Initial LIPS Method

To overcome cross reactive samples, RBD protein was used to outcompete the NLuc-RBD label[82]. A range of RBD antigen molarity was tested with $8x10^{-9}$ mol/L showing good affinity for RBD-specific IgG. The NLuc-RBD antigen was diluted in Denver LIPS + 0.05% casein to a concentration of $3.8x10^6$ – $4.2x10^6$ per 25ul. Sera (1ul, 4 replicates) were pipetted in to a 96 well plate. Samples were incubated with and without competition of RBD binding with

unlabelled RBD protein (kindly provided by Dr. Kapil Gupta) added at a final concentration of $8x10^{-9}$ mol/L. Immunocomplexes were precipitated and measured as outlined above.

This competition IgG assay did solve some of the cross-reactivity (unpublished data), but it also increased the cost of the assay. Another limitation of this LIPS assay is that it only detected IgG antibodies, so LIPS assays had to be concurrently developed to detect IgA and IgM antibodies to SARS-CoV-2. Having three separate assays limited the throughput of an assay system which already struggled with the bottleneck at the immunoprecipitation wash step.

2.5.3 Novel Bridging Assay Method

The Spike-RBD Bridging assay uses the same concept of the NLuc tagged RBD protein but in a plate-based format. Several optimisation conditions had already been shown in similar assays – either the liquid-phase LIPS assay described above or a similar bridging format using RBD-coated plates.

Condition	Assay it was optimised in	Outcome
NLuc RBD freeze-thaw cycles	RBD IgG LIPS	At least 3 freeze-thaw cycles are acceptable
Assay Reagent Dilution	RBD IgG LIPS	The standard 1:50 with a further 1:1 in TBST 0.15% Tween
Label Total Counts	RBD-coated bridging assay	$1x10^7$ LU
Label Incubation Length	RBD-coated bridging assay	2 hours
Blocking Agent	RBD-coated bridging assay	1% Casein in PBS
Serum Volume	RBD-coated bridging assay	1.5µl serum

Table 2-6 SARS-CoV-2 Spike-RBD Bridging assay conditions optimised in other previously or concurrently developed assay formats (data not shown).

Unlabelled spike antigen (Kapil Gupta, UK) diluted to 100ng/40µl was pipetted into every well of a 96-well high-binding OptiPlate™ (Perkin-Elmer, Waltham, MA, USA) and incubated for 18hrs at 4°C. The plate was washed 4 times in 20mM Tris 150mM NaCl pH 7.4 with 0.5% v/v Tween-20 (Denver LIPS) and blocked with 1% Casein in PBS (Thermo Scientific, Waltham,

MA, USA). The plate was left to air-dry for 2-3hrs before being stored with a sachet of desiccant in a sealed plastic bag at 4°C.

The NLuc-RBD antigen was diluted in Denver LIPS to a concentration of $9.5x10^6$-$1.05x10^7$ LU per 25µl. Sera (1.5µl, 2 replicates) were pipetted into a 96-well plate and incubated with 37.5µl diluted antigen for 2hrs at room temperature. Of this mixture, 26µl was transferred into the coated OptiPlate and incubated shaking (~700rpm) for 1.5hrs at 4°C. The plate was washed 8 times with Denver LIPS, excess buffer was removed by aspiration, then 40µl of a 1:1 dilution of the standard 1:50 Nano-Glo® substrate (Promega) in 20mM Tris 150mM NaCl pH 7.4 with 0.15% v/v Tween-20 (Denver buffer) was injected into each well before counting in a Hidex Sense Beta Luminometer (Turku, Finland).

2.6 Statistical Analysis

Raw LU are output by a luminometer. Signal-to-noise ratio (SNR) was calculated by dividing a sample's mean LU with the mean LU of the negative standard on that plate. The data have not been transformed, and the SNR were analysed using appropriate statistical tests, notably the Wilcoxon signed-rank test and the Freidman test. P values of less than 0.05 were considered statistically significant. Data analysis and graphing were performed using Graphpad Prism 8 statistical software and included scatter dot plots, Receiver Operator Characteristic (ROC) analysis, calculating the area under the ROC curve (AUC), and correlation.

3 Results

3.1 IA-2 Expression and Purification

Expression of PTP-IA-2 was performed as per the method described in 2.3.1. An expression gel is below, showing that the GST-tagged PTP-IA-2 fusion protein, ~66kDa, was present in the supernatant (S) and not in the cell pellet (CP), and increased in yield as expression progressed over the four-hour period (T = hours since first addition of IPTG).

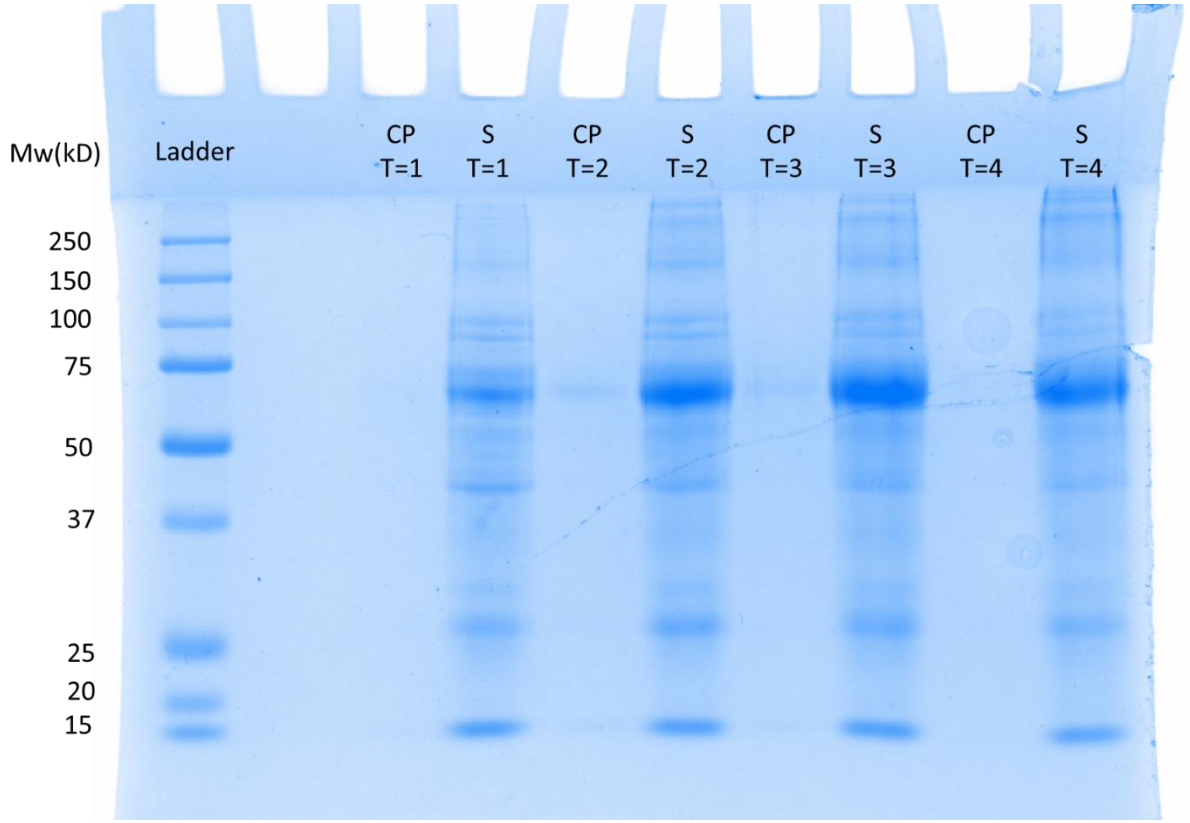

Figure 3-1 SDS-PAGE Gel showing expression of PTP-IA-2. Supernatant (S) and resuspended cell pellet (CP) sampled every hour (T) since the first addition of IPTG. Ladder was the Precision Plus Protein™ All Blue Prestained protein standards.

After expression, the protein was purified by FPLC and collected in 1ml fractions of varying concentrations. This process was repeated with the IA-2ic protein. Some of the highest concentration fractions, as indicated by the peaks in the graphs generated by the PrimeView software, of PTP-IA-2 and IA-2ic were run on the same gel to compare, indicating that the IA-2ic expression/purification was unsuccessful. This research group has historically found IA-2ic difficult to express.

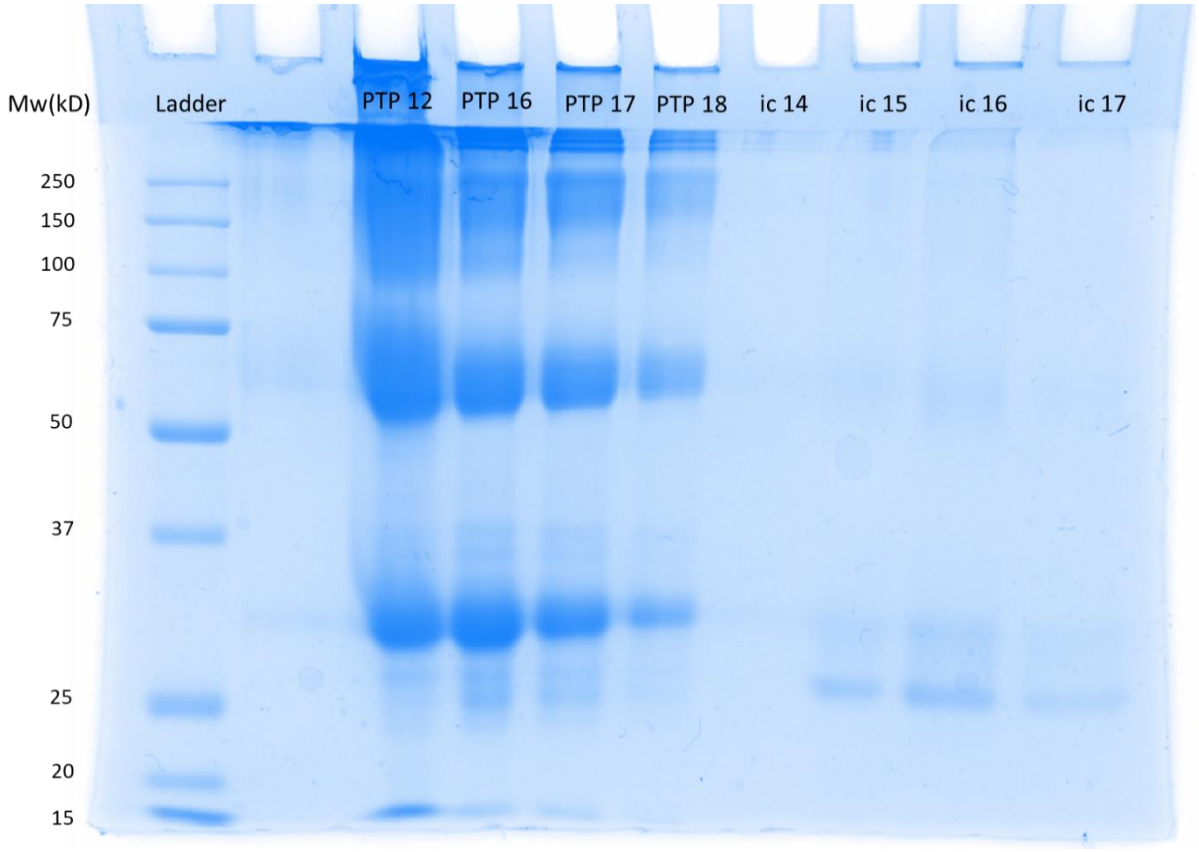

Figure 3-2 SDS-PAGE Gel showing FPLC-purified fractions of PTP-IA-2 and IA-2ic. Ladder was the Precision Plus Protein™ All Blue Prestained protein standard.

3.2 IA-2A Bridging Assay Variations

Optimisation of the IA-2A bridging assay began in 2019 as part of my undergraduate research project. There are three variations of the assay, in various stages of development. The standard, straight-coated PTP-IA-2-GST bridging assay is the primary focus of this thesis; however, several optimisation experiments were also conducted looking at a variation involving a glutathione-coated plate, which bound to the GST tag on the unlabelled autoantigen, and a neutravidin-coated plate, which would bind to the biotin once the unlabelled autoantigen was biotinylated. The standard version of the assay had already undergone previous optimisation experiments, for which I have been credited as part of my undergraduate degree, as well as one preliminary experiment with the glutathione version.

Many of the previously optimised conditions were assumed to also be optimal for the other assay variations, notably the incubation method and number of washes. Similarly, some of the conditions optimised in the glutathione-coated and neutravidin-coated versions of the assay were also applied to the standard format – e.g. label preparation, incubation lengths, and blocking method.

3.3 Glutathione Variation of the IA-2A Bridging Assay

3.3.1 The optimal concentration of PTP-IA-2-GST to coat the glutathione-coated optiplate is 5ng/well

It was hypothesised that the glutathione-coated plate would allow for a lower concentration of PTP-IA-2-GST to be used when coating the plates. To determine the optimal concentration, a range of concentrations were investigated over a number of distinct assays. The initial experiment looked at a fairly wide range of concentrations: 2.5ng/well, 12.5ng/well, and 25ng/well (figure 3-3-A).

This assay was in its infancy in terms of optimisation at this time, so the signal-to-noise ratios were generally quite poor. Possibly because of this, there appeared little statistical difference between the conditions ($p=0.1546$). However, there is clear graphical indication that the lower concentration of 2.5ng/well was superior in the spread of the results produced. As the lowest concentration tested appeared promising, a second experiment examined even lower concentrations and one between the two lower concentrations tested in the first experiment: 0.1ng/well and 0.2ng/well, and 5ng/well (figure 3-3-B). Again, the Friedman statistical test seemed of limited use ($p=0.1546$) but the ability of the assay to distinguish between known positives and negatives appeared greatly increased in the 5ng/well condition. Conditions closer to 5ng/well were tested next: 1ng/well, 2ng/well, and 5ng/well itself (figure 3-3-C). These three concentrations appeared most graphically similar, but statistically the SNRs differed ($p<0.0001$).

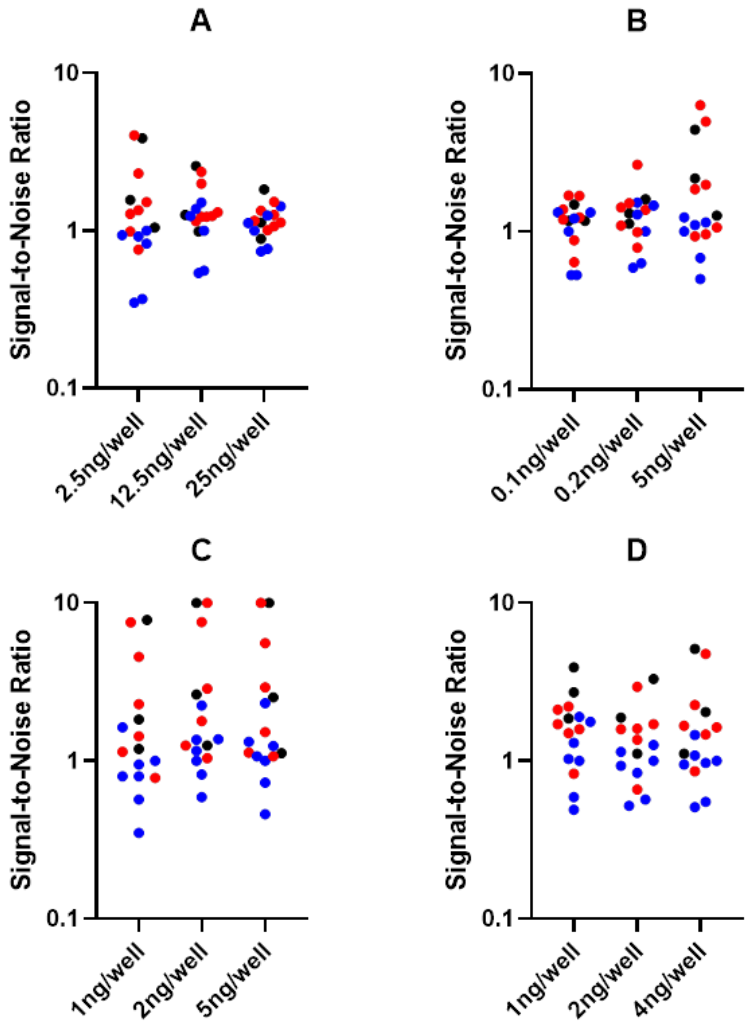

Figure 3-3 Glutathione IA-2A Bridging Optimisation: Coated Protein Concentration. A plot of signal-to-noise ratio (SNR) from investigating different concentrations of PTP-IA-2-GST used to coat glutathione-coated plates. Panel A is the first experiment, testing concentrations 2.5ng/well, 12.5ng/well, and 25ng/well. Panel B is the second experiment, testing 0.1ng/well, 0.2ng/well, and 5ng/well. Panel C is the third experiment, testing 1ng/well, 2ng/well, and 5ng/well. Four values above 10 (standard A and PR97 QC data from 2ng/well and 5ng/well), the highest being 13.6, were set to 10 for the graph, but the true values were used for the Freidman statistical test. Panel D is the fourth experiment, retesting similar concentrations to the previous experiment. Black points are the DK Standards A, C, and E. Red points are known positive samples and blue points are known negative samples, mostly from the BOX Family Study, and had been previously tested by IA-2 RBA. Each data point represents the SNR of the mean of two replicates.

For the third experiment, panel C, for the 1ng/well condition, the median LU was 31,252 LU for the known positives (including standards) and 13,755.5 LU for the known negatives. The ranges were 120,095.5 LU and 13,506.5 LU respectively. For the 2ng/well condition, the median LU was 31,832 LU for the known positives (including standards) and 13,998 LU for the known negatives. The ranges were 151,646 LU and 9,315 LU respectively. For the 5ng/well condition, the median LU was 25,512 LU for the known positives (including standards) and 10,740 LU for the known negatives. The ranges were 117,023.5 LU and 8,616 LU respectively.

Additional analysis focused on the differences between 2ng/well and 5ng/well. When comparing only the known positives and standards, there was little evidence of a difference (p=0.4258). However, when only the known negative samples were analysed, there was a notable difference (p=0.0313), and the median of the negatives was increased in the

2ng/well condition. This difference is slight, and based on few samples, so the experiment was repeated once more, this time including 4ng/well to see if that looked comparable to 5ng/well.

Going forward in the optimisation, 5ng/well was chosen as it provided good signal with some evidence of lower background. However, slightly lower concentrations are relatively comparable and could save costs, especially if the assay were to be performed at large-scales, so this condition may be revisited if development continues.

3.3.2 Cell-made single label preparation offers superior spread compared to other labels

Nano-luciferase labels can be made either by *in vitro* transcription/translation system (TnT®, Promega) or via cells. Two versions of the IA-2ic label were created, a dimer and monomer (single). Thus far all optimisation had been using the cell-derived single label, but this was compared to a TnT single and dimer, as well as a cell dimer, to investigate whether a different label preparation could improve the assay differentiation of SNR between known positives and negatives. Overall, there was a difference in both the positives ($p<0.0001$) and the negatives ($p=0.0003$). The TnT labels differ greatly from the cell-made labels, for both the single labels and the dimers (single $p<0.0001$, dimer $p=0.0024$). The dimer labels both have lower overall signal and a lot of clustering of results from positive and negative samples alike. Despite obvious graphical differences (Figure 3-4), the cell single and cell dimer are more similar ($p=0.1186$) than a cell and TnT label. The cell single label had the greatest range of SNR, and continued to be used going forward.

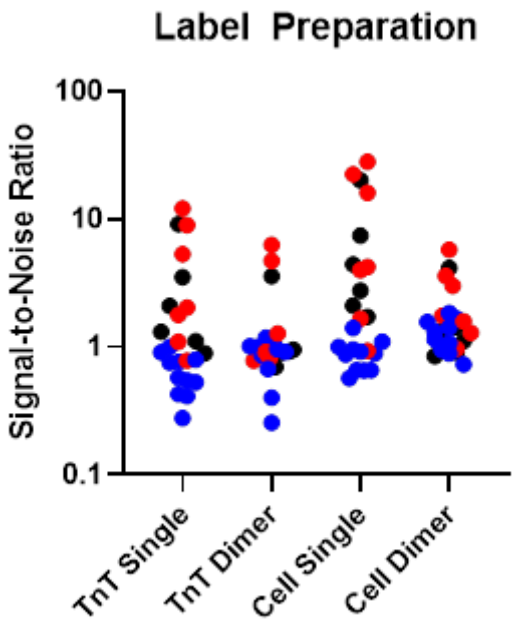

Figure 3-4 Glutathione IA-2A Bridging Optimisation: Label Preparation. A plot of signal-to-noise ratio (SNR) from investigating different preparations of the NLuc IA-2ic label. Black points are the DK Standards A-F. Red points are known positive samples and blue points are known negative samples, mostly from the BOX Family Study, and had been previously tested by IA-2 RBA. Each data point represents the SNR of the mean of two replicates. The black line denotes the median of the known positives (including standards).
For the TnT Single condition, the median LU was 67,155.5 LU for the known positives (including standards) and 19,053.5 LU for the known negatives. The ranges were 373,455 LU and 23,824 LU respectively. For the TnT Dimer condition, the median LU was 29,870.5 LU for the known positives (including standards) and 31,136.5 LU for the known negatives. The ranges were 181,781 LU and 30,108.5 LU respectively. For the Cell Single condition, the median LU was 52,196 LU for the known positives (including standards) and 10,915 LU for the known negatives. The ranges were 335,027.5 LU and 10,313.5 LU respectively. For the Cell Dimer condition, the median LU was 17,457 LU for the known positives (including standards) and 13,968 LU for the known negatives. The ranges were 59,863 LU and 13,543.5 LU respectively.

3.3.3 A 2 hour label incubation and 1.5 hour incubation in a coated plate is sufficient to discriminate well between positive and negative samples

A bridging assay has two incubation steps. Firstly, the incubation of the sera with the luciferase-tagged antigen. This mixture is then transferred into an antigen-coated optiplate and incubated again. The lengths of both incubations were investigated simultaneously in order to find the optimal combination. Sera and label were incubated together for either 2 hours at room temperature (RT) or overnight (16-24 hours). In each case the plates were wrapped/covered in foil to protect them from light. Following this incubation, the contents was transferred into a coated-optiplate before the second incubation. This incubation was either 1.5 hours or overnight, both shaking at 750rpm and again covered in foil. These timings were chosen to match other LIPS assays run in the laboratory. A summary of the conditions investigated is presented in table 3-1 below.

	Plate A	Plate B	Plate C	Plate D
Incubation 1 (sera + labelled antigen)	2 hours RT	2 hours RT	Overnight 4°C	Overnight 4°C
Incubation 2 (added to coated plate)	1.5 hours RT Shaking	~4 hours RT then Overnight (16-24 hours) 4°C	1.5 hours RT Shaking	~4 hours RT then Overnight (16-24 hours) 4°C

Table 3-1 Investigated incubation conditions for the Glutathione IA-2A Bridging Assay.

Overall, there was evidence of differences between the investigated combinations of conditions ($p<0.0001$), however this was limited to the positives/standards ($p=0.0002$) – there was less evidence of a difference in the negative samples ($p=0.633$), indicating the incubation length has little effect on the background of the assay. When considering the second incubation, there was little evidence of a difference between the two lengths, regardless of whether the first incubation was 2 hours ($p=0.5153$) or overnight ($p=0.2253$).

Conversely, the first incubation between serum and label did appear to have an effect, whether the second incubation was 1.5 hours (p=0.0005) or overnight (0=0.0012).

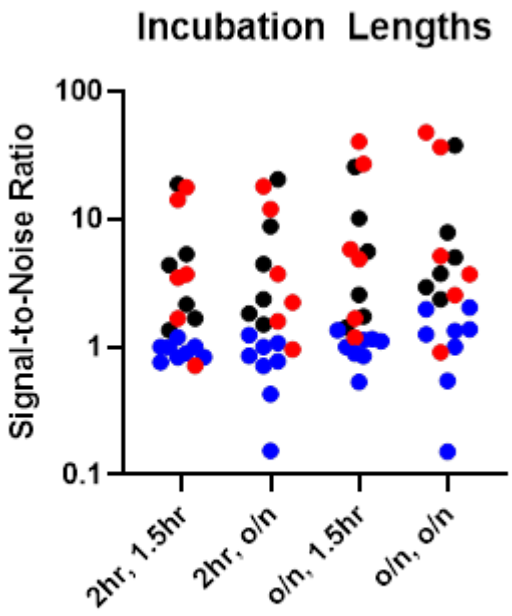

Figure 3-5 Glutathione IA-2A Bridging Optimisation: Incubation Lengths. A plot of signal-to-noise ratio (SNR) from investigating different incubation lengths. X axis labels are the length of the first incubation (sera and label) comma the length of the second incubation (shaking in the coated optiplate). O/n refers to an overnight incubation, described in table 3.4. Black points are the DK Standards A-F. Red points are known positive samples and blue points are known negative samples, mostly from the BOX Family Study, and had been previously tested by IA-2 RBA. Each data point represents the SNR of the mean of two replicates.

For the 2hr, 1.5hr condition, the median LU was 65,822.75 LU for the known positives (including standards) and 17,310.5 LU for the known negatives. The ranges were 329,940 LU and 7,891.5 LU respectively. For the 2hr, o/n condition, the median LU was 87,090.75 LU for the known positives (including standards) and 23,327.75 LU for the known negatives. The ranges were 543,716.5 LU and 31,188.5 LU respectively. For the o/n, 1.5hr condition, the median LU was 98,537 LU for the known positives (including standards) and 19,930.25 LU for the known negatives. The ranges were 739,354.5 LU and 15,531.5 LU respectively. For the o/n, o/n condition, the median LU was 65,821.25 LU for the known positives (including standards) and 19,384.75 LU for the known negatives. The ranges were 701,742 LU and 28,198.5 LU respectively.

Graphically, the 2 hour first incubation and overnight second incubation does look better, due to its improved top signal (Figure 3-5). However, the difference is subtle, and the medians of the result are very comparable. Increasing the incubation length to be overnight limits throughput. Although a two-day assay does not require more technician time, in a standard five-day work week only four assays could be performed instead of five. The 2 hour incubation followed be a 1.5 hour incubation condition looked sufficient that a 20% reduction in throughput was not deemed worth sacrificing for slightly better spread.

3.3.4 Blocking via incubation with 1% casein does not reduce background

A premade solution of 1% casein in PBS had been previously shown to be the best blocking agent. The method of application of this blocking agent was then investigated here. No blocking agent at all was compared with incubating the coated plates with either 50µl or 100µl of 1% casein in PBS (shaking at room temperature for 1 hour) or the method previously in use – adding 50µl, then flicking it out, and repeating this for a total of three additions and removals of the 1% casein (the "flicking out thrice") (Figure 3-6). After each of the blocking methods, plates were left out at room temperature to air-dry for 2-3 hours before being stored at 4°C in a sealed plastic bag with a sachet of desiccant until use.

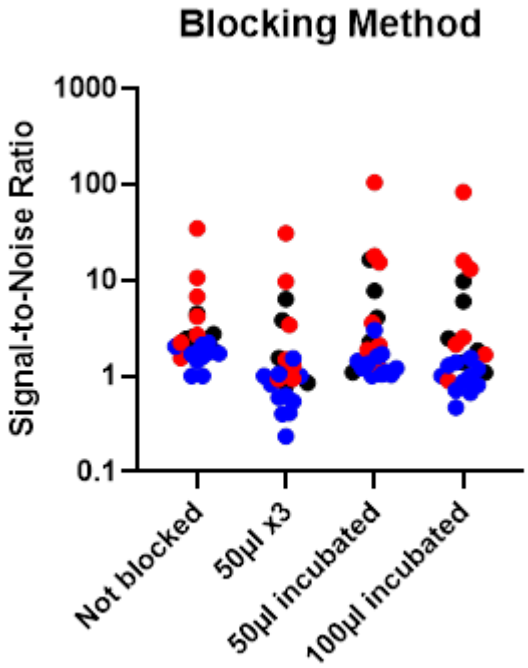

Figure 3-6 Glutathione IA-2A Bridging Optimisation: Blocking Method. A plot of signal-to-noise ratio (SNR) from investigating different blocking methods. The blocking buffer used was a commercial dilution of 1% casein in PBS. Commercial glutathione-coated plates additionally coated with 5ng/well PTP-IA-2-GST were blocked either by shaking at room temperature with 50µl or 100µl blocking buffer, or having 50µl added three times, with it flicked out in between each. Black points are the DK Standards A-F. Red points are known positive samples and blue points are known negative samples, mostly from the BOX Family Study, and had been previously tested by IA-2 RBA. Each data point represents the SNR of the mean of two replicates.

For the not blocked condition, the median LU was 7,716.5 LU for the known positives (including standards) and 4,947 LU for the known negatives. The ranges were 95,193 LU and 3,555 LU respectively. For the "flicking out thrice" condition, the median LU was 969 LU for the known positives (including standards) and 408 LU for the known negatives. The ranges were 19,639.5 LU and 845 LU respectively. For the 50µl incubated condition, the median LU was 990 LU for the known positives (including standards) and 331 LU for the known negatives. The ranges were 28,455 LU and 522.5 LU respectively. For 100µl incubated condition, the median LU was 878 LU for the known positives (including standards) and 357.5 LU for the known negatives. The ranges were 29,238 LU and 384 LU respectively.

The LU for some samples in this experiment were much lower than they had been previously. Between all methods, there was evidence for a difference in the negative

samples (p=0.0002) and the positives/standards (p<0.0001). When comparing individually however, there was little evidence of difference between the incubation methods and not blocking it (p=0.4820 and p=0.3146 for the 50µl and 100µl respectively). In contrast, the "flicking out thrice" method greatly reduced the binding overall (p<0.0001 comparing all and just the "flicking out thrice" method with no blocking). While this blocking method lowered the signal, the background was also greatly reduced, which was more desirable at this stage of the optimisation. Additionally, the signal of a negative sample appears increased in the 50µl incubated condition. The existing method of adding and flicking out the 1% casein was maintained going forwards.

3.4 Biotinylated Variation of the IA-2A Bridging Assay Results

3.4.1 Biotinylated IA-2 can be stored at -4°C or -80°C, at least short term, but glycerol reduces binding

For optimal throughput, large batches of IA-2 should be biotinylated at once and stored until use. This experiment investigated how stable the biotinylated protein was in different storage conditions. Aliquots were stored at either 4°C, -80°C, or in a suspension with 15% glycerol and then frozen at -80°C.

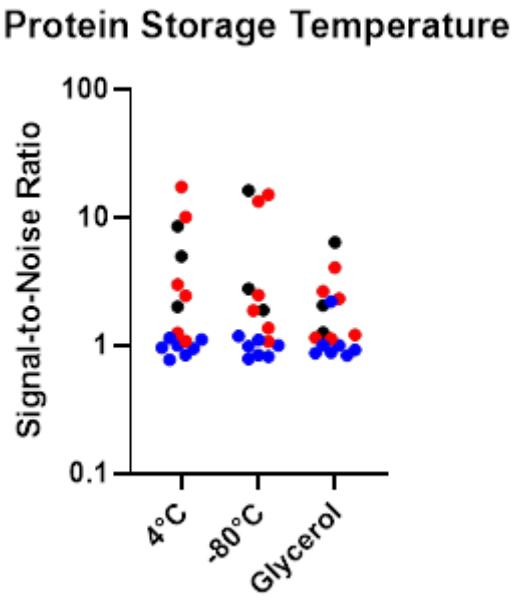

Figure 3-7 Biotinylated IA-2A Bridging Optimisation: Protein Storage Temperature. A plot of signal-to-noise ratio (SNR) from investigating different storage conditions of the biotinylated IA-2 antigen – either refrigerated or in a -80°C freezer neat or suspended at 15% in glycerol. Black points are the DK Standards A, C, and E. Red points are known positive samples and blue points are known negative samples, mostly from the BOX Family Study, and had been previously tested by IA-2 RBA. Each data point represents the SNR of the mean of two replicates.

For the 4°C condition, the median LU was 27,167.5 LU for the known positives (including standards) and 8,775 LU for the known negatives. The ranges were 147,552.5 LU and 3,363.5 LU respectively. For the -80°C condition, the median LU was 20,313 LU for the known positives (including standards) and 8,088.5 LU for the known negatives. The ranges were 124,307 LU and 3,222 LU respectively. For the -80°C with 15% glycerol condition, the median LU was 15,579.5 LU for the known positives (including standards) and 10,372.5 LU for the known negatives. The ranges were 39,706 LU and 10,372.5 LU respectively.

There was very little evidence for differences between the three investigated storage temperatures (p=0.2466), however this was mostly due to the negative samples (p=0.9563). When considering only the positives/standards, there was evidence of differences between the conditions (p=0.0080). Graphically, the positives seemed to spread better in the 4°C condition, although statistically there was little evidence of a difference between the 4°C and -80°C conditions (p>0.9999). The greatest difference was seen when glycerol was added and is especially noticeable in the raw LU; for example, the mean LU for DK standard A was over twice as high in the -80°C condition without glycerol compared to the -80°C with glycerol. Going forward, glycerol was not added. To reduce any unknown effects of freeze-thawing cycles, the refrigerated aliquot was used going forwards, with remaining aliquots frozen at -80°C for longer-term storage.

3.4.2 Incubating biotinylated IA-2 in the label buffer boosted signal compared to incubating it separately

To decide where to introduce the biotinylated IA-2 into the assay, an experiment was carried out where the biotinylated protein was either diluted in the label buffer, with the NLuc IA-2, and incubated with the serum before later being transferred to the neutravidin-coated plate, or incubated alone in the streptavidin-coated plate, with the sera and NLuc-IA-2 added later.

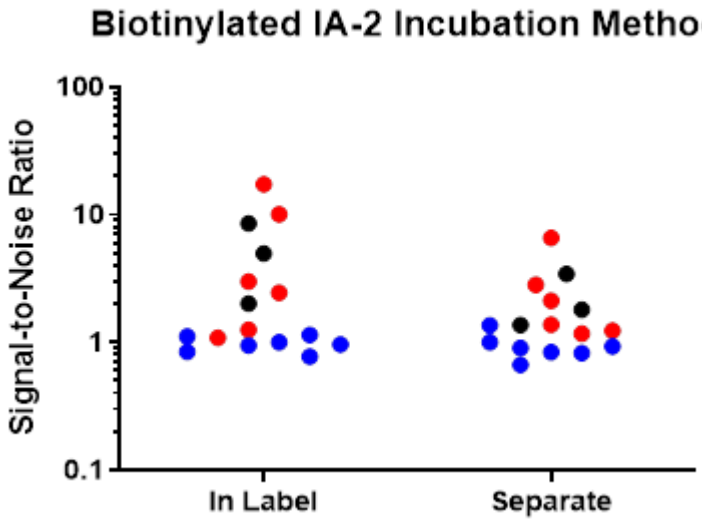

Figure 3-8 Biotinylated IA-2A Bridging Optimisation: Protein Incubation Method. A plot of signal-to-noise ratio (SNR) from investigating diluting the biotinylated IA-2 within the NLuc-IA-2 dilution (incubating it with the sera and label) or incubating it separately to the sera and label, in the neutravidin-coated plate. Black points are the DK Standards A-F. Red points are known positive samples and blue points are known negative samples, mostly from the BOX Family Study, and had been previously tested by IA-2 RBA. Each data point represents the SNR of the mean of two replicates.

For the "in label" condition, the median LU was 27,167.5 LU for the known positives (including standards) and 8,775 LU for the known negatives. The ranges were 147,552.5 LU and 3,363.5 LU respectively (this experiment was conducted in the same assay as the previous one, hence the results for "in label" incubation and 4°C storage are the same). For the "separate" condition, the median LU was 5,556 LU for the known positives (including standards) and 2,789.5 LU for the known negatives. The ranges were 16,672 LU and 2,139.5 LU respectively.

There was evidence for a difference (p=0.0054), and graphical analysis was clear that diluting the biotinylated protein with the label increased the spread of the known positive samples greatly. This was supported by separate statistical analysis, where there was little difference in the negatives (p=0.5625) but evidence of an effect on the positive samples and standards (p=0.0117), with a great decrease in the median LU of the positive samples when incubating the biotinylated IA-2 and the label separately. Going forward, the NLuc-IA-2 was diluted in Denver LIPS with biotinylated IA-2 diluted in it already.

3.4.3 Biotinylated IA-2 diluted to 10ng/well provided optimal signal without increasing background

An experiment was conducted to determine the optimal concentration of biotinylated IA-2. Half a neutravidin-coated optiplate was used to assay with NLuc IA-2 label, with a different concentration of biotinylated-IA-2 diluted in it: 2, 5, 10, 20, and 50ng/well.

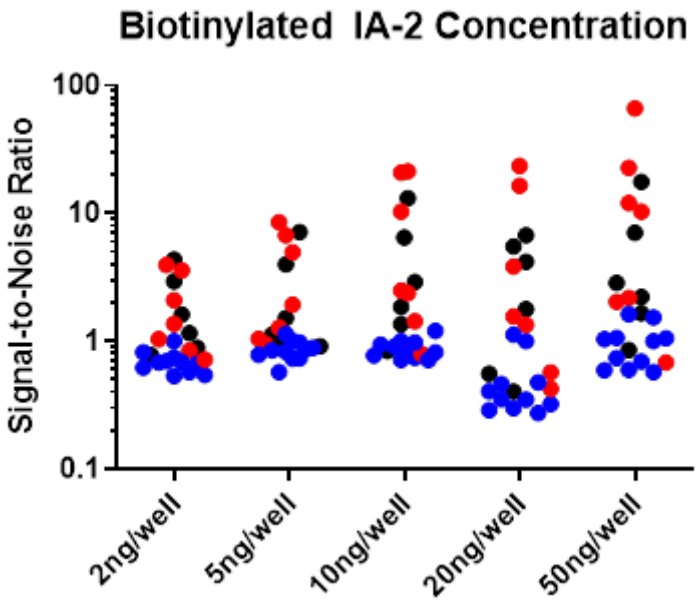

Figure 3-9 Biotinylated IA-2A Bridging Optimisation: Biotinylated IA-2 concentration. A plot of signal-to-noise ratio (SNR) from investigating a range of concentrations of biotinylated PTP-IA-2 diluted in the dilute label (Nluc-IA-2 in Denver LIPS). Black points are the DK Standards A-F. Red points are known positive samples and blue points are known negative samples, mostly from the BOX Family Study, and had been previously tested by IA-2 RBA. Each data point represents the SNR of the mean of two replicates.

For the 2ng/well condition, the median LU was 10,202.5 LU for the known positives (including standards) and 5,106.5 LU for the known negatives. The ranges were 27,219.5 LU and 3,476 LU respectively. For the 5ng/well condition, the median LU was 9,256.5 LU for the known positives (including standards) and 5,172 LU for the known negatives. The ranges were 46,599 LU and 3,425.5 LU respectively. For the 10ng/well condition, the median LU was 22,454 LU for the known positives (including standards) and 8,053.5 LU for the known negatives. The ranges were 185,253 LU and 19,211 LU respectively. For the 20ng/well condition, the median LU was 40,212 LU for the known positives (including standards) and 7,947 LU for the known negatives. The ranges were 521,823 LU and 19,211 LU respectively. For the 50ng/well condition, the median LU was 9,910 LU for the known positives (including standards) and 3,458 LU for the known negatives. The ranges were 227,110 LU and 3,641 LU respectively.

There was evidence of a difference in positives/standards between these concentrations, as expected ($p<0.0001$). The background did vary as concentration increased to a point, but there not convincing evidence of a difference between the negative samples at 10ng/well and 50ng/well ($p=0.4922$). However, there was evidence of a difference in signal ($p=0.0075$) between these two concentrations. Graphically, increasing concentration did seem to increase the signal, although at 50ng/well this was limited to one sample (the high positive

QC). It was decided that this limited improvement in spread was not worth the five-fold increase in protein (and associated increase in cost), so going forward 10ng/well was used, as this was where the pattern of consistently increasing signal with increasing concentration seemed to plateau.

3.4.4 Neutravidin-coated plates do not require additional blocking

A premade solution of 1% casein in PBS had been previously shown to be the best blocking agent, however the commercial plates pre-coated with neutravidin had already been blocked with SuperBlock during manufacture. To see whether this blocking was sufficient or whether we should also block the plates with casein, no additional blocking agent was compared with incubating the coated plates with either 50µl or 100µl 1% casein in PBS (shaking at room temperature for 1 hour) or the method previously in use – adding 50µl, then flicking it out, and repeating this for a total of three additions and removals of the 1% casein (colloquially referred to as the "flicking out thrice" method). After each of the blocking methods, plates were left out at room temperature to air-dry for 2-3 hours before being stored at 4°C in a sealed plastic bag with a sachet of desiccant until use.

There was evidence of a difference between the conditions ($p<0.0001$), however looking at the negative samples, there was no evidence of a difference in background with the "flicking out thrice" method that had worked well in other versions of the assay ($p=0.6250$), nor the incubation method (100µl $p=0.2324$). The neutravidin-coated plates were used straight from the packet going forward, with no additional blocking.

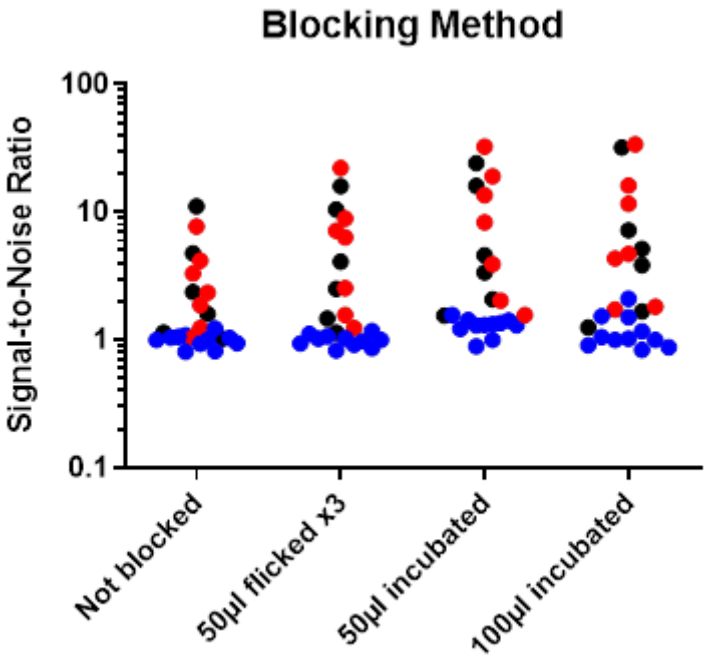

Figure 3-10 Biotinylated IA-2A Bridging Optimisation: Blocking Method. A plot of signal-to-noise ratio (SNR) from investigating a range of methods of blocking with 1% casein in PBS: No additional blocking buffer, the blocking buffer added thrice and flicking out in between, or two volumes of the blocking buffer incubating in the neutravidin-coated plates at room temperature. Black points are the DK Standards A-F. Red points are known positive samples and blue points are known negative samples, mostly from the BOX Family Study, and had been previously tested by IA-2 RBA. Each data point represents the SNR of the mean of two replicates.

For the "not blocked" condition, the median LU was 2,417.5 LU for the known positives (including standards) and 1,028.5 LU for the known negatives. The ranges were 10,412.5 and 437 LU respectively. For the "flicking out thrice" condition, the median LU was 2,751.5 LU for the known positives (including standards) and 671 LU for the known negatives. The ranges were 14,116 and 235.5 LU respectively. For the 50µl condition, the median LU was 2,305 LU for the known positives (including standards) and 656 LU for the known negatives. The ranges were 15,517.5 and 337 LU respectively. For the 100µl condition, the median LU was 2,402.5 LU for the known positives (including standards) and 520 LU for the known negatives. The ranges were 16,612.5 and 647 LU respectively.

3.4.5 Biotinylated IA-2 variation of the bridging assay suffered a 10-fold decrease in light units

At this stage in the development of the biotinylated IA-2 variation of the IA-2A bridging assay, we noticed the mean LU dropped significantly. At some point between the date of the second and third experiments shown on figure 3-11, the mean LU dropped 10-fold, although the SNRs were remarkably well preserved (see appendix 5.3.3 for assay reagent dilution optimisation results, which were achieved despite this drop in raw signal). This is not something that had occurred in any other variation of the assay, so it was presumed to be due to the biotinylated IA-2 in some way – possibly degradation due to extended storage at 4°C.

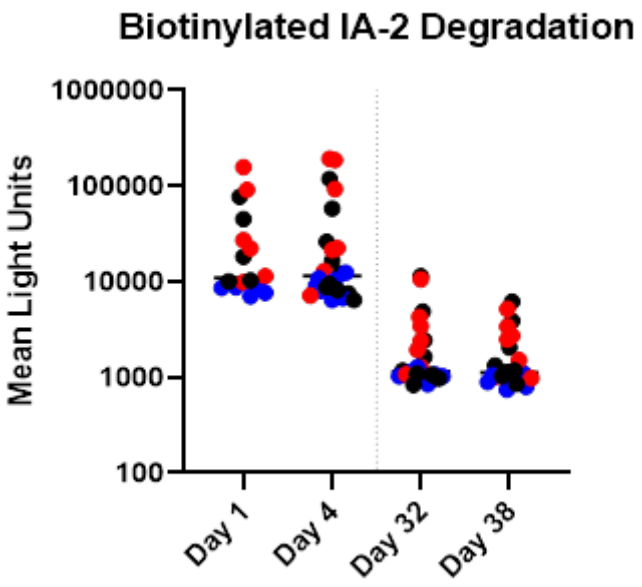

Figure 3-11 Biotinylated IA-2A Bridging Optimisation: Biotinylated IA-2 Degradation. A plot of light units (LU) from the same conditions of four recent optimisation experiments. Black points are the DK Standards A-F. Red points are known positive samples and blue points are known negative samples, mostly from the BOX Family Study, and had been previously tested by IA-2 RBA. Each data point represents the mean LU of two replicates. The black line denotes the median.

3.5 Standard IA-2A Bridging Assay Optimisation Results

The three formats of the bridging assay were optimised concurrently until it was decided to pause development of two to enable more progress to be made with one version. The most recent optimisation experiments from each assay at the time were analysed to compare the three methods, and these data are presented in figure 3-12.

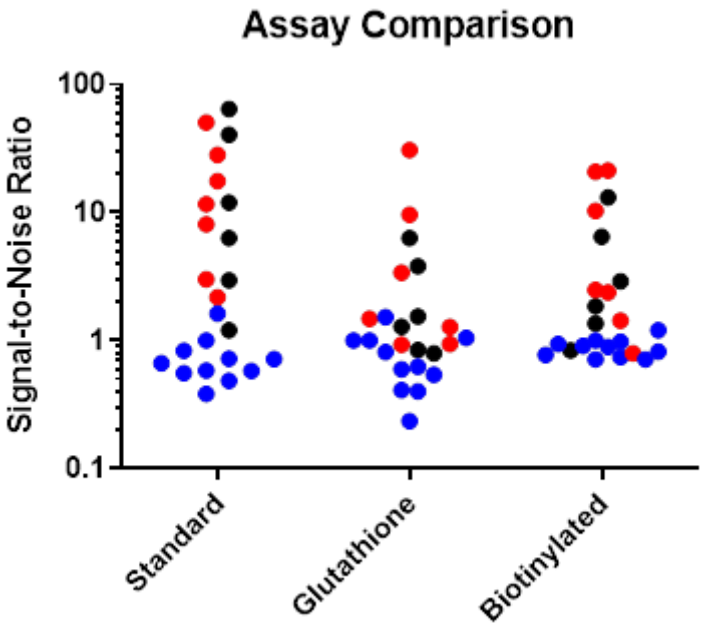

Figure 3-12-2 IA-2A Bridging Assay Format Comparison. A plot of signal-to-noise ratio (SNR) from the most optimised experiments (at the time) of each of the three formats of the IA-2A bridging assay. Black points are the DK Standards A-F. Red points are known positive samples and blue points are known negative samples, mostly from the BOX Family Study, and had been previously tested by IA-2 RBA. Each data point represents the SNR of the mean of two replicates.

For the standard/straight-coated condition, the median LU was 25,660 LU for the known positives (including standards) and 1,463 LU for the known negatives. The ranges were 138,810 and 2,725 LU respectively. For the glutathione condition, the median LU was 969 LU for the known positives (including standards) and 408 LU for the known negatives. The ranges were 19,639.5 and 845 LU respectively. For the biotinylated condition, the median LU was 22,454 LU for the known positives (including standards) and 8,053.5 LU for the known negatives. The ranges were 185,253 and 4,460 LU respectively.

The background of the three assay formats was similar (p=0.0665), however the SNR of the known positives/standards did vary (p=0.0009). The standard, or straight-coated, assay format graphically appeared to provide the best discrimination between negative and low positive samples, while also providing the greatest dynamic range – especially for the standard curve – and having the greatest median LU of positive samples. While it required a great deal more IA-2 antigen to coat the plates (200ng/well compared to 5 or 10ng/well), this could be expressed in-house, and saved money elsewhere by avoiding having to purchase commercial pre-coated plates. The biotinylated IA-2 format with the neutravidin-coated plates, and the version with the glutathione-coated plates (taking advantage of the existing GST-tag on the PTP-IA-2) were not optimised past what has already been described here.

3.5.1 Unlabelled PTP-IA-2 can be stored at -80°C or 4°C for up to 7 months

Unlabelled PTP-IA-2-GST was purified via FPLC, and then aliquots were stored at -80°C (frozen) and 4°C (refrigerated) for 7 months prior to their use. Two plates were coated, one with an aliquot of protein stored at each temperature, at a concentration of 400ng/well, and the same serum samples were assayed using both plates.

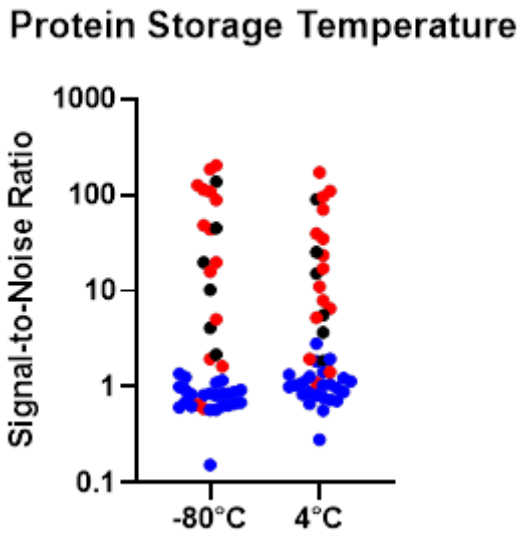

Figure 3-13 IA-2A Bridging Optimisation: Protein Storage Temperature. A plot of signal-to-noise ratio (SNR) from investigating storing unlabelled PTP-IA-2-GST at either -80°C or 4°C. Black points are the DK Standards A-F. Red points are known positive samples and blue points are known negative samples, mostly from the BOX Family Study, and had been previously tested by IA-2 RBA. Each data point represents the SNR of the mean of two replicates.

For the -80°C condition, the median LU was 195,829 LU for the known positives (including standards) and 8,242.5 LU for the known negatives. The ranges were 2,002,212 and 1,119,711 LU respectively. For the 4°C condition, the median LU was 37,849 LU for the known positives (including standards) and 3,552 LU for the known negatives. The ranges were 583,349 and 238,744 LU respectively.

While there did appear to be evidence of a difference in the positive/standard samples (p=0.0019), graphically the signal generally appeared to be maintained across the conditions (Figure 3-13). The background also varied between the conditions (p=0.1228), however again, both outcomes seemed satisfactory, so it was concluded that both storage temperatures preserved the protein well. The effect of freeze-thaw cycles or continued refrigerated storage will be investigated at a future date. In the meantime, the protein was split into smaller aliquots so it could be stored at -80°C while minimising how often it was thawed.

3.5.2 Increasing label total counts to $1x10^7$ improves signal without affecting background

To investigate the optimal total counts of the NLuc IA-2 cell single construct, the existing total counts of $4x10^6$ LU/25µl was compared with $1x10^7$ LU/25µl, both measured using the standard 1:50 dilution of NanoGlo assay reagent. The labelled antigen was incubated with sera for 2 hours at room temperature.

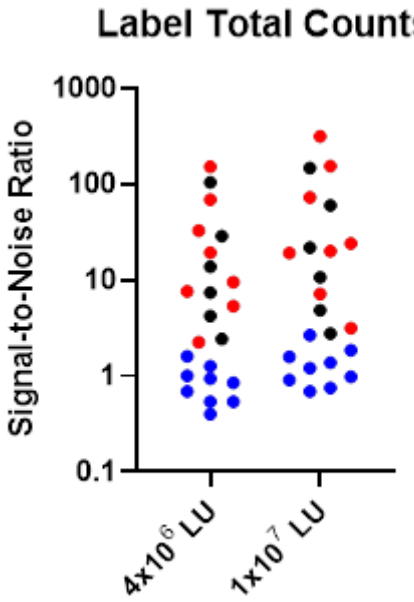

Figure 3-14 IA-2A Bridging Optimisation: Label Total Counts. A plot of signal-to-noise ratio (SNR) from investigating diluting NLuc-tagged IA-2 to 4 million light units vs 10 million light units. Black points are the DK Standards A-F. Red points are known positive samples and blue points are known negative samples, mostly from the BOX Family Study, and had been previously tested by IA-2 RBA. Each data point represents the SNR of the mean of two replicates.

For the $4x10^6$ LU condition, the median LU was 29,133 LU for the known positives (including standards) and 2,145.5 LU for the known negatives. The ranges were 376,848 LU and 3,035 LU respectively. For the $1x10^7$ LU condition, the median LU was 52,531 LU for the known positives (including standards) and 3,050 LU for the known negatives. The ranges were 783,323.5 LU and 4,956.5 LU respectively.

The SNR varied greatly between the two conditions ($p<0.0001$). When considering only the known negative samples, the SNR were similar ($p=0.1055$), indicating the background of the assay had not increased with the label concentration. In contrast, when analysing only the positive samples, including the standards, the SNRs of two conditions were distinct ($p<0.0001$), with a median SNR of 11.60 for $4x10^6$ compared to 20.91 for $1x10^7$.

An NLuc IA-2 antigen total counts of $1x10^7$ LU offered greater IA-2A binding and comparable assay background compared with $4x10^6$ LU. Further optimisation experiments used $1x10^7$ LU.

3.5.3 NanoGlo® Assay Reagent can be further diluted to reduce cost

The standard Assay Reagent is a 1:50 dilution of the substrate furimazine in the buffer included in the Promega NanoGlo® kit. Diluting this assay reagent further was investigated primarily to cut costs, as this is one of the more expensive reagents, but also to see if it could improve the assay.

The first experiment looking at this compared the standard 1:50 dilution with standard 1:50 assay reagent that had been diluted an additional 1:1 in Denver buffer (figure 3-15-A). The two conditions initially appeared graphically similar, but statistically this was not the case ($p=0.0004$). However, this difference appears to be mostly in the signal rather than the background, as the known negatives alone are much more similar ($p=0.8203$) than when comparing only the known positives and standards ($p<0.0001$). The median of the known positives and standards for the 1:50 dilution was 20.91, and in the further 1:1 it was 34.90. The additional dilution then, as well as cutting the cost of the reagent by 50%, seemed to improve the signal of the assay without affecting the background.

Based on this success, a second experiment was carried out to see whether the assay reagent could be diluted even further. The experiment compared the additional 1:1 dilution with a 1:3, 1:4, and 1:5 further dilutions of the standard 1:50 assay reagent (figure 3-15-B). The four conditions varied ($p=0.0002$), so each was compared individually with the 1:1 dilution. The 1:1 and 1:2 conditions still varied ($p=0.0006$), so closer analysis was again required (figure 3-15-C). When considering only the known negative samples, the two conditions were much more similar ($p=0.5625$), whereas the differences persisted in the known positives and standards ($p=0.0005$). The median and mean were lower in the 1:2 condition, indicating that while the background remained similar, diluting the assay reagent further reduced the signal.

An equipment error meant that four samples had no data collected, and there was one unexpectedly high known negative in the 1:2 condition, possibly due to spillover from adjacent positive samples. For these reasons, the 1:2 condition was looked at again, with more samples ($n=47$ compared to $n=21$) (figure 3-15-D). This time the two conditions looked very comparable ($p=0.3900$). Going forward the 1:50 assay reagent was diluted a further 1:2

with Denver buffer, which also brought it more in-line with other LIPS assays for islet autoantibodies.

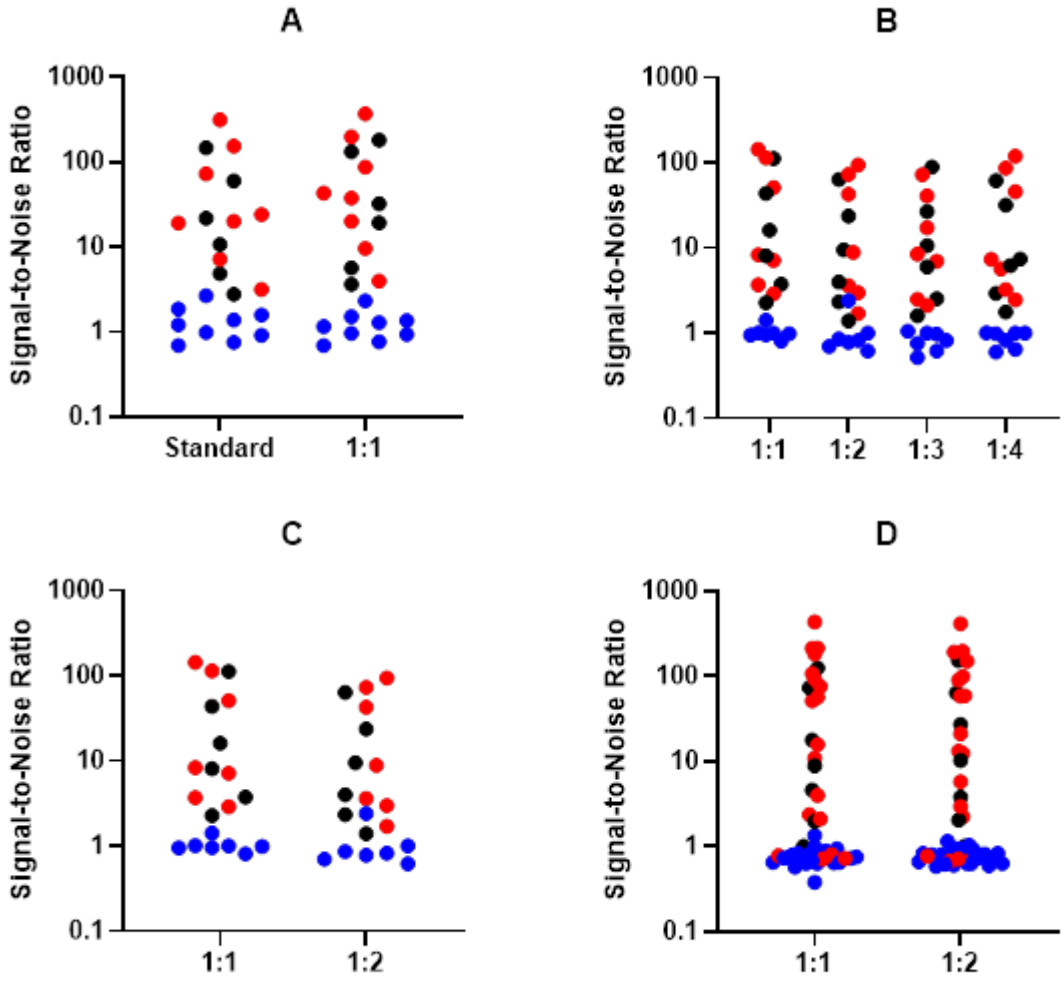

Figure 3-15 IA-2A Bridging Optimisation: Assay Reagent Dilution. A plot of signal-to-noise ratio (SNR) from varying dilutions of the standard 1:50 dilution of the furimazine substrate from Promega's NanoGlo® kit. Panel A depicts the first experiment comparing the standard 1:50 with a 1:1 dilution. Panel B is the follow-up experiment looking at a range of potential dilutions. Panel C is this same experiment but only looking at the 1:1 and 1:2 dilutions. Panel D is the final experiment again comparing 1:1 and 1:2. Black points are the DK Standards A-F. Red points are known positive samples and blue points are known negative samples, mostly from the BOX Family Study, and had been previously tested by IA-2 RBA. Each data point represents the SNR of the mean of two replicates.

For the final experiment, panel D, for the 1:1 LU condition, the median LU was 447.387 LU for the known positives (including standards) and 6,473.5 LU for the known negatives. The ranges were 3,760,788 LU and 14,913 LU respectively. For the 1:2 LU condition, the median LU was 259,060 LU for the known positives (including standards) and 7,468.5 LU for the known negatives. The ranges were 3,954,303 LU and 22,641 LU respectively

3.5.4 Additional reagents in label buffer do not improve assay performance

When the IA-2A bridging assay first began development, an experiment was conducted looking at whether the presence of EDTA in the label buffer had any effect. It was concluded at the time that EDTA did boost the signal of some low positive samples, so 5% EDTA was added to the Denver LIPS the NLuc-tagged IA-2 was diluted in from then on. Upon revisiting those data however, it was noted that the standard curve did not have the expected spread of LU. This, combined with the laboratory's recent successes adding 1% casein to the labels for other LIPS assays, prompted an experiment revisiting the potential label additives.

NLuc-tagged IA-2 was diluted to $1x10^7$ LU/25µl in Denver LIPS alone (control), or with 5% EDTA, 0.05% casein (1:20 of a pre-made solution of 1% casein in PBS), or 0.1% BSA.

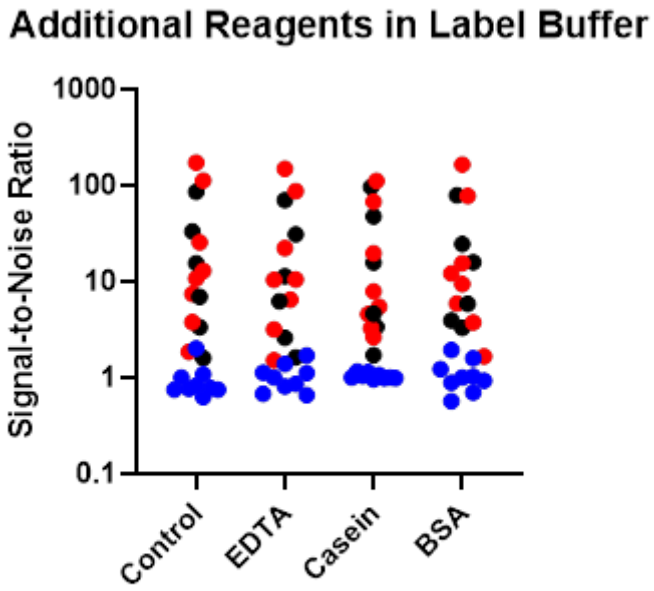

Figure 3-16 IA-2A Bridging Optimisation: Additional Reagents in Label Buffer. A plot of signal-to-noise ratio (SNR) from investigating the addition of either 5% EDTA, 0.1% casein (a 1:20 dilution of pre-diluted 1% casein in PBS), or 0.1% BSA, as well as a control condition of NLuc-IA-2 diluted simply in Denver LIPS alone. Previous to this experiment the 5% EDTA condition was the standard protocol. Black points are the DK Standards A-F. Red points are known positive samples and blue points are known negative samples, mostly from the BOX Family Study, and had been previously tested by IA-2 RBA. Each data point represents the SNR of the mean of two replicates.

For the control condition, the median LU was 39,543.8 LU for the known positives (including standards) and 2,597.5 LU for the known negatives. The ranges were 575,115 LU and 2,597.5 LU respectively. For the EDTA condition, the median LU was 32,534.5 LU for the known positives (including standards) and 3,100 LU for the known negatives. The ranges were 460,696 LU and 3,277.5 LU respectively. For the casein condition, the median LU was 12,441.8 LU for the known positives (including standards) and 1864.5 LU for the known negatives. The ranges were 204,733 LU and 364 LU respectively. For the BSA condition, the median LU was 30,292.8 LU for the known positives (including standards) and 2,813 LU for the known negatives. The ranges were 459,246 LU and 3,854 LU respectively.

Some differences in LU were noted, particularly the reduced binding when casein was added, but the SNRs were similar (p=0.3219). This can also be seen when analysing the positive/standard samples (p=0.0317), with the control condition maintaining the highest median LU amongst these

samples. The additional reagents were attempts to reduce the background, so this was analysed separately from the positive samples, however there was also no real evidence of an effect ($p=0.5222$). As the different additions to the label buffer did not improve the assay (and even seemed to reduce the signal) to make the protocol simpler and to save reagents and their associated costs, no additional reagents were diluted in the label buffer going forward.

3.6 IA-2A Bridging Assay Threshold Setting

The fully optimised standard IA-2A bridging assay method, described in 2.4, was used to test additional samples in order to set a threshold. Based on serum samples from 265 schoolchildren (aged 9-13 years), the threshold at the 97.5th percentile was 1.23 units, or 1.97 units at the 99th percentile. Few assays have been carried out since the threshold was set, so it may be amended in future as more sera from schoolchildren are tested. ROC curve analysis of these plus serum samples from 135 patients (aged 1-21), taken within 3 months of diagnosis, indicated an area under the ROC curve of 0.858 (95% CI 0.811 – 0.905). At a specificity of 99%, the assay was found to be 70% sensitive.

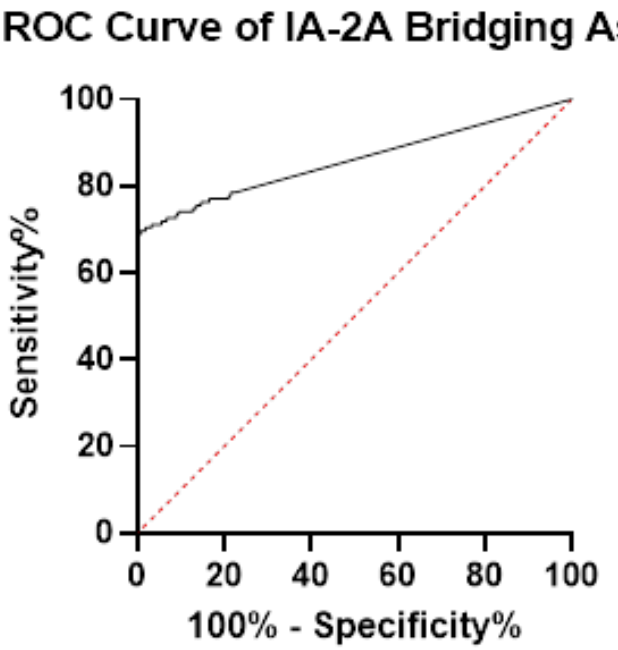

Figure 3-17 Receiver Operator Characteristic (ROC) Curve for the IA-2A Bridging Assay. Based on sera from 265 schoolchildren (aged 9-13 years) and 135 patients (aged 1-21), taken within 3 months of diagnosis, as described in figure 2-1. AUC = 0.858 (95% CI 0.811 – 0.905).

3.7 PTP-IA-2A Bridging Assay correlates well with PTP-IA-2 RBA

A blinded set of 150 serum samples was assayed by PTP-IA-2 RBA (method as described in Long et al. 2012[140]) as part of the IASP 2020 Workshop. These same samples were assayed with the standard PTP-IA-2-GST Bridging Assay. The two tests correlated well, with a spearman's correlation coefficient of 0.85, although two samples tested negative in the IA-

2A bridging assay, despite being from multiple islet autoantibody positive individuals and testing positive by RBA.

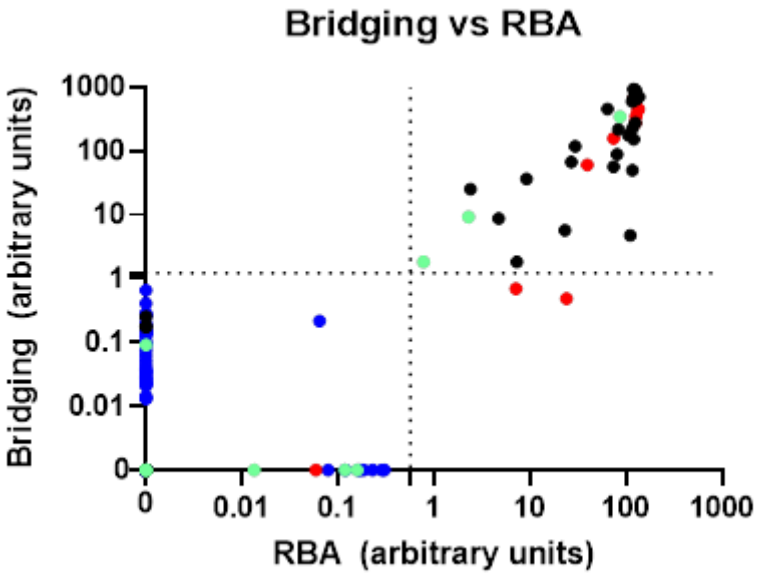

Figure 3-18 Plot of arbitrary units from 150 samples from the IASP2020 Workshop tested In both the PTP-IA-2A bridging assay and the PTP-IA-2A radiobinding assay. New onset n=38, black), controls (n=90, blue), multiple islet autoantibody positive (n=12, red), other blinded samples (n=10, teal). Dashed lines are the thresholds for each assay.

Signal-to-noise ratios were also calculated using the mean of the raw units (cpm for the RBA and LU for the bridging) from the 90 control samples. For the RBA, the median SNR of the 12 multiple islet autoantibody positive samples was 69.4, compared with 119.3 for the bridging assay.

3.8 Bridging assays frequently have great intra-assay variation

Sera were always plated twice, in adjacent wells, and percentage errors above 30% were investigated to see if it would affect whether the sample was assigned to be positive or negative overall. While this was rarely the case, and samples in this situation were always repeated, errors in high positive samples would lead to inaccurate measures of antibody titre. This occurred in both the IA-2A and Spike-RBD bridging assays.

To give an indication of the scale of this problem, when testing the 150 samples from the IASP 2020 workshop, 27.5% of the results had a percentage error greater than 30%, although less than half of these errors would have caused a sample to cross the positivity threshold. This is significantly greater than the frequency of percentage errors above 30% on the same samples tested in the equivalent RBA, which only had a 5.6% error rate and only two samples with errors that would affect their positivity status.

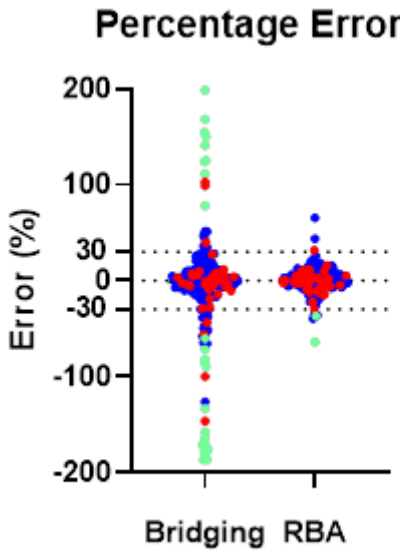

Figure 3-19 Graph comparing the percentage error (calculated from the counts of one replicate subtracted from the counts of the other, divided by their mean) of 150 IASP 2020 samples as tested in the IA-2A bridging assay and the PTP-IA-2 radiobinding assay. Samples positive in each assay are red, samples negative in each assay are blue, and samples that required repeating and were negative are teal. The largest errors tended to be in truly negative samples, possibly due to spillover, and it was usually only samples with one negative and one positive replicate which were repeated, hence there are no repeated positive samples. Dotted lines are at x=0, as well as the thresholds of replicate investigation 30% and -30%.

3.9 SARS-CoV-2 Bridging Assay Variations

Work initially began optimising a plate-based bridging assay using plates coated with unlabelled RBD. Optimisation of the spike-coated format of the assay began shortly after and the two assays were optimised concurrently until work on the RBD-coated format ceased to focus on the spike-coated assay. Some conditions optimised in the RBD-coated bridging assay were assumed to also be optimal for the spike-coated bridging assay. These

are summarised in table 2-6. Four concentrations of each protein were used to coat plate assayed in the same experiment.

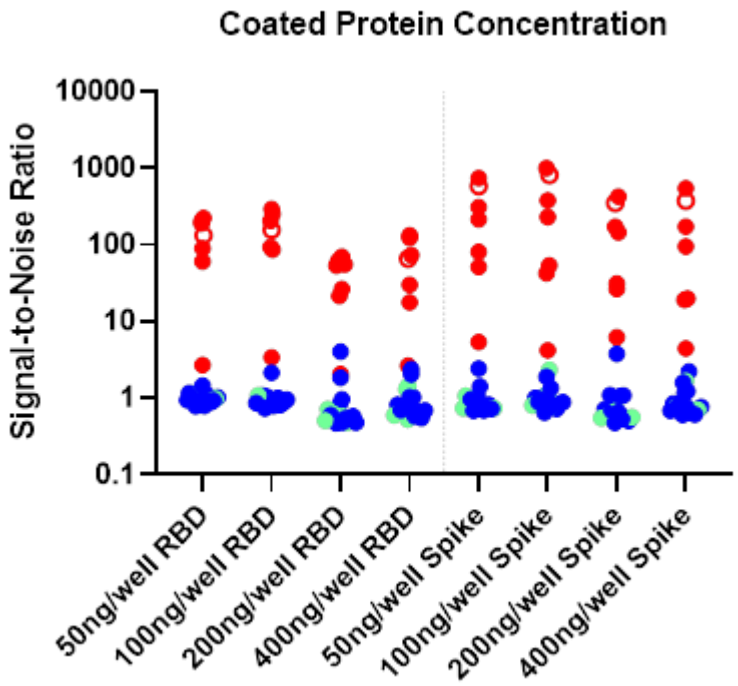

Figure 3-20 Spike-RBD Bridging Optimisation: Coated Protein. A plot of signal-to-noise ratio (SNR) from investigating the four different concentrations (50, 100, 200, and 400ng/well) of either receptor binding domain (RBD) or the whole spike antigen of SARS-CoV-2, diluted in PBS. Red points are known PCR test positive samples and blue points are known negative serum samples, mostly pre-pandemic. Red unfilled circles are samples from individuals who were symptomatic and suspected to have COVID-19 but were not PCR tested. Teal points are general population samples from the Capillary Testing for COVID-19 (CTC-19) study. Each data point represents the SNR of the mean of two replicates.

At 100ng/well, for the RBD condition, the median LU was 54,415 LU for the known positives (including standards) and 307.75 LU for the known negatives. The ranges were 100,332.5 LU and 492 LU respectively. For the Spike condition (also at 100ng/well), the median LU was 83,863 LU for the known positives (including standards) and 329.5 LU for the known negatives. The ranges were 362,134 LU and 454.5 LU respectively.

There was little evidence of a difference between the proteins, especially at the lower concentration 50ng/well (p=0.5600) or 100ng/well (p=0.9168). At 100ng/well, the SNRs both the negative samples (known negatives, so excluding CTC-19 samples) (p=0.4238) and the known positive samples (p=0.4688) were comparable. While both proteins looked initially promising, the spike-coated format was chosen to pursue going forward because of its improved dynamic range, despite the antigen being comparatively more difficult and expensive to obtain. These data are reanalysed in 3.9.2 to narrow down the optimal concentration of spike protein to coat plates with.

3.10 SARS-CoV-2 Spike-RBD Bridging Assay Optimisation Results

3.10.1 A variety of buffers could be used to dilute unlabelled protein to coat plates

To determine which buffer the unlabelled spike protein should be diluted in before being used to coat the plates, the protein was diluted to the same concentration (2.5mg/ml) in four buffers – Phosphate-Buffered Saline (PBS) pH7.4, a carbonate buffer pH9.6, and Tris-Buffered Saline (TBS) at pH7.6 and pH10. More detailed descriptions of the buffers are included in appendix 5.1.

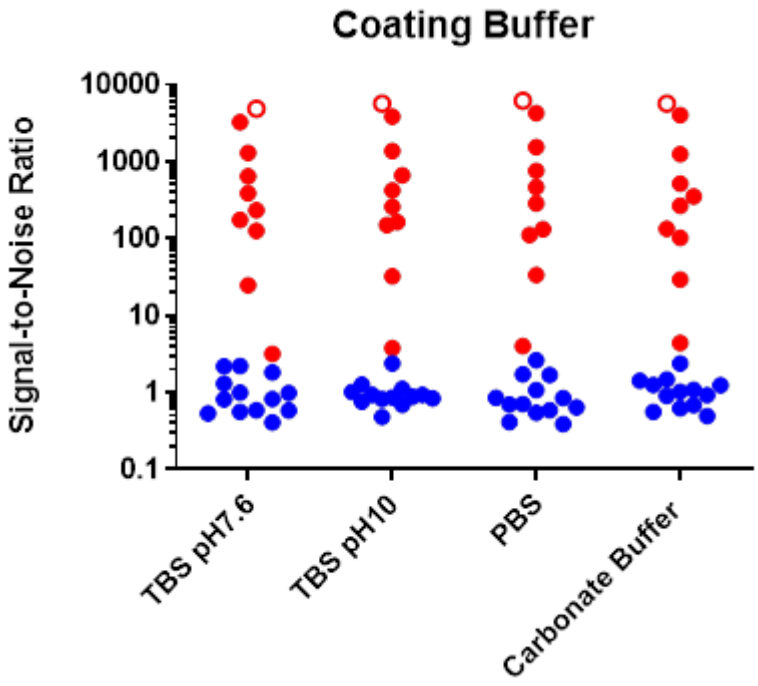

Figure 3-21 Spike-RBD Bridging Optimisation: Coated Protein Diluent. A plot of signal-to-noise ratio (SNR) from investigating the four different buffers to dilute the sike protein to 100ng/well in: Phosphate-Buffered Saline (PBS) pH7.4, a carbonate buffer pH9.6, and Tris-Buffered Saline (TBS) at pH7.6 and pH10. Red points are known PCR test positive samples and blue points are known negative serum samples, mostly pre-pandemic. Red unfilled circles are samples from individuals who were symptomatic and suspected to have COVID-19 but were not PCR tested. Each data point represents the SNR of the mean of two replicates.

For the TBS pH7.6 condition, the median LU was 404,905 LU for the known positives (including PCR unconfirmed symptomatic) and 943.75 LU for the known negatives. The ranges were 5,123,440 LU and 132,334 LU respectively. For the TBS pH10 condition, the median LU was 352,716.5 LU for the known positives (including PCR unconfirmed symptomatic) and 756.5 LU for the known negatives. The ranges were 4,748,064 LU and 125,071.5 LU respectively. For the PBS condition, the median LU was 369,699 LU for the known positives (including PCR unconfirmed symptomatic) and 614.25 LU for the known negatives. The ranges were 4,909,279 LU and 88,050 LU respectively. For the carbonate buffer condition, the median LU was 296,009.5 LU for the known positives (including PCR unconfirmed symptomatic) and 883.25 LU for the known negatives. The ranges were 4,752,336 LU and 111,640.5 LU respectively.

There initially seemed to be little evidence for differences between any of the four buffers ($p=0.1353$), especially when solely analysing the negative samples ($p=0.1558$). While some evidence

of a difference did arise when looking only at positive samples (0=0.0076), graphically the results looked very similar across all four conditions. Due to its relative inexpensiveness and simplicity to make, the decision was made to use PBS going forward.

3.10.2 Coating plates with 100ng/well is the optimal concentration of unlabelled spike protein

Several assays were carried out to determine which concentration of spike protein to coat the plates with. Initially, 50, 100, 200, and 400ng/well were tested, with evidence of a difference across the conditions (p=0.0013). The signal decreases as protein concentration increased, for example the median of the SNR from samples from PCR-positive or symptomatic/suspected COVID-19 patients was 228.74 in the 100ng/well condition, but dropped to 84.31 at 400ng/well.

With this in mind, a second experiment was performed looked at decreasing the coating concentration further – testing 12.5ng/well, 25ng/well, 50ng/well, and 100ng/well. Graphically, across both experiments, the background seemed unaffected by the coated protein concentration; and this was supported by statistical analysis of the second experiment's negative samples (p=0.9343). However, when considering all the samples (p=0.0028) or just the known positive samples (p=0.0006), there was evidence of a difference between the conditions in the second experiment.

The opposite pattern to the first experiment appeared. As the concentration of spike protein decreased, the median SNR of the samples from PCR-positive or symptomatic/suspected COVID-19 patients this time decreased also, e.g. from 209.66 in 100ng/well to 108.53 in 12.5ng/well. Coating each well with 100ng of spike protein seemed to be optimal in achieving high SNR amongst known positive samples, with the signal decreasing as the concentration departed from that optimum in either direction.

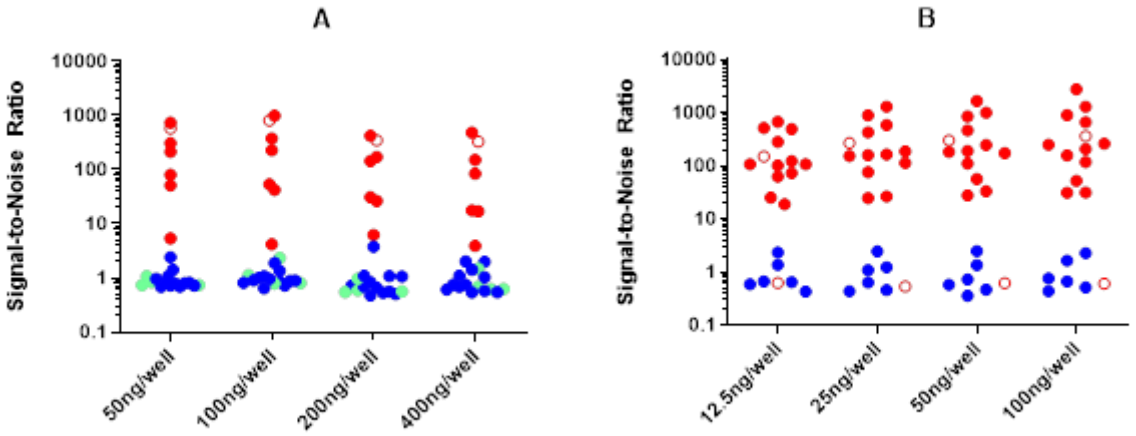

Figure 3-22 Spike-RBD Bridging Optimisation: Coated Protein Concentration. A: A plot of signal-to-noise ratio (SNR) from investigating four different concentrations (50, 100, 200, and 400ng/well) of SARS-CoV-2 spike antigen, diluted in PBS. B: A plot of SNR from a follow-up experiment investigating four concentrations (12.5, 25, 50, and 100ng/well) of SARS-CoV-2 spike antigen, diluted in PBS. Red points are known PCR test positive samples and blue points are known negative serum samples, mostly pre-pandemic. Red unfilled circles are samples from individuals who were symptomatic and suspected to have COVID-19 but were not PCR tested. Teal points are general population samples from the Capillary Testing for COVID-19 (CTC-19) study. Each data point represents the SNR of the mean of two replicates.

In the second experiment (panel B), for the 12.5ng/well condition, the median LU was 74,360 LU for the known positives (including PCR unconfirmed symptomatic) and 458 LU for the known negatives. The ranges were 466,389.5 LU and 359,468 LU respectively. For the 25ng/well condition, the median LU was 129,389.5 LU for the known positives (including PCR unconfirmed symptomatic) and 889 LU for the known negatives. The ranges were 1,061,637 LU and 477,720.5 LU respectively. For the 50ng/well, the median LU was 207,003 LU for the known positives (including PCR unconfirmed symptomatic) and 762.5 LU for the known negatives. The ranges were 2,762,763 LU and 900,693.5 LU respectively. For the 100ng/well condition, the median LU was 163,582 LU for the known positives (including PCR unconfirmed symptomatic) and 641.5 LU for the known negatives. The ranges were 1,481,859 LU and 756,912 LU respectively.

3.10.3 Reducing the number of washes increases the background of the assay

The assay had been washed via two runs of a four-wash programme on a BioTek ELx405 plate washer. To determine whether the number of washes in the assay could be reduced from eights washes to four (a single run of the programme), two plates were assayed together, with one washed four times and one eight times.

The original analysis (figure 3-23) showed little evidence for a difference between the two conditions (p=0.2467), but graphically the background did appear slightly raised in the four washes condition,

despite being statistically very similar (p=0.6322). The additional cycle of the automated washer did not take much time or use much buffer, so the eight-wash method persisted going forwards.

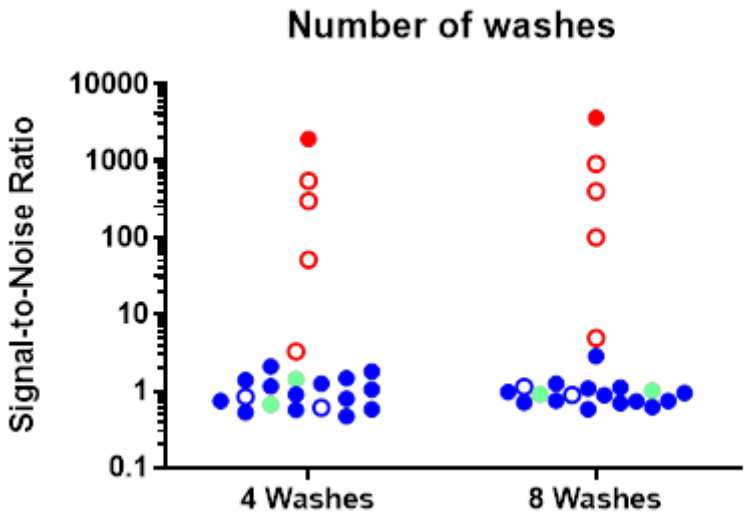

Figure 3-23 Spike-RBD Bridging Optimisation: Number of Washes. A plot of signal-to-noise ratio (SNR) from investigating washing plates with four cycles or eight cycles of Denver LIPS, performed with a BioTek ELx405 plate washer. This experiment was later repeated (data not shown). Red points are known PCR test positive samples and blue points are known negative serum samples, mostly pre-pandemic. Red unfilled circles are serum samples from individuals who were symptomatic and suspected to have COVID-19 but were not PCR tested. Blue unfilled circles are known negative plasma samples. Teal points are general population samples from the Capillary Testing for COVID-19 (CTC-19) study. Each data point represents the SNR of the mean of two replicates.

For the 4 washes condition, the median LU was 380,259 LU for the known positives (including PCR unconfirmed symptomatic) and 1,103.25 LU for the known negatives. The ranges were 2,448,804 LU and 2,047.5 LU respectively. For the 8 washes condition, the median LU was 276,970 LU for the known positives (including PCR unconfirmed symptomatic) and 610.5 LU for the known negatives. The ranges were 2,502,776 LU and 1,553 LU respectively.

Later, the experiment was repeated with more samples (data not shown) and this time there was a difference (p<0.0001), with the PCR-negative or pre-pandemic samples being unaffected (p=0.0946) but the median SNR of the PCR-positive, symptomatic, or standard serum samples being decreased in the four wash condition (19.91 vs 29.53 in the eight wash condition). This provided evidence that the correct decision was made at the time - while the background is genuinely not affected, the decreased washes did somehow decrease signal.

3.10.4 Coated plates can be stored up to 3 months at 4°C

Plates needed to be coated with spike and then blocked the next morning, which took time each assay day and limited the number of days assays could be performed on. To determine how long plates coated with spike protein could be stored, an assay was performed using the same samples on plates coated with 100ng/well spike protein the previous day, one month prior, two months prior, or six months prior and stored at 4°C in a sealed plastic bag with a sachet of desiccant.

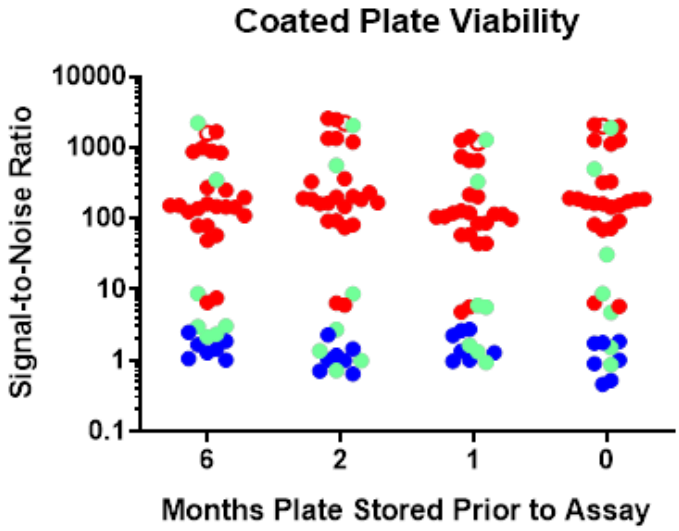

Figure 3-24 Spike-RBD Bridging Optimisation: Coated Plate Viability. A plot of signal-to-noise ratio (SNR) from investigating assaying with plates coated with 100ng/well up to six months prior to being used in an assay. Plates were stored at 4°C in a sealed plastic bag with a sachet of desiccant. Red points are known PCR test positive samples and blue points are known negative serum samples, mostly pre-pandemic. Red unfilled circles are samples from individuals who were symptomatic and suspected to have COVID-19 but were not PCR tested. Teal points are general population samples from the Capillary Testing for COVID-19 (CTC-19) study. Each data point represents the SNR of the mean of two replicates.

For the 6 month condition, the median LU was 278,464 LU for the known positives (excluding standards) and 2,669.5 LU for the known negatives. The ranges were 3,098,720 LU and 13,118.5 LU respectively. For the 2 month condition, the median LU was 282,016 LU for the known positives (excluding standards) and 1,483.5 LU for the known negatives. The ranges were 3,825,040 LU and 2,432 LU respectively. For the 1 month condition, the median LU was 276,088 LU for the known positives (excluding standards) and 3,219 LU for the known negatives. The ranges were 3,416,666 LU and 4,235 LU respectively. For the 0 month condition, the median LU was 361,276.5 LU for the known positives (excluding standards) and 2,034 LU for the known negatives. The ranges were 4,273,848 LU and 2,823.5 LU respectively.

The background of the assay remained unaffected by storage even up to 6 months ($p=0.2615$), but the signal did vary ($p<0.0001$). The median SNR of positive standards, QCs, and sera from PCR-positive COVID-19 patients ranged from 105.59 to 170.97 – around a 1.6-fold increase - and was not considered meaningful. Plates stored for up to six months were considered acceptable to use going forward.

3.10.5 Room temperature label incubation is sufficient to achieve good and distinct range of positive signal

To determine whether the 2-hour label incubation should be at room temperature or at 4°C, two plates were assayed together, with one incubated in the refrigerator and the other not.

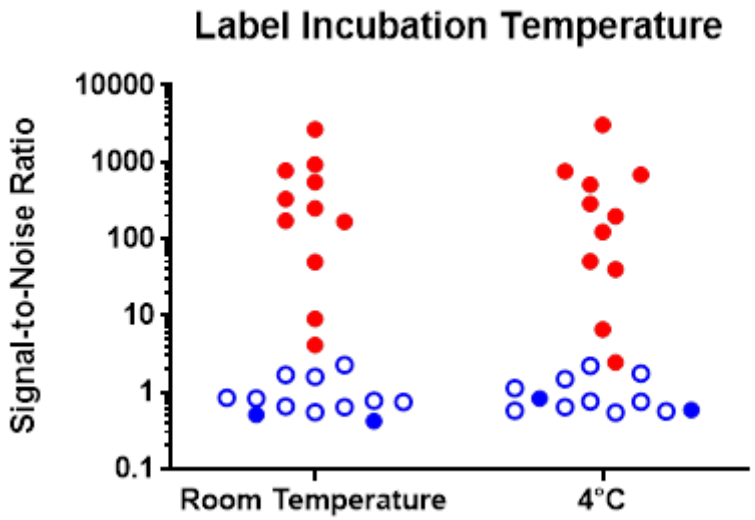

Figure 3-25 Spike-RBD Bridging Optimisation: Label Incubation temperature. A plot of signal-to-noise ratio (SNR) from investigating incubating sera (1.5µl) and NLuc-RBD label (37.5µl) for 2 hours at either room temperature or at 4°C. Red points are known PCR test positive samples and blue points are known negative serum samples, mostly pre-pandemic. Blue unfilled circles are known negative plasma samples. Each data point represents the SNR of the mean of two replicates.

For the room temperature condition, the median LU was 345,024.5 LU for the known positives (including PCR unconfirmed symptomatic) and 1,049.5 LU for the known negatives. The ranges were 3,685,488 LU and 2,555 LU respectively. For the 4°C condition, the median LU was 237,098.5 LU for the known positives (including PCR unconfirmed symptomatic) and 917.5 LU for the known negatives. The ranges were 3,691,717 LU and 2,017.5 LU respectively.

There was evidence of a difference between the two conditions (p=0.0233). There was less evidence of a difference in the known negative samples (p=0.8311) compared to a similar number of known positive samples (p=0.537). The medians were incredibly comparable however, and graphically the room temperature condition appeared to show better discrimination between the known negative and positive samples. Not having to refrigerate the incubation also made the assay logistically easier to carry out in a laboratory which runs many other assays which are clearly improved by refrigerated incubations.

3.10.6 Casein in Label Buffer does not lower the background

In concurrently developed liquid phase assays, casein in the label buffer appeared to reduce the background (data not shown). To determine whether the background of the bridging assay could also be lowered by this, several different experiments ended up needing to

occur. In the first experiment, NLuc-RBD label was diluted in Denver LIPS buffer containing either 0.05%, 0.1%, 0.2%, or no casein. Higher concentrations of casein were not considered viable as the casein was already 1% in PBS so the more casein added, the more Denver LIPS is replaced with PBS.

There was evidence of a difference between the groups, (p=0.0131), however this difference does not appear to be in the negative samples (p=0.9396). There were differences in the signal (p=0.0038), but these differences fluctuated with no obvious casein-causative pattern (the median SNR of the positive samples increased with 0.05% casein but decreased greatly at 0.1% before peaking at 0.2% casein) and were not great enough to be considered meaningful (the greatest difference was about a 1.8-fold change between 0.1% and 0.2% casein).

While it seemed that casein had no effect on the assay background, the first experiment had relatively few samples (negative n=6) per condition, so it was repeated looking at 0.05% casein with additional, mostly negative (n=22), samples. This provided what we believed to be a definitive answer on the question of reducing background – there was little evidence for a difference between the two conditions (p=0.1355).

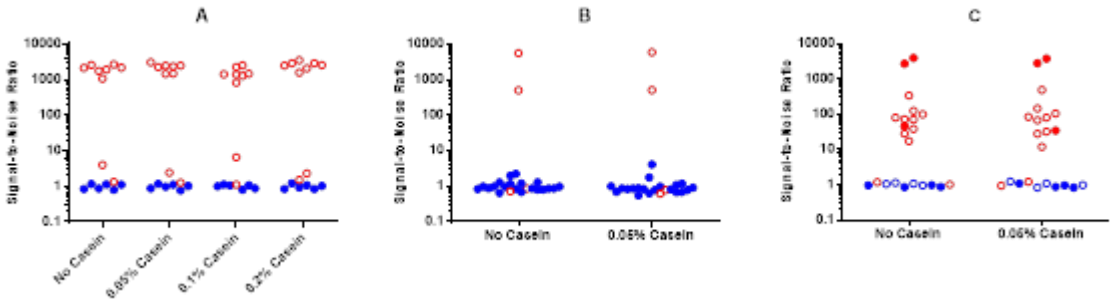

Figure 3-26 Spike-RBD Bridging Optimisation: Casein in Label Buffer. A plot of signal-to-noise ratio (SNR) from three experiments investigating varying concentrations of casein in the label buffer. Casein was diluted from a 1% solution in PBS. Panel A shows investigation of a range of concentrations – 0.05%, 0.1%, and 0.2% compared with no casein. Panels B and C look at 0.05% casein in a larger sample set, B with more negative samples, and C with more positive samples to look at the difference casein had on background and signal respectively. Red points are known PCR test positive samples and blue points are known negative serum samples, mostly pre-pandemic. Blue unfilled circles are known negative plasma samples. Each data point represents the SNR of the mean of two replicates.

In the third experiment, panel C, for the no casein condition, the median LU was 42,667.5 LU for the known positives (including PCR unconfirmed symptomatic) and 579.25 LU for the known negatives. The ranges were 2,356,750 LU and 163 LU respectively. For the 0.05% casein condition, the median LU was 41,036.75 LU for the known positives (including PCR unconfirmed symptomatic) and 540.25 LU for the known negatives. The ranges were 2,105,684 LU and 225 LU respectively.

However, we decided to re-visit the condition once more, to similarly assess the effect on positive signal in more samples. This third experiment provided a much more definitive

answer, with little evidence for difference between the conditions regardless of whether you considered all the samples (p=0.9493) or only the known/suspected positive samples (p=0.8077). It was therefore decided not to include casein in the label buffer going forward.

3.11 Spike-RBD Bridging Threshold Setting

Based on sera from 401 pre-pandemic individuals, the threshold based on Youden's index (a compromise between best sensitivity and specificity) percentile was 0.75 units. In a ROC analysis with an additional 46 samples from PCR-confirmed positive COVID-19 patients, the AUC was 0.997 (95% CI 0.993-1.000).

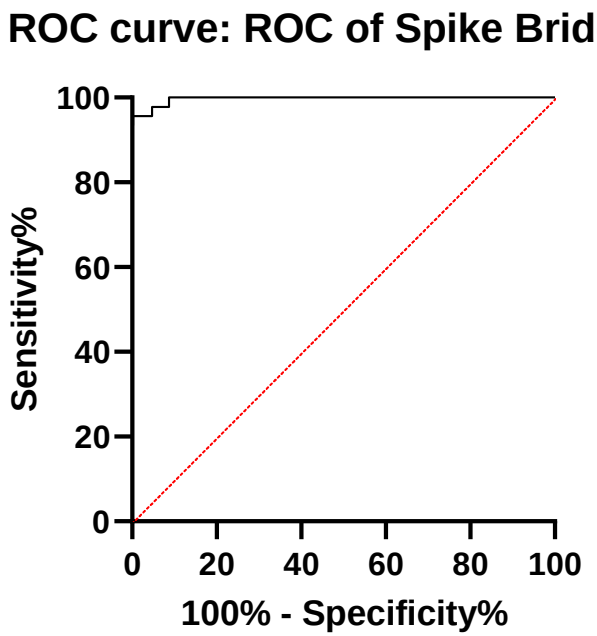

Figure 3-27 Receiver Operator Characteristic (ROC) Curve for the Spike-RBD bridging assay. Based on sera from 401 control individuals, taken pre-pandemic or from people who tested negative by PCR, and 46 samples from COVID-19 patients who tested positive by PCR. AUC = 0.997 (95% CI 0.993-1.000).

3.12 Comparison with the Roche assay

The Roche Elecsys assay format is an ECL assay described in section 1.5.4. First approved in early May 2020[141], the test was one of the first available. While there has been difficulty and hesitation to declare a gold standard[142], the Roche Elecsys N assay would be a frontrunner, with a clinical sensitivity of 99.5% and specificity of 99.8% by 14 days post-positive PCR test[143]. Samples (n=182) were tested in both the Roche Elecsys N assay and the Spike-RBD Bridging assay. These samples were taken before the vaccines to the spike protein were

developed, so positivity in either test is indicative of natural infection, although each assay is still detecting antibodies to different viral proteins.

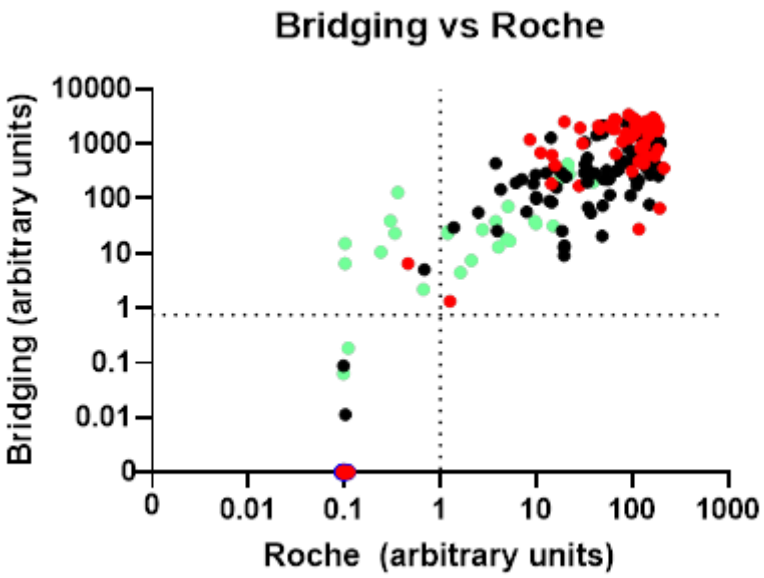

Figure 3-28 Graph comparing results of 182 samples in the Roche N and Spike-RBD bridging antibody tests. No SARS-CoV-2 infection (blue, n=6), acute infection (<3 weeks since positive PCR test or symptom onset, teal, n=32), early convalescence (3-12 weeks since positive PCR test or symptom onset, black, n=89), late convalescence (<12 weeks since positive PCR test or symptom onset, red, n=55). The two assays agree in negativity in 15 samples, including all 6 pre-pandemic samples. There are nine samples, mostly acute infections, which the bridging assay detects as positive but the Roche assay does not.

Signal-to-noise ratios were also calculated using the mean of the raw units (units as plotted above for Roche and mean and LU for the bridging) from the 6 pre-pandemic control samples. For the acute samples, the median SNR was 24.4 in the Roche assay and 111.3 in the bridging assay. For the early convalescent samples, the median SNR was 496.1 in the Roche assay and 1,697.2 in the bridging assay. For the late convalescent samples, the median SNR was 1,097.8 in the Roche assay and 9,431.5 in the bridging assay.

The bridging test detected anti-spike antibodies in 7 samples from individuals with acute SARS-CoV-2 infection which the Roche test did not pick up. This agrees with the Roche assay's reported much lower clinical sensitivity of (60.2%) <7 days from positive PCR test, although contradicts reports of antibodies to the N protein appearing earlier in the disease than antibodies to the spike protein.

3.13 Spike-RBD Bridging Assay Validation

The Spike-RBD bridging assay, along with three concurrently developed isotype-specific liquid-phase LIPS assays, was validated in 807 samples via great collaborative effort as described in Halliday et al. 2022[144]. Separate thresholds based on Youden's Index were set depending on disease progression. At a specificity of 98.5% the sensitivity was 78.7% in patients with acute COVID-19 infection (<21 days since positive PCR test or symptom onset), 92.4% in COVID-19 patients in early convalescence (3-12 weeks since positive PCR test or

symptom onset), and 94.3% in COVID-19 patients in late convalescence (>12 weeks since positive PCR test or symptom onset).

4 Discussion

Over the course of this MSc project, two novel assays with low blood volume requirements and high throughput potential have been optimised and validated. Through careful investigation of a range of conditions, including concentration of free luciferase-tagged antigen and of unlabelled antigen bound to the plate, these assays achieved good specificity and sensitivity in the well-characterised cohorts described in this thesis. Many existing antibody detection methods in both the field of T1D and SARS-CoV-2 are ill-suited for large-scale screening due to use of radioisotypes, large sample volume requirements, or being considered too high cost. The IA-2A and Spike-RBD bridging assays described in this thesis have acted as proof of concept for a novel "bridging assay" format well-suited to large-scale screening.

4.1 SARS-CoV-2 Spike-RBD Antibody bridging Assay

The bridging assay for antibodies to SARS-CoV-2's spike protein was highly sensitive and specific even at acute stages of COVID-19. It was able to identify all three relevant isotypes (IgG, IgA, and IgM – data not shown), meaning target populations could be screened with a single assay. At a specificity of 98.5%, the sensitivity ranged from 78.7% in acute COVID-19 to 94.3% by late convalescence. While there is the possibility of cross-reactivity with antibodies to SARS-COV-1[145], prevalence of these antibodies is expected to be low (there have been no reported cases of the first Severe Acute Respiratory Syndrome (SARS) anywhere in the world since 2004[146]). Reports of cross-reactivity with other coronaviruses in more common circulation, such as HKU1, 229 E, OC43, NL63, vary by method[147,148].

4.2 PTP-IA-2A Bridging Assay

This bridging assay for islet autoantibodies to the PTP region of IA-2 was 70% sensitive at a specificity of 99%, based on sera from 265 schoolchildren (aged 9-13) and 135 individuals with T1D (aged 1-21, samples taken within three months of diagnosis). Islet autoantibody bridging assays will benefit from being submitted to future IASP workshops. This will facilitate comparisons not only with the other assays run in the Bristol laboratory, but with a vast array of islet autoantibody tests being performed in laboratories across the world.

4.3 Strengths of the bridging assay format

The bridging assay format builds on existing methods, utilising the plate-bound antigen from an indirect ELISA[106], and the luciferase conjugate reporter system from LIPS assays[149]. The IA-2A bridging assay has shown that the format is capable of good agreement with the gold standard RBA, while circumventing the need for radioisotopes and centrifugation immunoprecipitation. The luminescence signal is generated through reagents which are easier to store and dispose of than radioisotopes. This also allows the assay to be transferred to more laboratories – an obvious advantage in large-scale screening.

4.3.1 Bridging assays detect all isotypes of antibody response

Unlike assays involving a specific secondary antibody or Ig-agarose/Sepharose, bridging assays detect all immunoglobulin isotypes. This is of benefit when screening for conditions where there is a breadth of isotype response – for example, when detecting autoantibodies to tissue transglutaminase, the IgA response is of particular use, so much so that some RBA methods add anti-IgA agarose in addition to protein A Sepharose[150]. With a bridging assay, this IgA response would be detected at no extra cost. This feature can also reduce the number of different tests needed to get a complete antibody profile – for example, there exist distinct liquid-phase LIPS assays for IgG, IgA, and IgM responses to SARS-CoV-2[82,144]. If you wanted to test for the total antibody response, the LIPS method would require testing the sample thrice compared with a single bridging assay, although the bridging does not provide the proportions of each response, only the sum. Being able to detect all isotypes also improves the sensitivity of the assay, as individuals positive only for one isotype are less often missed. Other solid-phase assays only detect one isotype of antibody, determined by reagents such as the secondary antibody in an ELISA. Assay formats such as the sVNT and ADAP tend to detect all isotypes as well, although ADAP can be altered to detect a particular one, which gives the system broader applications compared with the bridging format[151]. The variety of electrochemiluminescence methods mean some are isotype-specific due to their conjugate antibodies, while others, like the Roche ECLIA/CMIA and islet autoantibody multiplex ECL, are more akin to the bridging assay, being solely able to detect all isotypes.

The bridging assay's ability to detect all isotypes of antibody, while useful for screening, may limit the assay's use in a research context. For example, if trying to answer questions about a specific isotype or subclass response, the bridging format is of limited use. Alternative

assays such as LIPS, ELISAs, or electrochemiluminescence assays are better-suited for this, as the Ig-agarose/Sepharose or conjugate antibodies can be exchanged depending on the isotype of antibody requiring detection.

4.3.2 Bridging assays only capture specific antibodies

Non-specific antibodies are able to bind to the Ig-agarose/Sepharose used in assays such as RBA and LIPS via their constant regions. These non-specific antibodies will not be detected, as there is no other labelled antigen present, but the Ig-agarose/Sepharose (an expensive reagent) must be added in excess to prevent saturation. Conversely, the bridging assay format utilises the bivalent nature of immunoglobulins' variable regions, meaning both the binding of the antibody to the reporter system and the trapping of the antibody to the solid-phase are both specific antigen-antibody binding. The plates are coated with the specific antigen and blocked with 1% casein to prevent non-specific binding. Each antibody having to bind its complementary antigen twice in order to be detected may increase the specificity of the assay format. This is also the case in assays such as the Roche ECLIA tests, and is theorised to be responsible for differences between tests that utilise this bivalent antibody binding and other chemiluminescence assays which only require the antibodies to bind a single antigen[152].

Bridging assays also capture any binding antibodies, rather than only neutralising antibodies as in tests such as the sVNT and some ELISA methods[152]. While neutralising antibodies are strongly correlated with protection/immunity[153], they are only a fraction of the total antibody response; tests that also detect non-neutralising antibodies may be able to elucidate more of the breadth of the humoral response to SARS-CoV-2.

4.3.3 Bridging assays can be sensitive and specific

Achieving a balance of specificity and sensitivity is an essential consideration when setting a threshold for an assay. While the Spike-RBD bridging assay proves the bridging format is capable of exceptional sensitivity and specificity compared to the Roche Elecsys N assay, the IA-2A bridging assay does not appear to overcome all its existing competitors in terms of sensitivity – for example, at 95% specificity, the IA-2A sensitivity of ADAP was reported to be 74%, slightly greater than that of the IA-2A bridging assay[127]. However, the IA-2A bridging assay's sensitivity was greater than several less novel methods, 70% compared to 62% in an

RBA and 54% in a plate-based ELISA[154], although these gold standards are also rivalled in sensitivity and specificity by more novel methods like ADAP and ECL[155]. These measures of sensitivity will depend on the sample set tested and the specificity, controlled through the threshold for positivity. Additionally, most IA-2A assays measure antibodies to full-length IA-2ic, so are difficult to directly compare to the IA-2A bridging assay which only detects antibodies to the PTP region of IA-2. Use of the full-length antigen could improve the sensitivity of the IA-2A bridging assay.

Overall, the two bridging assays that have been developed as part of this project do succeed in being sensitive and specific, and correlated well with other existing methods, be it an islet autoantibody RBA or the Roche SARS-CoV-2 antibody test.

Islet autoantibodies are rare in the general population, so tests for them need to be highly specific. This can come at the detriment of their sensitivity. Another reason the sensitivity of islet autoantibody assays tend to be lower than that of tests for anti-viral antibodies is that the antibodies are less consistently produced. For example, it has been reported that there is a 98.8% total anti-spike antibody seroconversion rate in individuals with COVID-19[156], whereas one study found that only 78% of individuals newly diagnosed with T1D have IA-2A[140].

4.3.4 The Spike-RBD Bridging assay detects even acute infection

Experiments described in this thesis show that anti-spike antibodies can be detected by the Spike-RBD bridging assay within three weeks of SARS-CoV-2 infection, while the Elecys Anti-SARS-CoV-2 N protein Roche assay finds that antibodies are usually detected 21 days after infection. This contradicts reports that antibodies to the N protein appear earlier in infection than antibodies targeting the spike protein[63]. It is possible that the limited sensitivity of the Roche N assay in the early stages of infection, coupled with the Spike-RBD bridging assay's consistently good sensitivity, enables this effect to be overcome. However, it is notable that the bridging/Roche comparison included very few pre-pandemic samples, therefore it cannot be ruled out that the threshold for the Roche Elecsys N assay is more specific than that of the Spike-RBD bridging.

Other SARS-CoV-2 antibody tests, like the sVNT, also suffered from reduced sensitivity in early infection[157], giving the Spike-RBD bridging assay a markedly lower false negative rate,

as early testing (<21 days of symptom onset) is more reliable. This also means the bridging assay can give a better estimate of current seroprevalence, without the three-week delay in positive antibody result.

4.3.5 Bridging assays require very low sample volume

Another criterion to consider for large-scale screening is a low sample volume requirement. While many existing tests also fulfil this desire, bridging assays are no different, requiring just 2-3µl of sera. Its serum volume requirements are most comparable to LIPS assays, and there is no requirement for any dilution or pre-treatment as in some methods like sVNT[158] or ECL assays[114]. The ADAP method uses slightly more sample, especially in the automated protocol[129], but the bridging assay may also require an increased sample volume if automated to that level in the future.

Requiring such low volumes of sera means there would be no need for invasive large-volume veinous blood draws[159]. Capillary blood sampling would be the method of choice for serological screening of large populations because of a number of benefits it has compared to traditional venous blood draws, which are generally more painful[50,160,161], are commonly associated with fear or phobia[162], and require a trained phlebotomist which costs money, time, and requires travel for the patient/participant. Finger prick sampling is preferred by people being screened[50] as well as parents of children being screened[163], and allows individuals to collect the samples themselves. This may improve acceptability, with one study finding 82% of participants preferred self-collection of capillary blood samples to outpatient venepuncture[50]. Additionally, recent experience with lateral flow antigen testing for SARS-CoV-2 has shown that if large-scale screening is desired, individuals need to be able to collect their own samples themselves because there are not enough healthcare professionals to support such a widespread initiative.

Capillary blood sampling by postage allows much cheaper sample collection, at approximately £5 to send a kit and have it returned to the laboratory. This method also has additional conveniences in recruitment, for example during COVID-19 lockdowns where individuals could not attend a non-urgent medical appointment, or when attempting to recruit whole families such as in the BOX Family Study, where not all first-degree relatives of

the proband necessarily attend the clinic visit where recruitment occurred, so home postal kits may have a better chance at recruiting the desired relatives.

The Fr1da study relied on phlebotomists taking the samples from the young participants, which may have improved sample volumes collected, but greatly increased the cost of the programme as the clinicians were reimbursed €10 per recruited participant[49]. While Fr1da[49] and other studies report success in collecting sufficient volumes of sera via capillary sampling, with minimal pain to the participant[159], there are limited published data on participants performing the capillary blood draw on themselves. However, this has been investigated as part of TrialNet, and that study found 84% of samples were sufficient in volume for testing of GADA, IA-2A, ZnT8A, and IAA[50]. The BOX Family Study has used this sample collection method since 2015[164], indicating its success.

This method of sample collection may not be possible for large-scale screening with tests such as the ELISA (as used in Fr1da[49]) or sVNT, which require larger volumes of serum not commonly achieved with home capillary pricks.

The Spike-RBD bridging assay was also used to test a small number of saliva samples (which can also be easily collected via postal kits) with promising results, especially at higher sample volumes (data not shown).

4.3.6 Bridging assays are low cost to perform

The Bristol laboratory where the bridging assay was developed is currently progressing toward United Kingdom Accreditation Service accreditation for RBA and LIPS assays, so the costing business case is under discussion with the University of Bristol Finance Department. Current bridging assay cost estimates are therefore preliminary.

The cost of assays is not always easy to ascertain, however it can be assumed that reagents such as conjugated antibodies (as in CMIA methods) are relatively expensive. Bridging assays are low cost compared to many existing antibody detection methods. One of the more expensive reagents for the NLuc bridging assays is the substrate provided in the Nano-Glo® kits from Promega. However, in both applications detailed here, the luciferase substrate has been able to be diluted to reduce the cost - in half for the Spike-RBD Bridging assay, and by two thirds for the IA-2A Bridging assay. This cost-saving measure has also been effective in several unpublished LIPS assays. The removal of the requirement for Ig-

agarose/Sepharose, which accounts for over a quarter of the cost of an RBA or LIPS assay, also reduces the cost of bridging assays significantly over these liquid-phase competitors.

The other potentially substantial costs are the proteins – unlabelled to coat plates, and NLuc-tagged to generate signal. Commercially purchasing protein could increase costs above that of the time it takes a technician to express and purify it in-house. More analysis must be done, however it is likely that the bridging assay cost will remain lower than for-profit commercial assays or tests otherwise requiring numerous specific constructs.

As shown in this project, the concentration of protein needed to coat plates varies by antigen. If a particular antigen appears to require a very high concentration then it may be financially wiser to utilise one of the alternative coating methods demonstrated here. The economic benefit is dependent on the comparative costs of protein expression or commercially bought antigen versus pre-coated plates and tag attachment, but by using a GST or biotin tag to coat glutathione or streptavidin/NeutrAvidin-coated plates, it is possible to achieve a functional assay with much lower concentrations of antigen.

Until a multiplex bridging assay is developed, the method will not be competitive to use to screen large populations for a several islet autoantibodies due to needing to test the same sample multiple times. The ADAP multiplex test for GADA, IA-2A, and IAA costs about 2.5 times that of an equivalent electrochemiluminescence test from MSD. Both of these novel tests currently cost much more than older multiplex methods such as the three-screen ELISA, the RSR list price of which is around one quarter to one third of the cost of this MSD kit[48,101]. However, Fr1da appears to have been able to utilise this ELISA at less than a third of its listed cost, between €1.40-3.60 per sample[48], indicating that many of these assays' costs may end up being lower if implemented in large-scale screening.

4.3.7 Bridging assays can be high throughput

The bridging assay format is relatively high throughput (for example, in a standard 35-hour work week, approximately 24 plates could be assayed, equating over 800 samples), however automation is largely considered vital to improve assay throughput to such a degree where general population screening would be considered feasible. A recent ADAP paper describes a 4 to 6-fold increase in throughput with the automated method compared with the manual method, and an annual throughput of up to 72,000 samples per instrument per year[129].

While automation was not included as part of this project, the plate-based format could facilitate future attempts to automate the assay. Indeed, the Spike-RBD bridging assay plate-coating profile has been set up on a TECAN robot. Unlike the related RBA and LIPS assays, there is no immunoprecipitation that requires centrifugation - in fact the equivalent wash step is already largely automated via a BioTek ELx405 Plate Washer. The SARS-CoV-2 Spike-RBD bridging assay also has increased throughput over its liquid phase equivalent for IgG LIPS, which has highly concordant results but requires competing with unlabelled RBD protein, effectively halving the throughput[144]. It is not yet clear whether circumventing competitive displacement is an overall strength of the assay format, but this would be an advantage of any future bridging assay detecting IAA[100].

Even in its current state of limited automation, a bridging assay result can be generated in just one day, and large quantities of plates can be counted at once using the stacker and auto-loading mechanical arm of the Hidex Sense Beta luminometer. One of the more technician-time-intensive aspects of the assay is blocking the coated plates with 1% casein, but even this should be amenable to automation if the assay were to be scaled up for widespread rollout.

For two plates (~75 samples plus standards and controls) the time required for each step of the assay is summarised in table 4-1 below. In addition to this there are incubations (freshly coated plates left overnight, blocked plates air-dry for 2-3 hours, sera and label incubated for 2 hours, mixture incubated in coated plate for 1.5 hours) which total 3.5 hours on the day of the assay, during which time the technician(s) could be doing other work. Interpolation of the raw LU to standardised units, checking of quality control parameters, and input of data into results databases to make use of it requires additional technician time, but the assay is still capable of a fast turnaround which may improve acceptability of a screening programme to the public.

Process	Time Required (for 1 technician, manually)	Potential for Automation?
Diluting antigen and coating plates	10 minutes	Yes, preliminary automation has been tested off-site via a Tecan Liquid Handling system
Blocking coated plates	20 minutes	Yes
Aliquoting sera into plates	45 minutes	Possibly but would require a large dead volume of serum, so unlikely to be automated in the event of large-scale screening
Diluting NLuc-tagged antigen	15 minutes	No, but time required does not increase with number of plates
Adding dilute label to sera	10 minutes	Yes
Transferring 26µl to coated plate	15 minutes	Not at current volumes
Washing plates	10 minutes	Yes, already automated with a BioTek ELx405 Plate Washer
Counting plates	20 minutes	Yes, already automated with the stacker of a Hidex Sense Beta luminometer
General set-up, making buffers, etc	20 minutes	No

Table 4-1 Table summarising bridging assay steps and automation potential.

4.4 Limitations of the bridging assay format

4.4.1 Bridging assays have great intra-assay variation

The main limitation of the bridging assay format as it currently stands is the high error and repeat rate observed. This was especially notable in the Spike-RBD bridging assay when measuring vaccine responses, likely due to the incredibly high antibody titres. Attempts to rectify this issue included experimenting with coloured additives in the diluted protein used to coat plates, to ensure all wells were coated evenly. For the Spike-RBD Bridging assay, the volume of sera and label were scaled up, resulting in 1.5µl of serum incubated with 37.5µl of label (as opposed to the previous 1µl and 25µl), 26µl of which was transferred to the coated plate later in the assay. Other troubleshooting involved centrifuging microplates before removing their lids, or purchasing different, more secure sealing lids/mats altogether. This will continue to be considered as development and validation of additional bridging assays occurs. The replicate error rates were highly variable across plates/assay dates and are potentially influenced by laboratory temperature or other environmental factors. While it is unlikely false negative/positive results would be reported, especially if the low serum volume requirement was utilised for confirmational testing, the repeat rate may be higher than other methods, and that would bring additional cost.

This sort of information is rarely published, but existing methods are likely better than the bridging assay in this regard.

4.4.2 Plate-based assays can suffer from epitope obscuration

The bridging assay requires coating plates with antigen, which risks obscuring key epitopes. Whereas liquid-phase assays like the RBA and LIPS capture antibodies through binding of the fragment crystallizable (Fc) region of the immunoglobulin molecule to Ig-agarose/Sepharose beads, the bridging assay utilises the specific binding of the fragment antigen-binding (Fab) region to the plate-bound antigen. When the antigen is initially added to the high-binding plates, its orientation may be random, and a portion of the molecule would be accessible to antibodies. The complex kinetics at play here mean there may be a risk each time a plate is coated that the antigenic epitope in question is obscured to the extent that antibody binding is severely reduced, potentially resulting in false negative

results and great inter-assay variation. This phenomenon could be a contributor to the non-perfect correlation between the PTP-IA-2A results as measured by RBA and bridging.

This variation in solid-phase molecular orientation could also be the reason for the long-standing rates of discordance between the ELISA and RBA in DASP/IASP workshops[165]. Pending further studies of the way antigens coat plates and how stochastic this process is, more expensive liquid-phase assays like ADAP, ECL, and LIPS may have an advantage over the plate-based bridging platform. However, quality control samples allow inter-assay variations to be monitored, and there has been minimal evidence of epitope obscuration being an issue with the bridging assay format so far.

4.4.3 Bridging assays rely on existing luciferase constructs and Promega kits

Another limitation is the bridging assay's reliance on the Nano-Glo® kit from Promega. This product is expensive, although it is further diluted to mitigate that cost, and the bridging assay is still cheaper than many of its antibody assay peers. There could be issues with supply chains, or product discontinuation, but luciferases are becoming a popular reporting system, and unbranded alternatives are likely available. This is a theoretical limitation of many assays, for example there are limited suppliers of iodinated insulin for IAA RBAs. The machine and consumables for an ECL assay were also from a single supplier[166], as well as the bespoke liquid handling system currently automating ADAP[129]. On the other hand, Promega is an international company that offers shipping worldwide, which is a strength compared to products required in other assays which may only be available in certain countries.

The use of luciferase tags could also potentially impede the assay's ability to be multiplexed. This is firstly because there are currently only three different luciferase reporters on the market: Firefly Luciferase (FLuc), Renilla Luciferase (RLuc), and the NanoLuc Luciferase implemented here. This already means it would not currently be possible to screen for all islet autoantibodies in a single assay with antigen specific reporters. Additionally, the reporter conjugates NLuc and RLuc are unable to be multiplexed together. This incompatibility therefore restricts the multiplex possibility even further, although a combined signal reporter approach would still be possible, and incredibly useful when screening for things as rare as islet autoantibodies.

4.4.4 The Spike-RBD bridging assay is unable to differentiate between responses to vaccination and natural SARS-CoV-2 infection

Throughout the course of this project, global vaccination efforts have succeeded in rolling out a number of vaccines to the spike protein of SARS-CoV-2 (Pfizer BioNTech, Sputnik V, AstraZeneca, Moderna, etc) and whole virus approaches are in development (Valneva). Individuals who have been vaccinated using spike-based vaccines should mount an antibody response to the spike protein, and therefore test positive in this Spike-RBD bridging assay. Individuals who have been naturally infected with SARS-CoV-2 should mount a broader immune response, but this would include the highly immunogenic spike protein, so these individuals also test positive in the Spike-RBD bridging. In order to differentiate between these two responses (vaccine response and the humoral response to a natural infection), a different test would be needed, one that tests for the nucleocapsid (N) protein. The current vaccines do not target this protein, therefore the presence of antibodies to the virus' N protein is likely indicative of a natural infection.

Two approaches were developed for this. Work began on a bridging assay similar to the method optimised in this project but with an NLuc-tagged N protein label and plates coated with N protein. In addition to this, we carried out an ELISA method provided by Dr. Alice Halliday and her team in Cellular and Molecular Medicine, University of Bristol. The ELISA protocol is based on the RBD screening and spike confirmatory ELISA assays described by Krammer, Schumacher, and Amanet et al[167]. With assays to both spike and N protein available, work can proceed in tandem elucidating the humoral immune response in individuals (with and without type 1 diabetes) to both vaccine doses and natural infection.

Having a separate assay to detect antibodies to N protein is the common approach, with many ECLIA and ELISA methods having spike or N-specific tests, for example Roche's Elecsys Anti-SARS-CoV-2 and Elecsys Anti-SARS-CoV-2 S. With MSD's CLIA method however, depending on the antigens immobilised in their panel, multiplex detection of antibodies to spike and N protein (as well as to 8 other antigens) would be possible, with separate readout for each.

4.4.5 The biotinylated IA-2 is not suitable for long-term storage at 4°C

As described in 3.4.5, the biotinylated IA-2 version of the IA-2A bridging assay suffered a 10-fold decrease in light units, believed to be caused by degradation of the biotinylated antigen. Being stored at 4°C degrees, this was not unexpected, hence other aliquots of the protein were kept at -80°C for longer-term storage. While development of the biotinylated IA-2 version of the assay did not continue, it is expected that the deep-frozen aliquots of the biotinylated IA-2 would have continued to perform well, and could have been aliquoted into smaller volumes to minimise freeze-thaw cycles while being routinely stored at -80°C.

4.4.6 The IA-2A bridging assay uses a truncated antigen

A limitation of the IA-2A bridging assay as it stands is its reliance on GST-tagged PTP-IA-2 to coat the plates. While there is often epitope spreading of the autoantibody response to target the PTP region, it is the JM domain which contains the regions usually recognised in early pre-diabetes[35,168]. The PTP-IA-2A bridging assay is therefore fundamentally limited in its sensitivity due to the false negatives of individuals who are negative for anti-PTP region antibodies but positive for anti-JM region antibodies - although these individuals would typically be too young to be rapidly approaching disease onset. It would therefore be preferable to alter the assay to use plates coated with the entire intracellular region of IA-2 (IA-2ic). A pGEX6 plasmid containing genes to express GST-tagged IA-2ic was kindly provided by Dr. Michael Christie, and was transformed and expressed as described in the methods section, but the expression was unsuccessful, as previous attempts in pET42, pET332, and pET49 vectors had also been, with no obvious reason. This could be circumvented by the purchase of IA-2ic from companies such as RSR[101], although this would significantly increase the cost compared with expressing the protein in-house.

The use of this truncated protein is more a limitation of this project rather than the bridging format in general, as alternative epitopes of IA-2 could likely be substituted in with ease, requiring limited additional optimisation, as shown by early experiments coating plates with just the RBD portion of the spike protein.

4.5 Application: General Population Screening for Islet Autoantibodies

The primary application of a test suitable for large-scale screening of islet autoantibodies would be general population screening as a way of predicting T1D. This is something that

has been talked about for decades[169] and is now getting closer[170]. There are many benefits to the individual of being screened for pre-type 1 diabetes. The studies BABYDIAB, Diabetes Prediction in Skåne (DiPiS), TEDDY, DAISY, and DIPP, all found their paediatric participants presented with less DKA and lower HbA_{1c}[170]. Screening programmes could also identify at-risk individuals for recruitment into intervention trials, in order to research ways of preventing clinical onset of T1D.

Many of the WHO's criteria for screening have been satisfied for T1D (it is an important health problem; there is an accepted treatment; there are facilities for diagnosis and treatment; there is a recognisable latent and early symptomatic stage; there is an agreed policy on whom to treat as patients; case-finding could be a long-term continuous process)[171]. However, there are criteria which have yet to be fulfilled. Research remains to be done on whether a screening programme is acceptable to the population[171] (especially given the low uptake of testing and known psychological consequences of awareness to an increased risk of an incurable chronic disease[172]). Additionally, there is more to discover regarding the natural history of T1D and understanding the process of progression from islet autoantibody positivity to clinical disease onset[171].

The third and final criterion as yet deemed uncertain by the WHO is the economic balance of case-finding vs potential medical expenditure[171]. In the UK, it is estimated that the average cost of one patient's single episode of DKA is £2064[173], so this is how much money a screening programme could save the NHS per successfully identified at-risk individual. In the US however, as of 2015, saving the T1D-complications' healthcare costs would not be expected recover the cost of a potential screening programme[174], although this may be different in countries with universal healthcare. To date however, the expected financial worth of improvements to short-term and long-term quality of life through better metabolic control in individuals and families have not been fully evaluated.

While the existence of islet autoantibodies and their serological tests is satisfactory to the WHO, many existing tests fall short of the logistical challenges involved in such large-scale screening. Furthermore, features of the test affecting the participant burden (such as collection method and its relation to required sample volume) could improve acceptability of a screening programme. These, as well as the low cost, are the gaps that the IA-2A bridging assay aims to fill.

While the time to develop clinical type 1 diabetes can vary, seroconversion of islet autoantibodies can begin in early childhood. When deciding the age at which to screen a population, allowing full seroconversion to occur while ensuring individuals have not progressed to clinical disease is vital, so screening between the ages of two and six years appears optimal for good sensitivity. However, a better strategy could be to screen a smaller range of younger individuals, between 2 and 3 years of age, to catch early seroconverters before disease onset, followed by a second screen of the initially islet autoantibody negative individuals, to avoid missing those who seroconverted later[4,175]. Seroconversion to IAA is often the first to occur[175,176] followed by GADA[176], and it is these, but not IA-2A, which are more likely to be detected at these ideal screening age ranges[177]. However, a screening strategy can include an initial screen for some autoantibodies and then follow-up with the important remaining markers in those who screen positive. For example, the Fr1da study had success screening for GADA, IA-2A, and ZnT8A by multiplex ELISA and then confirming results and testing IAA in positives by RBA[49]. One justification for this is that IA-2A appears to be an important marker of progression to type 1 diabetes, as it is the most frequent autoantibody at diagnosis[176]. In the unlikely event of large-scale screening for a single islet autoantibody, IA-2A could be a stronger choice compared with single persistent IAA or GADA positive individuals who are much less likely to progress to disease[178].

The IA-2A bridging assay therefore could prove a useful tool in the goal of large-scale screening, and has acted as proof of concept for development of equivalent assays for other islet autoantibodies.

Prevalence of T1D in the UK is currently estimated to be around 400,000[65] of an estimated 67 million people living in the UK (0.6%). In new-onset T1D in Europe, the weighted mean prevalence of IA-2A has been found to be 74.9%[179]. Combining these statistical estimates, the total prevalence of IA-2A in the UK could be assumed to be around 0.45%. This is a reasonable but imperfect estimate as it combines percentage estimates from the UK with those from the whole of Europe, and does not include individuals positive for IA-2A who do not have T1D.

Because of this low incidence of islet autoantibodies in the general population, the majority of IA-2A bridging assay positive results may be false positives, meaning the positive predictive value would be very low, as with any islet autoantibody test. Similarly, the

negative predictive value would be very high because if the test is negative it is very likely true, again due to the low incidence.

The positive predictive value of the IA-2A bridging assay could be improved by raising the threshold of positivity, although this would sacrifice some sensitivity by missing some low IA-2A titre positive individuals. Another way to improve the positive predictive value in a screening programme would be to introduce a secondary test, for example using an ELISA, RBA, or LIPS assay as a follow-up confirmatory test. This method has been successfully implemented in several screening studies, including Fr1da which initially screened with a multiplex ELISA and then followed-up any positive individuals with RBAs[49]. The IA-2A bridging assay requires just 2µl of serum, leaving plenty of sample remaining for use in a confirmatory second test.

This low serum volume requirement is the one of the main advantages the bridging format has over the three-screen ELISA, which required 25µl of serum[49], and is likely to persist into a multiplex version of the assay. Testing children from the general population with a bridging assay and then confirming positive results by a low-volume liquid-phase RBA or LIPS assay may be an appropriate method of screening. Indeed, the two different formats of assay could also help identify/circumvent any issues related to obscured epitopes, while the low positive rate in the initial screen provides lower sample numbers more appropriate for the limited throughput of these secondary assays, as in Fr1da. This strategy would be especially effective if a multiplex islet autoantibody bridging method was developed.

Alternatively, single antibody bridging assays could be used as the confirmatory test in place of the previous gold standard RBA used in Fr1da. With this approach, ADAP may be a competitive choice for the initial screen, due to its existing automation strategy. This is contingent on the method's ability to be carried out in other laboratories, which has thus far proved challenging[180], and the cost to be significantly reduced, which should be feasible due to it being a PCR-based method. If the ADAP method meets these conditions and can demonstrate sensitive prediction of high-risk individuals (this has not been published), and the bridging assay served as a specific and sensitive confirmation of islet autoantibody positive individuals, this method of screening could be viable.

An ADAP multiplex screen positive rate of just 0.5%, in the context of three-year-olds in the UK general population, amounts to nearly 4,000 individuals[181] who would require confirmatory testing. This subset is small enough to be managed by the limited throughput of many existing methods, but large enough the bridging assay's cost effectiveness would make it an option competitive to alternative tests such as RBA or electrochemiluminescence assays.

4.6 Application: Large-scale screening for anti-SARS-Cov-2 spike antibodies

The Spike-RBD bridging assay began development in the Spring of 2020, before any vaccine was licensed in the UK, and had the potential to be a useful data-collection tool in large-scale serology screening. Since then, several vaccines have been developed, all targeting the spike protein, meaning the assay should detect an individual as positive if they are either vaccinated or have been naturally infected, or both, with no way to distinguish between the two. The ability of an assay detecting anti-spike antibodies to give a measure of disease prevalence is therefore limited in areas high vaccination uptake. However, while there has been intense investigation of infection and vaccination responses in the West, the COVID-19 vaccine distribution has been globally uneven. Much of Africa, as well as a handful of countries in Asia and other areas of the world, have had very limited access to the vaccines[86,182]. There are plans in place to help address this disparity[183], but until this is achieved assays such as this Spike-RBD bridging assay could help address questions of disease prevalence in these underserved areas.

The Spike-RBD bridging assay could have other applications in society. For example, in areas of the world with strict COVID-19 protection rules, a positive result in the Spike-RBD bridging assay (if accredited to give clinical advice) could be used in lieu of a vaccination record to prove immunity, in order to gain access to a workplace or public venue. This would allow equity to those individuals who were not vaccinated (currently estimated to be 7.4% of the UK population[184] - a large cohort which the Spike-RBD bridging assay would be well-suited to screen).

Having alternative assay formats available is important in understanding the breadth of the immune response, and this can be directly translational, especially when considering public health costs or mortality. Tests such as the Spike-RBD bridging assay could be used to inform

life-saving policy regarding, for example, booster doses of a vaccine - should everyone in a population be given one dose of a vaccine or should the most vulnerable in that population be given two doses, and the less vulnerable none?

As of 23rd March 2022, there have been 20,515,998 cumulative positive tests for COVID-19 in the UK[185]. This is not an ideal estimate of prevalence considering testing regimes did change over time, definitions of cases vary by nation, it is unlikely all test results are reported, and this possibly includes multiple positive tests from the same individual. If we assume this to be a reasonable estimate, this would give an estimated 30.6% incidence in the 67 million-strong population of the UK - a much higher prevalence than IA-2A. Taking the 98.5% specificity and 92.4% sensitivity the Spike-RBD Bridging has shown in convalescent COVID-19 patients, this would give a positive predictive value of ~96% and a negative predictive value of ~97% (a 3% probability of having had COVID-19 despite the negative Spike-RBD Bridging result). The expected rates of true and false positive and negative results are summarised in table 4-2 below.

	True Positive	True Negative
Test Positive	29%	1%
Test Negative	2%	68%

Table 4-2 Table showing the estimated rates of true positives, false positives, true negatives, and false negatives of COVID-19 patients in early convalescence (3-12 weeks since positive PCR test or symptom onset) by the Spike-RBD bridging assay, assuming a disease prevalence of 30.6%.

The Spike-RBD bridging assay was developed and validated using samples almost exclusively from the UK, however we do not expect anti-viral immune responses to vary drastically around the world (in contrast to T1D, which is preceded very differently across the globe[179]). These have also been calculated based on UK disease prevalence, but prevalence is likely to also be high in areas the test could be rolled out in, so the strong predictive values should be maintained.

4.7 Conclusion and Future Work

Planned future work includes continuing the validation of the IA-2A bridging assay, testing it in populations stratified by risk, and application of the Spike-RBD bridging assay to populations with and without type 1 diabetes. While demographic information such as ethnicity is incomplete in the BOX Family Study, the majority of samples tested, including

the schoolchildren used to set a threshold, were Caucasian. It remains to be seen how both assays will perform in more diverse populations.

While expressing IA-2ic in-house has proved difficult, commercial IA-2ic could be purchased from companies such as RSR[101]. The use of this larger antigen may facilitate a more sensitive screening assay for IA-2A. Further work would also continue to investigate and mitigate the issues of high errors between sample replicates.

When screening large populations, multiplex assays are highly sought after, to save the additional time, costs, and sample volume of running several singleplex assays on the same sample. Whether the bridging assay format is suitable for multiplexing remains to be seen, but development will almost certainly progress in that direction, potentially developing similar bridging assays for the other islet autoantibodies, with the aim of a multiplex assay able to test for all islet autoantibodies while maintaining the high specificity and sensitivity achieved by the IA-2A bridging assay. Multiplexing of the SARS-CoV-2 bridging assays would be largely redundant for clinical or screening purposes, as the presence of antibodies to the spike protein is already a measure of response to both natural infection and vaccine in a single assay, although discerning between these two responses with a multiplexed N and spike assay could be interesting.

Until then, work will proceed validating the N protein bridging assay, and then using this assay in tandem with the Spike-RBD bridging assay to screen samples from the COVID-19 substudy of the BOX Family Study, and the related general population CTC-19 study, to elucidate any differences between the humoral response to natural SARS-CoV-2 infection in individuals with and without type 1 diabetes, regardless of vaccination status.

More broadly, luciferase bridging assays have now been established as an alternative method of antibody detection specifically geared towards large-scale screening. Swapping the antigen for coating the plate and the labelled reporter antigen, with minimal other differences in protocol, allows the test to be used for a wide range of applications, not least in studies of autoimmunity and infectious disease as described here. The assay format's low serum volume requirement, low cost, and possibility for automation could make it an indispensable tool for screening large populations for a range of antibody biomarkers.

5 Appendix

5.1 Buffers

	Buffer Name	Buffer Constituents
Expression Buffers	Lysogeny broth / Luria-Bertani broth (LB)	• Tryptone 2g • Yeast extract 1g • NaCl 2g • 200ml dH_20
	LB agar	• Tryptone 2g • Yeast extract 11g • NaCl 2g • Agar 3g • 200ml dH_2O
FPLC Buffers	Binding Buffer A (for GSTrap + equilibration wash buffer for anti-His affinity)	• 3.765g Tris (MELFORD TRIS Base Ultrapure [Tris(hydroxymethyl) aminomethane]) • 500ml dH_20 • 4.383g NaCl • pH 7.5 • 0.077g Dithiothreitol (DTT) on day of use
	High Salt Wash Buffer B	• 3.765g Tris • 500ml ddH_20 • 8.766g NaCl • pH 7.5 • 0.077g DTT on day of use
	Elution Buffer C	• 0.606g Tris • 0.307g reduced glutathione • 100ml dH_20 • pH 8
SDS-PAGE Buffers and Gels	Resolving/Separating Gel Buffer / 1.5M Tris pH 8.8	• 90.8g Tris • 400ml dH_20 • pH 8.8 • Brought to 500ml with ddH20
	Stacking Gel Buffer / 0.5M Tris pH 6.8	• 30.3g Tris • 400ml dH_20 • pH 6.8 • Brought to 500ml with ddH20
	12% Separating Gel	• 6.4ml 30% acrylamide • 4ml 1.5M Tris pH 8.8 • 160µl 10% ammonium persulfate (APS) • 160µl 10% SDS • 16µl tetramethylethylenediamine (TEMED) • 5.3ml dH_2O
	6% Stacking Gel	• 2ml 30% acrylamide • 2.5ml 0.5M Tris pH 6.8 • 100µl 10% SDS • 100µl 10% APS

		• 10µl TEMED • 5.3ml dH_2O
	Loading Dye (2 x sample loading buffer (non-reducing)	• 0.5ml 1M Tris-HCL • pH 7 • 2.5ml 20% SDS • 2ml glycerol • 2mg bromophenol blue • Brought to 10ml with ddH20
	10x TRIS-glycine running buffer	• 30.2g Tris • 144g glycine • 800ml dH_20 • 10g SDS brought to 1L • Dilute to 1x working buffer
	Destain Solution	• 150ml methanol • 50ml glacial acetic acid • 300ml dH_20
Assay Buffers	Denver	• 4.844g Tris • 17.44g NaCl • 2L dH_2O • ~7ml (pH 7.4) HCl (5M) • 3ml Tween 20
	Denver LIPS	• 4.844g Tris • 17.44g NaCl • 2L dH_2O • ~7ml (pH 7.4) HCl (5M) • 10ml Tween 20
	Phosphate-Buffered Saline (PBS)	• 500ml dH_2O • 1x 5g Gibco® PBS tablet • pH 7.45 without adjustment
	Carbonate Buffer	• Anhydrous Na2CO3, 1.5 g • Anhydrous NaHCO3, 2.93 g • 2L dH_2O • pH to 9.6

Table 5-1 Table showing all buffers used in this project and their recipes.

5.2 IA-2ic Sequencing Results

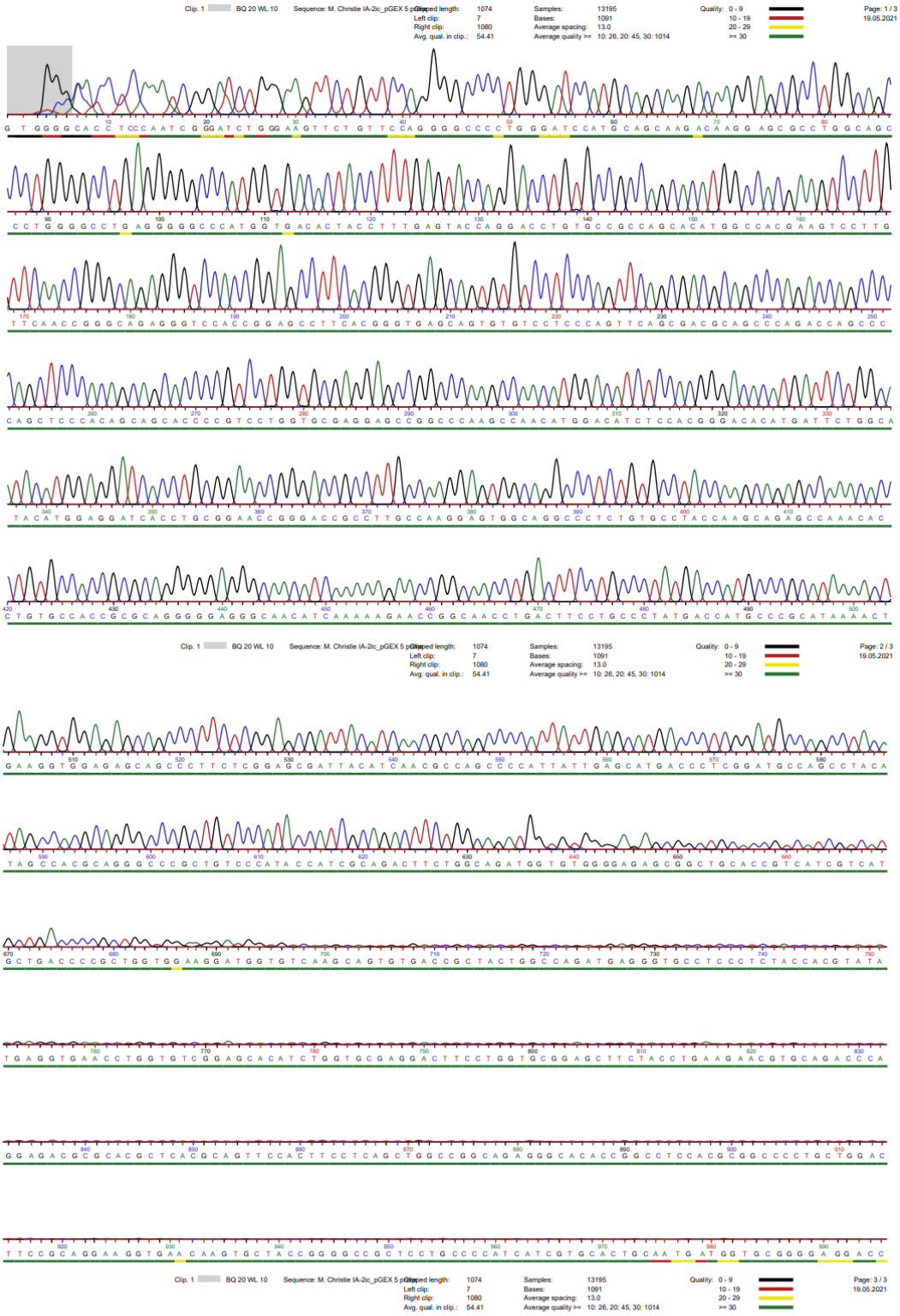

Figure 5-1 Five prime IA-2ic sequencing results.

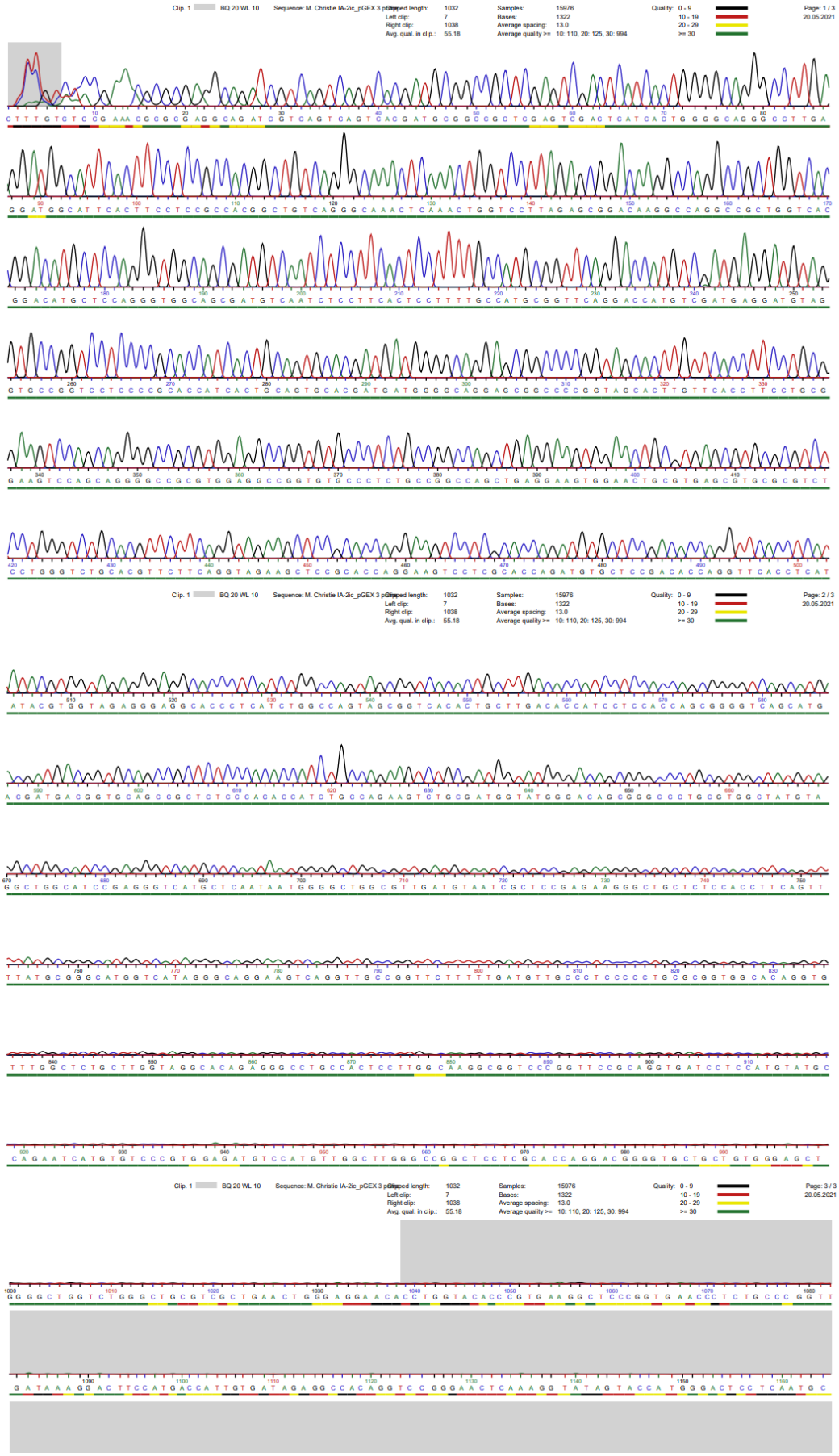

Figure 5-2 Three prime IA-2ic sequencing results.

5.3 Alternate IA-2A Bridging Assay Format Methods

Table 5-2 details conditions optimised in the standard, "straight-coated" IA-2A bridging assay which were carried forward into the alternative formats of this assay. These formats of the assay were not fully optimised. Detailed below are the methods as they stood at the end of this project, although the conditions detailed may or may not be revisited if future optimisation occurs.

Condition	Outcome
Incubation method	"Indirect" method, incubating sera and label together before transferring to the coated plate
EDTA in label	Include 5% EDTA in the Denver label buffer to boost the positive signal slightly
Label incubation buffer	Denver + 5% EDTA as the label buffer, no BSA or SuperBlock
Number of washes	Wash the plates 8 times (2 runs of the ELISA wash programme)

Table 5-2 Table showing assay conditions used in the glutathione and biotinylated versions of the IA-2A bridging assay but which were only optimised in the "straight-coated"/standard IA-2A bridging assay.

5.3.1 Glutathione-Coated Plate Variation of the IA-2A Bridging Assay Method

PTP-IA-2-GST antigen diluted to 5ng/40µl was pipetted into every well of a 96-well glutathione-coated plate (Thermo Scientific Pierce) and incubated for 18hrs at 4°C. The plate was washed 4 times in 20mM Tris 150mM NaCl pH 7.4 with 0.5% v/v Tween-20 (Denver LIPS) and blocked with 1% Casein in PBS (Thermo Scientific, Waltham, MA, USA). The plate was left to air-dry for 2-3hrs before being stored with a sachet of desiccant in a sealed plastic bag at 4°C.

The NLuc-IA-2 antigen was diluted in Denver LIPS + 5% EDTA to a concentration of $1x10^7$ LU ±5% per 25µl. Sera (1µl, 2 replicates) were pipetted into a 96-well plate and incubated with 25µl diluted NLuc antigen for 2hrs at room temperature. This mixture was transferred into the coated OptiPlate and incubated shaking (~700rpm) for 20hrs, at room temperature until the end of the working day and then at 4°C overnight. The plate was washed 8 times with Denver LIPS, excess buffer was removed by aspiration, then 40µl of a 1:2 dilution of the

standard 1:50 Nano-Glo® substrate (Promega) and 20mM Tris 150mM NaCl pH 7.4 with 0.15% v/v Tween-20 (Denver) was injected into each well before counting in a Berthold Centro 963 Microplate Luminometer (Germany).

5.3.2 Biotinylated IA-2 Variation of the IA-2A Bridging Assay Method

This format of the assay was not fully optimised. Below is the method as it stood at the end of this project.

The NLuc-IA-2 antigen was diluted in Denver LIPS + 5% EDTA + 10ng/40µl to a concentration of $1x10^7$ LU ±5% per 25µl. Sera (1µl, 2 replicates) were pipetted into a 96-well plate and incubated with 25µl diluted NLuc antigen for 2hrs at room temperature. This mixture was transferred into a neutravidin-coated optiplate (Thermo Scientific Pierce) and incubated shaking (~700rpm) for 1.5hrs at room temperature. The plate was washed 8 times with Denver LIPS, excess buffer was removed by aspiration, then 40µl of a 1:2 dilution of the standard 1:50 Nano-Glo® substrate (Promega) and 20mM Tris 150mM NaCl pH 7.4 with 0.15% v/v Tween-20 (Denver) was injected into each well before counting in a Berthold Centro 963 Microplate Luminometer (Germany).

5.3.3 NanoGlo® Assay Reagent can be further diluted to reduce cost in the biotinylated IA-2 format of the bridging assay

The standard makeup of the assay reagent is a 1:50 dilution of the substrate furimazine in the buffer provided in the Promega kit. This kit is one of the greater expenses involved in this bridging assay, so preserving these reagents could dramatically reduce the cost. Here, this 1:50 dilution was diluted 1:2 in Denver buffer, which had been shown in other assays to have little effect on the results of the assay.

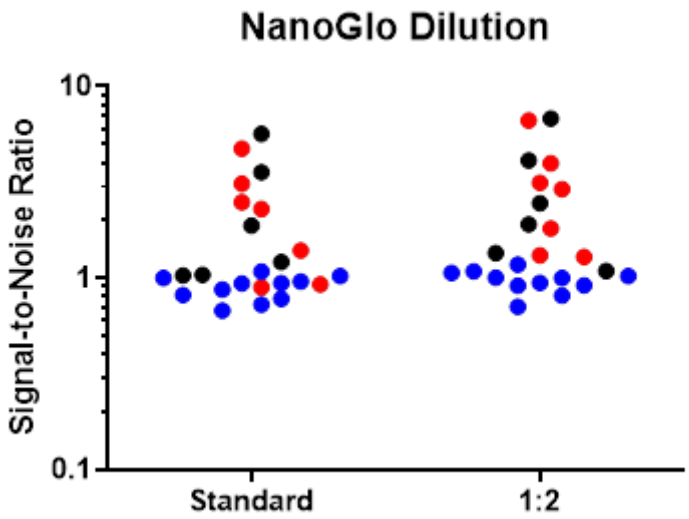

Figure 5-3 Biotinylated IA-2A Bridging Optimisation: Assay Reagent Dilution. A plot of light units (LU) from the same conditions of four recent optimisation experiments. Black points are the DK Standards A-F. Red points are known positive samples and blue points are known negative samples, mostly from the BOX Family Study, and had been previously tested by IA-2 RBA. Each data point represents the mean LU of two replicates.

This experiment was subject to a 10-fold decrease in LU, possibly due to denaturation of the biotinylated-IA-2 protein. For the standard assay reagent dilution condition, the median LU was 2,056.5 LU for the known positives (including standards) and 1,025 LU for the known negatives. The ranges were 5,207 LU and 440 LU respectively. For the further 1:2 dilution condition, the median LU was 2,725 LU for the known positives (including standards) and 1,108 LU for the known negatives. The ranges were 6,315.5 LU and 516.5 LU respectively.

This additional dilution did not affect the background ($p=0.0840$). While it did seem to have an effect on the SNR of the positive samples, including standards, ($p<0.0002$) the median SNR was actually increased in the 1:2 condition, and graphically it appears the additional dilution improved the distinction between low positive samples and the negative samples.

If optimisation of this version of the IA-2A bridging assay continues, the assay reagent will be diluted 1:2.

6 Bibliography

1. Wilcox G. Insulin and insulin resistance. *Clin Biochem Rev.* 2005;26(2):19-39.
2. Narayan KM, Boyle JP, Thompson TJ, Sorensen SW, Williamson DF. Lifetime risk for diabetes mellitus in the United States. *Jama.* 2003;290(14):1884-1890.
3. Atkinson MA, Eisenbarth GS, Michels AW. Type 1 diabetes. *Lancet (London, England).* 2014;383(9911):69-82.
4. Insel RA, Dunne JL, Ziegler AG. General population screening for type 1 diabetes: has its time come? *Current opinion in endocrinology, diabetes, and obesity.* 2015;22(4):270-276.
5. Thiruvoipati T, Kielhorn CE, Armstrong EJ. Peripheral artery disease in patients with diabetes: Epidemiology, mechanisms, and outcomes. *World journal of diabetes.* 2015;6(7):961-969.
6. Cade WT. Diabetes-related microvascular and macrovascular diseases in the physical therapy setting. *Phys Ther.* 2008;88(11):1322-1335.
7. Huo L, Harding JL, Peeters A, Shaw JE, Magliano DJ. Life expectancy of type 1 diabetic patients during 1997-2010: a national Australian registry-based cohort study. *Diabetologia.* 2016;59(6):1177-1185.
8. Audit NPD. National Paediatric Diabetes Audit Report 2012-15: Part 2: Hospital Admissions and Complications. In:2017.
9. Winkler C, Schober E, Ziegler AG, Holl RW. Markedly reduced rate of diabetic ketoacidosis at onset of type 1 diabetes in relatives screened for islet autoantibodies. *Pediatr Diabetes.* 2012;13(4):308-313.
10. Steck AK, Larsson HE, Liu X, et al. Residual beta-cell function in diabetes children followed and diagnosed in the TEDDY study compared to community controls. *Pediatr Diabetes.* 2017;18(8):794-802.
11. Barker JM, Goehrig SH, Barriga K, et al. Clinical characteristics of children diagnosed with type 1 diabetes through intensive screening and follow-up. *Diabetes care.* 2004;27(6):1399-1404.
12. Hekkala AM, Ilonen J, Toppari J, Knip M, Veijola R. Ketoacidosis at diagnosis of type 1 diabetes: Effect of prospective studies with newborn genetic screening and follow up of risk children. *Pediatr Diabetes.* 2018;19(2):314-319.
13. Simmons KM, Gottlieb PA, Michels AW. Immune Intervention and Preservation of Pancreatic Beta Cell Function in Type 1 Diabetes. *Current diabetes reports.* 2016;16(10):97.
14. Herold KC, Bundy BN, Long SA, et al. An Anti-CD3 Antibody, Teplizumab, in Relatives at Risk for Type 1 Diabetes. *N Engl J Med.* 2019;381(7):603-613.
15. Ohno Y, Aoki N, Nishimura A. In vitro production of interleukin-1, interleukin-6, and tumor necrosis factor-alpha in insulin-dependent diabetes mellitus. *The Journal of clinical endocrinology and metabolism.* 1993;77(4):1072-1077.
16. Peleg AY, Weerarathna T, McCarthy JS, Davis TM. Common infections in diabetes: pathogenesis, management and relationship to glycaemic control. *Diabetes Metab Res Rev.* 2007;23(1):3-13.
17. Da Silva Xavier G. The Cells of the Islets of Langerhans. *Journal of clinical medicine.* 2018;7(3).
18. Kulkarni RN. The islet beta-cell. *The international journal of biochemistry & cell biology.* 2004;36(3):365-371.
19. In't Veld P. Insulitis in human type 1 diabetes: The quest for an elusive lesion. *Islets.* 2011;3(4):131-138.
20. Leete P, Willcox A, Krogvold L, et al. Differential Insulitic Profiles Determine the Extent of β-Cell Destruction and the Age at Onset of Type 1 Diabetes. *Diabetes.* 2016;65(5):1362-1369.

21. Willcox A, Richardson SJ, Bone AJ, Foulis AK, Morgan NG. Analysis of islet inflammation in human type 1 diabetes. *Clinical and experimental immunology.* 2009;155(2):173-181.
22. Christie MR. Delving Into the Type 1 Diabetic Islet: Evidence That B-Cell Infiltration of Islets Is Linked to Local Hyperimmunity and Accelerated Progression to Disease. *Diabetes.* 2016;65(5):1146-1148.
23. Zhao Y, Scott NA, Quah HS, et al. Mouse pancreatic beta cells express MHC class II and stimulate CD4(+) T cells to proliferate. *Eur J Immunol.* 2015;45(9):2494-2503.
24. Robertson CC, Inshaw JRJ, Onengut-Gumuscu S, et al. Fine-mapping, trans-ancestral and genomic analyses identify causal variants, cells, genes and drug targets for type 1 diabetes. *Nat Genet.* 2021;53(7):962-971.
25. Oram RA, Patel K, Hill A, et al. A Type 1 Diabetes Genetic Risk Score Can Aid Discrimination Between Type 1 and Type 2 Diabetes in Young Adults. *Diabetes care.* 2016;39(3):337-344.
26. Sharp SA, Weedon MN, Hagopian WA, Oram RA. Clinical and research uses of genetic risk scores in type 1 diabetes. *Curr Opin Genet Dev.* 2018;50:96-102.
27. Dean L, McEntyre J. Genetic Factors in Type 1 Diabetes. In*.* Vol The Genetic Landscape of Diabetes. Bethesda (MD): National Center for Biotechnology Information (US); 2004.
28. Insel RA, Dunne JL, Atkinson MA, et al. Staging presymptomatic type 1 diabetes: a scientific statement of JDRF, the Endocrine Society, and the American Diabetes Association. *Diabetes care.* 2015;38(10):1964-1974.
29. Palmer JP, Asplin CM, Clemons P, et al. Insulin antibodies in insulin-dependent diabetics before insulin treatment. *Science.* 1983;222(4630):1337-1339.
30. Baekkeskov S, Aanstoot HJ, Christgau S, et al. Identification of the 64K autoantigen in insulin-dependent diabetes as the GABA-synthesizing enzyme glutamic acid decarboxylase. *Nature.* 1990;347(6289):151-156.
31. Wenzlau JM, Juhl K, Yu L, et al. The cation efflux transporter ZnT8 (Slc30A8) is a major autoantigen in human type 1 diabetes. *Proceedings of the National Academy of Sciences of the United States of America.* 2007;104(43):17040-17045.
32. McLaughlin KA, Richardson CC, Ravishankar A, et al. Identification of Tetraspanin-7 as a Target of Autoantibodies in Type 1 Diabetes. *Diabetes.* 2016;65(6):1690-1698.
33. Payton MA, Hawkes CJ, Christie MR. Relationship of the 37,000- and 40,000-M(r) tryptic fragments of islet antigens in insulin-dependent diabetes to the protein tyrosine phosphatase-like molecule IA-2 (ICA512). *J Clin Invest.* 1995;96(3):1506-1511.
34. Bottazzo GF, Florin-Christensen A, Doniach D. Pillars Article: Islet-cell Antibodies in Diabetes Mellitus with Autoimmune Polyendocrine Deficiencies. Lancet. 1974. 304: 1279-1283. *Journal of immunology (Baltimore, Md : 1950).* 2017;199(9):3014-3018.
35. McLaughlin KA, Richardson CC, Williams S, et al. Relationships between major epitopes of the IA-2 autoantigen in Type 1 diabetes: Implications for determinant spreading. *Clin Immunol.* 2015;160(2):226-236.
36. Torii S. Expression and function of IA-2 family proteins, unique neuroendocrine-specific protein-tyrosine phosphatases. *Endocr J.* 2009;56(5):639-648.
37. Ziegler AG, Rewers M, Simell O, et al. Seroconversion to Multiple Islet Autoantibodies and Risk of Progression to Diabetes in Children. *Jama.* 2013;309(23):2473-2479.
38. Gorus FK, Balti EV, Vermeulen I, et al. Screening for insulinoma antigen 2 and zinc transporter 8 autoantibodies: a cost-effective and age-independent strategy to identify rapid progressors to clinical onset among relatives of type 1 diabetic patients. *Clinical and experimental immunology.* 2013;171(1):82-90.
39. Achenbach P, Warncke K, Reiter J, et al. Stratification of type 1 diabetes risk on the basis of islet autoantibody characteristics. *Diabetes.* 2004;53(2):384-392.
40. Leslie RD, Atkinson MA, Notkins AL. Autoantigens IA-2 and GAD in Type I (insulin-dependent) diabetes. *Diabetologia.* 1999;42(1):3-14.

41. Kukko M, Kimpimäki T, Korhonen S, et al. Dynamics of diabetes-associated autoantibodies in young children with human leukocyte antigen-conferred risk of type 1 diabetes recruited from the general population. *The Journal of clinical endocrinology and metabolism.* 2005;90(5):2712-2717.
42. Barker JM, Barriga KJ, Yu L, et al. Prediction of autoantibody positivity and progression to type 1 diabetes: Diabetes Autoimmunity Study in the Young (DAISY). *The Journal of clinical endocrinology and metabolism.* 2004;89(8):3896-3902.
43. Ziegler AG, Kick K, Bonifacio E, et al. Yield of a Public Health Screening of Children for Islet Autoantibodies in Bavaria, Germany. *Jama.* 2020;323(4):339-351.
44. Ziegler AG, Hummel M, Schenker M, Bonifacio E. Autoantibody appearance and risk for development of childhood diabetes in offspring of parents with type 1 diabetes: the 2-year analysis of the German BABYDIAB Study. *Diabetes.* 1999;48(3):460-468.
45. Bingley PJ, Christie MR, Bonifacio E, et al. Combined analysis of autoantibodies improves prediction of IDDM in islet cell antibody-positive relatives. *Diabetes.* 1994;43(11):1304-1310.
46. Ziegler AG, Rewers M, Simell O, et al. Seroconversion to multiple islet autoantibodies and risk of progression to diabetes in children. *Jama.* 2013;309(23):2473-2479.
47. Steck AK, Johnson K, Barriga KJ, et al. Age of islet autoantibody appearance and mean levels of insulin, but not GAD or IA-2 autoantibodies, predict age of diagnosis of type 1 diabetes: diabetes autoimmunity study in the young. *Diabetes care.* 2011;34(6):1397-1399.
48. Karl FM, Winkler C, Ziegler AG, Laxy M, Achenbach P. Costs of Public Health Screening of Children for Presymptomatic Type 1 Diabetes in Bavaria, Germany. *Diabetes care.* 2022;45(4):837-844.
49. Raab J, Haupt F, Scholz M, et al. Capillary blood islet autoantibody screening for identifying pre-type 1 diabetes in the general population: design and initial results of the Fr1da study. *BMJ Open.* 2016;6(5):e011144.
50. Liu Y, Rafkin LE, Matheson D, et al. Use of self-collected capillary blood samples for islet autoantibody screening in relatives: a feasibility and acceptability study. *Diabetic medicine : a journal of the British Diabetic Association.* 2017;34(7):934-937.
51. Hasöksüz M, Kiliç S, Saraç F. Coronaviruses and SARS-COV-2. *Turk J Med Sci.* 2020;50(Si-1):549-556.
52. Schoeman D, Fielding BC. Coronavirus envelope protein: current knowledge. *Virol J.* 2019;16(1):69.
53. Information NCfB. Severe acute respiratory syndrome coronavirus 2 reference genome. 2020.
54. Cascella M, Rajnik M, Cuomo A, Dulebohn SC, Di Napoli R. Features, Evaluation, and Treatment of Coronavirus. In: *StatPearls.* Treasure Island (FL): StatPearls Publishing Copyright © 2020, StatPearls Publishing LLC.; 2020.
55. Perlman S, Netland J. Coronaviruses post-SARS: update on replication and pathogenesis. *Nat Rev Microbiol.* 2009;7(6):439-450.
56. Astuti I, Ysrafil. Severe Acute Respiratory Syndrome Coronavirus 2 (SARS-CoV-2): An overview of viral structure and host response. *Diabetes Metab Syndr.* 2020;14(4):407-412.
57. Wong SK, Li W, Moore MJ, Choe H, Farzan M. A 193-amino acid fragment of the SARS coronavirus S protein efficiently binds angiotensin-converting enzyme 2. *J Biol Chem.* 2004;279(5):3197-3201.
58. Chan JF, Yuan S, Kok KH, et al. A familial cluster of pneumonia associated with the 2019 novel coronavirus indicating person-to-person transmission: a study of a family cluster. *Lancet (London, England).* 2020;395(10223):514-523.
59. Grant MC, Geoghegan L, Arbyn M, et al. The prevalence of symptoms in 24,410 adults infected by the novel coronavirus (SARS-CoV-2; COVID-19): A systematic review and meta-analysis of 148 studies from 9 countries. *PloS one.* 2020;15(6):e0234765.

60. Sanyaolu A, Okorie C, Marinkovic A, et al. Comorbidity and its Impact on Patients with COVID-19. *SN Compr Clin Med.* 2020:1-8.
61. GOV.UK. COVID-19 confirmed deaths in England (to 31 January 2021): report. 2022; https://www.gov.uk/government/publications/covid-19-reported-sars-cov-2-deaths-in-england/covid-19-confirmed-deaths-in-england-report. Accessed 22/02/2022.
62. Harari D, Keep M, Brien P. Coronavirus: Economic Impact. *Research Briefing* 2021; https://commonslibrary.parliament.uk/research-briefings/cbp-8866/#:~:text=Economic%20impact%20to%20date,in%201921%20on%20unofficial%20estimates. Accessed 10/03/2022, 2022.
63. Shah VK, Firmal P, Alam A, Ganguly D, Chattopadhyay S. Overview of Immune Response During SARS-CoV-2 Infection: Lessons From the Past. *Front Immunol.* 2020;11:1949.
64. Grifoni A, Weiskopf D, Ramirez SI, et al. Targets of T Cell Responses to SARS-CoV-2 Coronavirus in Humans with COVID-19 Disease and Unexposed Individuals. *Cell.* 2020;181(7):1489-1501.e1415.
65. JDRF. Type 1 diabetes facts and figures. 2022; https://jdrf.org.uk/information-support/about-type-1-diabetes/facts-and-figures/.
66. Diagnosis and classification of diabetes mellitus. *Diabetes care.* 2014;37 Suppl 1:S81-90.
67. Allard R, Leclerc P, Tremblay C, Tannenbaum TN. Diabetes and the severity of pandemic influenza A (H1N1) infection. *Diabetes care.* 2010;33(7):1491-1493.
68. Booth CM, Matukas LM, Tomlinson GA, et al. Clinical features and short-term outcomes of 144 patients with SARS in the greater Toronto area. *Jama.* 2003;289(21):2801-2809.
69. Fadini GP, Morieri ML, Longato E, Avogaro A. Prevalence and impact of diabetes among people infected with SARS-CoV-2. In: *J Endocrinol Invest.* Vol 43.2020:867-869.
70. Guo W, Li M, Dong Y, et al. Diabetes is a risk factor for the progression and prognosis of COVID-19. *Diabetes Metab Res Rev.* 2020:e3319.
71. Deng SQ, Peng HJ. Characteristics of and Public Health Responses to the Coronavirus Disease 2019 Outbreak in China. *Journal of clinical medicine.* 2020;9(2).
72. Apicella M, Campopiano MC, Mantuano M, Mazoni L, Coppelli A, Del Prato S. COVID-19 in people with diabetes: understanding the reasons for worse outcomes. *Lancet Diabetes Endocrinol.* 2020;8(9):782-792.
73. Zhou J, Tan J. Diabetes patients with COVID-19 need better blood glucose management in Wuhan, China. *Metabolism.* 2020;107:154216.
74. Wang S, Ma P, Zhang S, et al. Fasting blood glucose at admission is an independent predictor for 28-day mortality in patients with COVID-19 without previous diagnosis of diabetes: a multi-centre retrospective study. *Diabetologia.* 2020;63(10):2102-2111.
75. Barron E, Bakhai C, Kar P, et al. Associations of type 1 and type 2 diabetes with COVID-19-related mortality in England: a whole-population study. *Lancet Diabetes Endocrinol.* 2020;8(10):813-822.
76. Agarwal S, Agarwal SK. Endocrine changes in SARS-CoV-2 patients and lessons from SARS-CoV. *Postgrad Med J.* 2020;96(1137):412-416.
77. Cristelo C, Azevedo C, Marques JM, Nunes R, Sarmento B. SARS-CoV-2 and diabetes: New challenges for the disease. *Diabetes Res Clin Pract.* 2020;164:108228.
78. Yao XH, Li TY, He ZC, et al. [A pathological report of three COVID-19 cases by minimal invasive autopsies]. *Zhonghua Bing Li Xue Za Zhi.* 2020;49(5):411-417.
79. Kusmartseva I, Wu W, Syed F, et al. Expression of SARS-CoV-2 Entry Factors in the Pancreas of Normal Organ Donors and Individuals with COVID-19. *Cell Metab.* 2020;32(6):1041-1051.e1046.
80. Barrett CE, Koyama AK, Alvarez P, et al. Risk for Newly Diagnosed Diabetes >30 Days After SARS-CoV-2 Infection Among Persons Aged <18 Years - United States, March 1, 2020-June 28, 2021. *MMWR Morb Mortal Wkly Rep.* 2022;71(2):59-65.

81. AlRashidi FT, Gillespie KM. Biomarkers in Islet Cell Transplantation for Type 1 Diabetes. *Current diabetes reports.* 2018;18(10):94.
82. Secchi M, Bazzigaluppi E, Brigatti C, et al. COVID-19 survival associates with the immunoglobulin response to the SARS-CoV-2 spike receptor binding domain. *J Clin Invest.* 2020.
83. Care DoHaS. Health Secretary sets out plan to carry out 100,000 coronavirus tests a day. *Press Release* 2020; https://www.gov.uk/government/news/health-secretary-sets-out-plan-to-carry-out-100000-coronavirus-tests-a-day.
84. Agency MHpR. Target Product Profile: antibody tests to help determine if people have recent infection to SARS-CoV-2: Version 2. 2020; https://www.gov.uk/government/publications/how-tests-and-testing-kits-for-coronavirus-covid-19-work/target-product-profile-antibody-tests-to-help-determine-if-people-have-recent-infection-to-sars-cov-2-version-2.
85. Mahase E. Covid-19: Two antibody tests are "highly specific" but vary in sensitivity, evaluations find. *Bmj.* 2020;369:m2066.
86. Organisation WH. WHO Coronavirus (COVID-19) Dashboard. 2022; https://covid19.who.int/. Accessed 07/02/2022.
87. Bonifacio E, Achenbach P. Birth and coming of age of islet autoantibodies. *Clinical and experimental immunology.* 2019;198(3):294-305.
88. Bonifacio E, Yu L, Williams AK, et al. Harmonization of glutamic acid decarboxylase and islet antigen-2 autoantibody assays for national institute of diabetes and digestive and kidney diseases consortia. *The Journal of clinical endocrinology and metabolism.* 2010;95(7):3360-3367.
89. Lampasona V, Schlosser M, Mueller PW, et al. Diabetes antibody standardization program: first proficiency evaluation of assays for autoantibodies to zinc transporter 8. In: *Clin Chem.* Vol 57. United States2011:1693-1702.
90. NIBSC. Coronavirus (COVID-19)-related research reagents available from the NIBSC. 2021; https://www.nibsc.org/science_and_research/idd/cfar/covid-19_reagents.aspx.
91. Pilcher CC, Elliott RB. A sensitive and reproducible method for the assay of human islet cell antibodies. *Journal of immunological methods.* 1990;129(1):111-117.
92. TrialNet TD. Frequently Asked Questions. 2018; https://www.trialnet.org/frequently-asked-questions.
93. Takahashi K, Tasaka H, Hasegawa Y. [Sensitivity and specificity for detection of islet cell cytoplasmic antibodies using rat pancreatic sections]. *Nihon Rinsho Meneki Gakkai Kaishi.* 1995;18(2):188-196.
94. Kohnert KD, Rjasanowski I, Hehmke B, Hamann J, Keilacker H, Michaelis D. The detection of autoantibodies to pancreatic islet cells by immunoenzyme histochemistry. *Diabetes Res.* 1994;25(1):1-12.
95. Winter WE, Harris N, Schatz D. Immunological Markers in the Diagnosis and Prediction of Autoimmune Type 1a Diabetes. *Clin Diabetes.* 2002;20(4):183-191.
96. Bingley PJ, Bonifacio E, Shattock M, et al. Can islet cell antibodies predict IDDM in the general population? *Diabetes care.* 1993;16(1):45-50.
97. Bingley PJ, Bonifacio E, Williams AJ, Genovese S, Bottazzo GF, Gale EA. Prediction of IDDM in the general population: strategies based on combinations of autoantibody markers. *Diabetes.* 1997;46(11):1701-1710.
98. Bingley PJ, Williams AJ, Gale EA. Optimized autoantibody-based risk assessment in family members. Implications for future intervention trials. *Diabetes care.* 1999;22(11):1796-1801.
99. Wyatt R, Williams, A. J. K. Islet Autoantibody Detection by Radioimmunoassay. In: Gillespie KM, ed. *Type-1 Diabetes Methods and Protocols.* Humana Press; 2016:57-83.
100. Williams AJ, Bingley PJ, Bonifacio E, Palmer JP, Gale EA. A novel micro-assay for insulin autoantibodies. *J Autoimmun.* 1997;10(5):473-478.

101. Autoimmunity RLf. PRODUCT RANGE - KITS & REAGENTS. 2020; https://www.rsrltd.com/products.html.
102. Fritzler MJ, Wiik A, Fritzler ML, Barr SG. The use and abuse of commercial kits used to detect autoantibodies. *Arthritis Res Ther.* 2003;5(4):192-201.
103. Achenbach P, Koczwara K, Knopff A, Naserke H, Ziegler AG, Bonifacio E. Mature high-affinity immune responses to (pro)insulin anticipate the autoimmune cascade that leads to type 1 diabetes. *J Clin Invest.* 2004;114(4):589-597.
104. Yu L, Miao D, Scrimgeour L, Johnson K, Rewers M, Eisenbarth GS. Distinguishing persistent insulin autoantibodies with differential risk: nonradioactive bivalent proinsulin/insulin autoantibody assay. *Diabetes.* 2012;61(1):179-186.
105. Delic-Sarac M, Mutevelic S, Karamehic J, et al. ELISA Test for Analyzing of Incidence of Type 1 Diabetes Autoantibodies (GAD and IA2) in Children and Adolescents. *Acta informatica medica : AIM : journal of the Society for Medical Informatics of Bosnia & Herzegovina : casopis Drustva za medicinsku informatiku BiH.* 2016;24(1):61-65.
106. Brooking H, Ananieva-Jordanova R, Arnold C, et al. A sensitive non-isotopic assay for GAD65 autoantibodies. *Clinica chimica acta; international journal of clinical chemistry.* 2003;331(1-2):55-59.
107. Törn C, Mueller PW, Schlosser M, Bonifacio E, Bingley PJ. Diabetes Antibody Standardization Program: evaluation of assays for autoantibodies to glutamic acid decarboxylase and islet antigen-2. *Diabetologia.* 2008;51(5):846-852.
108. Kawasaki E, Okada A, Uchida A, et al. Discrepancy of glutamic acid decarboxylase 65 autoantibody results between RSR radioimmunoassay and enzyme-linked immunosorbent assay in patients with type 1 diabetes is related to autoantibody affinity. *J Diabetes Investig.* 2019;10(4):990-996.
109. Greenbaum CJ, Palmer JP, Kuglin B, Kolb H. Insulin autoantibodies measured by radioimmunoassay methodology are more related to insulin-dependent diabetes mellitus than those measured by enzyme-linked immunosorbent assay: results of the Fourth International Workshop on the Standardization of Insulin Autoantibody Measurement. *The Journal of clinical endocrinology and metabolism.* 1992;74(5):1040-1044.
110. International ECL. Glutamic Acid Decarboxylase (GAD) Antibodies. https://www.exeterlaboratory.com/test/gad-antibodies/. Accessed 07/02/2022.
111. Chen S, Willis J, Maclean C, et al. Sensitive non-isotopic assays for autoantibodies to IA-2 and to a combination of both IA-2 and GAD65. *Clinica chimica acta; international journal of clinical chemistry.* 2005;357(1):74-83.
112. Bingley PJ, Bonifacio E, Mueller PW. Diabetes Antibody Standardization Program: first assay proficiency evaluation. *Diabetes.* 2003;52(5):1128-1136.
113. Kikkas I, Mallone R, Tubiana-Rufi N, et al. A simple and fast non-radioactive bridging immunoassay for insulin autoantibodies. *PloS one.* 2013;8(7):e69021.
114. Yu L. Islet Autoantibody Detection by Electrochemiluminescence (ECL) Assay. In: Gillespie KM, ed. *Type-1 Diabetes Methods and Protocols.* Humana Press; 2016:85-91.
115. Jia X, He L, Gu Y, High H, Yu L. A High-Throughput Electrochemiluminescence 7-Plex Assay Simultaneously Screening for Type 1 Diabetes and Multiple Autoimmune Diseases. *J Vis Exp.* 2020(159).
116. Jia X, Gu Y, High H, Yu L. Islet autoantibodies in disease prediction and pathogenesis. *Diabetol Int.* 2020;11(1):6-10.
117. Yu L. Islet Autoantibody Detection by Electrochemiluminescence (ECL) Assay. *Methods Mol Biol.* 2016;1433:85-91.
118. Bolton JS, Chaudhury S, Dutta S, et al. Comparison of ELISA with electro-chemiluminescence technology for the qualitative and quantitative assessment of serological responses to vaccination.

119. Jeong S, Lee N, Lee SK, et al. Comparing Results of Five SARS-CoV-2 Antibody Assays Before and After the First Dose of ChAdOx1 nCoV-19 Vaccine among Health Care Workers. *J Clin Microbiol.* 2021;59(9):e0110521.
120. Maine GN, Krishnan SM, Walewski K, Trueman J, Sykes E, Sun Q. Clinical and analytical evaluation of the Abbott AdviseDx quantitative SARS-CoV-2 IgG assay and comparison with two other serological tests. *Journal of immunological methods.* 2022;503:113243.
121. England PH. *Evaluation of Roche Elecsys AntiSARS-CoV-2 S serology assay for the detection of anti-SARS-CoV-2 S antibodies.* 2021.
122. Perkmann T, Perkmann-Nagele N, Breyer MK, et al. Side-by-Side Comparison of Three Fully Automated SARS-CoV-2 Antibody Assays with a Focus on Specificity. *Clin Chem.* 2020;66(11):1405-1413.
123. Bradley BT, Bryan A, Fink SL, et al. Anti-SARS-CoV-2 Antibody Levels Measured by the AdviseDx SARS-CoV-2 Assay Are Concordant with Previously Available Serologic Assays but Are Not Fully Predictive of Sterilizing Immunity. *J Clin Microbiol.* 2021;59(9):e0098921.
124. Tsai CT, Robinson PV, Spencer CA, Bertozzi CR. Ultrasensitive Antibody Detection by Agglutination-PCR (ADAP). *ACS Cent Sci.* 2016;2(3):139-147.
125. Karp DG, Cuda D, Tandel D, et al. Sensitive and Specific Detection of SARS-CoV-2 Antibodies Using a High-Throughput, Fully Automated Liquid-Handling Robotic System. *SLAS Technol.* 2020;25(6):545-552.
126. Lampasona V, Pittman DL, Williams AJ, et al. Islet Autoantibody Standardization Program 2018 Workshop: Interlaboratory Comparison of Glutamic Acid Decarboxylase Autoantibody Assay Performance. *Clin Chem.* 2019;65(9):1141-1152.
127. Cortez FJ, Gebhart D, Robinson PV, et al. Sensitive detection of multiple islet autoantibodies in type 1 diabetes using small sample volumes by agglutination-PCR. *PloS one.* 2020;15(11):e0242049.
128. de Jesus Cortez F, Lind A, Ramelius A, et al. Multiplex agglutination-PCR (ADAP) autoantibody assays compared to radiobinding autoantibodies in type 1 diabetes and celiac disease. *Journal of immunological methods.* 2022:113265.
129. Cortez FJ, Gebhart D, Tandel D, et al. Automation of a multiplex agglutination-PCR (ADAP) type 1 diabetes (T1D) assay for the rapid analysis of islet autoantibodies. *SLAS Technol.* 2021.
130. Dust K, Hedley A, Nichol K, et al. Comparison of commercial assays and laboratory developed tests for detection of SARS-CoV-2. *J Virol Methods.* 2020;285:113970.
131. Burbelo PD, Lebovitz EE, Notkins AL. Luciferase immunoprecipitation systems for measuring antibodies in autoimmune and infectious diseases. *Translational research : the journal of laboratory and clinical medicine.* 2015;165(2):325-335.
132. Burbelo PD, Groot S, Dalakas MC, Iadarola MJ. High definition profiling of autoantibodies to glutamic acid decarboxylases GAD65/GAD67 in stiff-person syndrome. *Biochem Biophys Res Commun.* 2008;366(1):1-7.
133. Burbelo PD, Hirai H, Leahy H, et al. A new luminescence assay for autoantibodies to mammalian cell-prepared insulinoma-associated protein 2. *Diabetes care.* 2008;31(9):1824-1826.
134. Liberati D, Wyatt RC, Brigatti C, et al. A novel LIPS assay for insulin autoantibodies. *Acta diabetologica.* 2018;55(3):263-270.
135. England CG, Ehlerding EB, Cai W. NanoLuc: A Small Luciferase is Brightening up the Field of Bioluminescence. In*.* Vol 5. Bioconjug Chem. 2016 May 18; 27(5): 1175–1187.2017:1175-1187.
136. Tan CW, Chia WN, Qin X, et al. A SARS-CoV-2 surrogate virus neutralization test based on antibody-mediated blockage of ACE2-spike protein-protein interaction. *Nat Biotechnol.* 2020;38(9):1073-1078.
137. Danh K, Karp DG, Robinson PV, et al. Detection of SARS-CoV-2 neutralizing antibodies with a cell-free PCR assay. *medRxiv.* 2020.

138. Arvan P, Pietropaolo M, Ostrov D, Rhodes CJ. Islet autoantigens: structure, function, localization, and regulation. *Cold Spring Harb Perspect Med.* 2012;2(8).
139. Siev M, Yu X, Prados-Rosales R, Martiniuk FT, Casadevall A, Achkar JM. Correlation between serum and plasma antibody titers to mycobacterial antigens. *Clin Vaccine Immunol.* 2011;18(1):173-175.
140. Long AE, Gillespie KM, Rokni S, Bingley PJ, Williams AJ. Rising incidence of type 1 diabetes is associated with altered immunophenotype at diagnosis. *Diabetes.* 2012;61(3):683-686.
141. Roche. Roche's COVID-19 antibody test receives FDA Emergency Use Authorization and is available in markets accepting the CE mark. 2020; https://diagnostics.roche.com/global/en/news-listing/2020/roches-covid-19-antibody-test-receives-fda-emergency-use-authorization.html.
142. Public Health England PD, Nuffield Department of Medicine, University of Oxford, Oxford University Hospitals NHS Foundation trust. Evaluation of sensitivity and specificity of four commercially available SARS-CoV-2 antibody immunoassays. In: England PH, ed: Public Health England; 2020.
143. Diagnostics R. Elecsys ® Anti-SARS-CoV-2. Immunoassay for the qualitative detection of antibodies (incl. IgG) against SARS-CoV-2. 2022; https://diagnostics.roche.com/gb/en/products/params/elecsys-anti-sars-cov-2.html#productInfo.
144. Halliday A, Long AE, Baum HE, et al. Development and evaluation of low-volume tests to detect and characterise antibodies to SARS-CoV-2. *medRxiv.* 2022:2022.2005.2003.22274395.
145. Tai W, He L, Zhang X, et al. Characterization of the receptor-binding domain (RBD) of 2019 novel coronavirus: implication for development of RBD protein as a viral attachment inhibitor and vaccine. *Cell Mol Immunol.* 2020;17(6):613-620.
146. NHS. SARS (severe acute respiratory syndrome). 2019; https://www.nhs.uk/conditions/sars/. Accessed 19th April, 2021.
147. Iyer AS, Jones FK, Nodoushani A, et al. Persistence and decay of human antibody responses to the receptor binding domain of SARS-CoV-2 spike protein in COVID-19 patients. *Sci Immunol.* 2020;5(52).
148. Secchi M, Bazzigaluppi E, Brigatti C, et al. COVID-19 survival associates with the immunoglobulin response to the SARS-CoV-2 spike receptor binding domain. *J Clin Invest.* 2020;130(12):6366-6378.
149. Burbelo PD, Kisailus AE, Peck JW. Detecting protein-protein interactions using Renilla luciferase fusion proteins. *Biotechniques.* 2002;33(5):1044-1048, 1050.
150. Bazzigaluppi E, Lampasona V, Barera G, et al. Comparison of tissue transglutaminase-specific antibody assays with established antibody measurements for coeliac disease. *J Autoimmun.* 1999;12(1):51-56.
151. Tsai CT, Mukai K, Robinson PV, et al. Isotype-specific agglutination-PCR (ISAP): A sensitive and multiplex method for measuring allergen-specific IgE. *J Allergy Clin Immunol.* 2018;141(5):1901-1904.e1915.
152. Theel ES, Johnson PW, Kunze KL, et al. SARS-CoV-2 Serologic Assays Dependent on Dual-Antigen Binding Demonstrate Diverging Kinetics Relative to Other Antibody Detection Methods. *J Clin Microbiol.* 2021;59(9):e0123121.
153. Pang NY, Pang AS, Chow VT, Wang DY. Understanding neutralising antibodies against SARS-CoV-2 and their implications in clinical practice. *Mil Med Res.* 2021;8(1):47.
154. Kawasaki E, Yamaguchi H, Hattori H, Egashira T, Eguchi K. Autoantibodies to IA-2 in type 1 diabetes: measurements with a new enzyme-linked immunosorbent assay. *Ann N Y Acad Sci.* 2002;958:241-246.
155. Gu Y, Zhao Z, High H, Yang T, Yu L. Islet Autoantibody Detection by Electrochemiluminescence (ECL) Assay. *J Clin Cell Immunol.* 2017;8(6).
156. Lou B, Li TD, Zheng SF, et al. Serology characteristics of SARS-CoV-2 infection after exposure and post-symptom onset. *Eur Respir J.* 2020;56(2).

157. Meyer B, Reimerink J, Torriani G, et al. Validation and clinical evaluation of a SARS-CoV-2 surrogate virus neutralisation test (sVNT). *Emerg Microbes Infect.* 2020;9(1):2394-2403.
158. Nie J, Li Q, Wu J, et al. Establishment and validation of a pseudovirus neutralization assay for SARS-CoV-2. *Emerg Microbes Infect.* 2020;9(1):680-686.
159. Serafin A, Malinowski M, Prażmowska-Wilanowska A. Blood volume and pain perception during finger prick capillary blood sampling: are all safety lancets equal? *Postgrad Med.* 2020;132(3):288-295.
160. Windich-Biermeier A, Sjoberg I, Dale JC, Eshelman D, Guzzetta CE. Effects of distraction on pain, fear, and distress during venous port access and venipuncture in children and adolescents with cancer. *J Pediatr Oncol Nurs.* 2007;24(1):8-19.
161. Migdal M, Chudzynska-Pomianowska E, Vause E, Henry E, Lazar J. Rapid, needle-free delivery of lidocaine for reducing the pain of venipuncture among pediatric subjects. *Pediatrics.* 2005;115(4):e393-398.
162. McLenon J, Rogers MAM. The fear of needles: A systematic review and meta-analysis. *J Adv Nurs.* 2019;75(1):30-42.
163. Gesualdo PD, Bautista KA, Waugh KC, et al. Feasibility of screening for T1D and celiac disease in a pediatric clinic setting. *Pediatr Diabetes.* 2016;17(6):441-448.
164. Gillespie KM, Fareed R, Mortimer GL. Four decades of the Bart's Oxford study: Improved tests to predict type 1 diabetes. *Diabetic medicine : a journal of the British Diabetic Association.* 2021;38(12):e14717.
165. Williams AJ, Lampasona V, Schlosser M, et al. Detection of Antibodies Directed to the N-Terminal Region of GAD Is Dependent on Assay Format and Contributes to Differences in the Specificity of GAD Autoantibody Assays for Type 1 Diabetes. *Diabetes.* 2015;64(9):3239-3246.
166. Bingley PJ, Williams AJ. Islet autoantibody testing: an end to the trials and tribulations? *Diabetes.* 2013;62(12):4009-4011.
167. Amanat F, Stadlbauer D, Strohmeier S, et al. A serological assay to detect SARS-CoV-2 seroconversion in humans. *Nat Med.* 2020;26(7):1033-1036.
168. Naserke HE, Ziegler AG, Lampasona V, Bonifacio E. Early development and spreading of autoantibodies to epitopes of IA-2 and their association with progression to type 1 diabetes. *Journal of immunology (Baltimore, Md : 1950).* 1998;161(12):6963-6969.
169. Knip M. Can we predict type 1 diabetes in the general population? *Diabetes care.* 2002;25(3):623-625.
170. Narendran P. Screening for type 1 diabetes: are we nearly there yet? *Diabetologia.* 2019;62(1):24-27.
171. Wilson JMG, Jungner G, World Health O. Principles and practice of screening for disease / J. M. G. Wilson, G. Jungner.
172. Tillerås KH, Kjoelaas SH, Dramstad E, Feragen KB, von der Lippe C. Psychological reactions to predictive genetic testing for Huntington's disease: A qualitative study. *J Genet Couns.* 2020;29(6):1093-1105.
173. Dhatariya KK, Skedgel C, Fordham R. The cost of treating diabetic ketoacidosis in the UK: a national survey of hospital resource use. *Diabetic medicine : a journal of the British Diabetic Association.* 2017;34(10):1361-1366.
174. Meehan C, Fout B, Ashcraft J, Schatz DA, Haller MJ. Screening for T1D risk to reduce DKA is not economically viable. *Pediatr Diabetes.* 2015;16(8):565-572.
175. Ziegler AG, Bonifacio E, Group B-BS. Age-related islet autoantibody incidence in offspring of patients with type 1 diabetes. *Diabetologia.* 2012;55(7):1937-1943.
176. Ilonen J, Lempainen J, Hammais A, et al. Primary islet autoantibody at initial seroconversion and autoantibodies at diagnosis of type 1 diabetes as markers of disease heterogeneity. *Pediatr Diabetes.* 2018;19(2):284-292.
177. Roll U, Fuchtenbusch M, Ziegler A-G, Christie MR, Payton MA, Hawkes CJ. Perinatal Autoimmunity in Offspring of Diabetic Parents: The German Multicenter BABY-DIAB

Study: Detection of Humoral Immune Responses to Islet Antigens in Early Childhood. *45.* 1996(7):967-973.
178. Decochez K, De Leeuw IH, Keymeulen B, et al. IA-2 autoantibodies predict impending type I diabetes in siblings of patients. *Diabetologia.* 2002;45(12):1658-1666.
179. Ross C, Ward ZJ, Gomber A, et al. The Prevalence of Islet Autoantibodies in Children and Adolescents With Type 1 Diabetes Mellitus: A Global Scoping Review. *Front Endocrinol (Lausanne).* 2022;13:815703.
180. Tombs MA. *Value of Autoantibodies to Tetraspanin-7 as Markers of Type 1 Diabetes*: School of Life Sciences, University of Lincoln; 2020.
181. Statistics OfN. Population of young children (aged 0-4) in the United Kingdom from 1971 to 2020, by single year of age. *Demographics* 2020; https://www.statista.com/statistics/766134/uk-young-children-population-by-single-year-of-age/.
182. Massinga Loembé M, Nkengasong JN. COVID-19 vaccine access in Africa: Global distribution, vaccine platforms, and challenges ahead. *Immunity.* 2021;54(7):1353-1362.
183. WHO. Vaccine Equity. In:2022.
184. GOV.UK. Coronavirus (COVID-19) in the UK: Vaccinations in United Kingdom. 2022; https://coronavirus.data.gov.uk/details/vaccinations.
185. GOV.UK. Cases in the United Kingdom. *Coronavirus (COVID-19) in the UK* 2022; https://coronavirus.data.gov.uk/details/cases.